The Dissertation Committee for Minyoung Park
certifies that this is the approved version of the following dissertation:

Designing Medium Access Control Protocols for Multiple-Input-Multiple-Output Wireless Networks

Committee:

Scott M. Nettles, Supervisor

Edward J. Powers

Gustavo de Veciana

Robert W. Heath, Jr.

Brian T. Kelley

Designing Medium Access Control Protocols for Multiple-Input-Multiple-Output Wireless Networks

by

Minyoung Park, B.S.E., M.S.E

Dissertation

Presented to the Faculty of the Graduate School of

The University of Texas at Austin

in Partial Fulfillment

of the Requirements

for the Degree of

Doctor of Philosophy

The University of Texas at Austin

August 2005

To my family

for their love and support

Acknowledgments

I would like to thank my supervisor, Dr. Scott Nettles, for his guidance and support throughout my research at the University of Texas at Austin. He showed me the fundamentals of research and guided me with great insights, broad and profound knowledge, and encouragement.

I am indebted to Dr. Robert Heath Jr. for his helpful directions and advice on wireless communications, to Dr. Edward Powers for his warm encouragement on my research, to Dr. Gustavo de Veciana for his guidance on network analysis, and to Dr. Brian Kelley for his helpful advice on the practical issues of communication systems.

I would also like to thank my colleagues, Seong-Kyu Song, Hari Shankar, Pisai Setthawong, Yihong Zhou, Soon-Hyeok Choi, Gibeom Kim, Sangwoo Lee, and Ketan Mandke for their helpful advice and discussions on my research.

My friends who started this long academic journey with me and helped me finish this journey are hereby acknowledged. I would like to thank Byungchul Jang, Seyeong Choi, Changyong Shin, Jihwan Chun, Jonghoon Baek, Taeho Jung, and Changhyun Paek for their sincere friendship. My years in Austin were pleasant and enjoyable because of them.

Furthermore, I would like to thank the Ministry of Information and Communication of Korea for its financial support during my study at the University of Texas at Austin.

Finally, I would like to dedicate this dissertation to my wife Soyoung Kim, to my daughter Jimin and soon to be born child, to my parents and parents-in-law, and to my brother and sister for their love, support, and encouragement. Without them, it would have been impossible to accomplish this.

Minyoung Park

The University of Texas at Austin
August 2005

Designing Medium Access Control Protocols for Multiple-Input-Multiple-Output Wireless Networks

Publication No. _____

Minyoung Park, Ph.D.
The University of Texas at Austin, 2005

Supervisor: Scott M. Nettles

Carrier Sense Multiple Access with Collision Avoidance (CSMA/CA) and the request-to-send (RTS)/ clear-to-send (CTS) control packet exchange mechanism based medium access control (MAC) protocols, such as the IEEE 802.11 MAC protocol, are extremely successful in single-hop environments. Unfortunately, in multi-hop environments, they suffer from unfair access to the channel due to a side effect of carrier sense and do not perfectly address the hidden node problem and thus degrade network performance.

Fortunately, Multiple-Input-Multiple-Output (MIMO) technologies, which employ multiple antennas on both the transmitter and the receiver, provide capa-

bilities to mitigate interference from neighboring nodes, to mitigate fading, and to increase the capacity of a link. We claim that designing MAC protocols jointly with flexible MIMO physical layer technologies can address the problems of conventional MACs and higher layer protocols for multi-hop wireless networks.

To show this, we first propose a MAC protocol, Mitigating Interference using Multiple Antennas MAC (MIMA-MAC), which mitigates interference from neighboring nodes by using MIMO in its spatial multiplexing mode. We show that the MIMA-MAC can address the problems caused by neighboring interference and can also increase the utilization of network resources. We further enhance the MIMA-MAC and propose the Mitigating Interference using Multiple Antennas with Antenna Selection diversity MAC (MIMA/AS-MAC), which fully utilizes multiple antennas by employing antenna selection diversity together with spatial multiplexing to mitigate fading as well as to suppress interference from neighboring nodes. For a multi-hop network, we show that the MIMA-MAC can improve TCP performance by mitigating neighboring interference. We further enhance the MIMA/AS-MAC and propose the TCP enhanced MIMA/AS-MAC, which increases the efficiency of small packet transmission. Finally, we explore ways of designing cross-layer MAC protocols that can address the problems of a system using reactive ad hoc routing protocols by controlling transmission modes based on the type of packets and channel conditions.

Contents

List of Tables

List of Figures

Chapter 1

Introduction

Most of the telecommunication architectures currently used for wired or wireless networks use a "layered" protocol architecture such as the Open System Interconnection (OSI) architecture [1]. Each layer is designed independently and thus it is possible to change each layer easily without affecting the other layers in the protocol stack. Although, this layered design makes the complex problems of protocol design and maintenance easier, when the physical layer changes from a static and reliable wired channel to a dynamic and unreliable wireless channel, the higher layer protocols that have been designed and optimized based on wired networks often perform poorly. This is because they have not taken into account the effects of the wireless channel such as fading and interference. This indicates that we need to introduce a "cross-layer" design approach in which each layer is designed jointly with other layers so as to achieve better performance.

IEEE 802.11 wireless ethernet technologies [2] are already extremely successful and their importance is growing daily. There is, however, growing evidence that IEEE 802.11's medium access control (MAC) protocol, when used in the Distributed Coordination Function (DCF) mode needed by multi-hop networks, is *unfair* and suffers from *throughput degradation*. For example, Xu and Saadawi show in [3] that

adjacent traffic flows in the network can experience significantly unfair access to the wireless channel. Moreover, Xu *et al.* show in [4] that throughput degradation can occur due to interference from hidden nodes. This is despite 802.11's MAC having been designed to avoid the hidden node problem by using a request-to-send/clear-to-send (RTS/CTS) scheme.

As we will illustrate in Chapter 2, these problems arise because IEEE 802.11's carrier sense multiple access with collision avoidance (CSMA/CA) with RTS/CTS MAC design allows some nodes to monopolize the channel as a side effect of carrier sense, while interference from hidden nodes causes collisions reducing throughput.

These problems of 802.11 further degrade the performance of TCP for multi-hop wireless networks since TCP tries to fill the pipe full to maximize link utilization, which naturally generates neighboring interference that 802.11 cannot mitigate. As a result, the source of the TCP flow reduces its transmission rate to the point where simultaneous transmissions in the pipe are far enough apart that they do not interfere each other's transmission. This eventually results in throughput degradation.

Besides the problems of 802.11, which arise from interference from neighboring nodes, another important issue that degrades the performance of a multi-hop wireless network is *fading* of the wireless channel, which also causes packet drops. TCP is a good example that shows the effect of packet drops caused by other than congestion in the network because TCP is built on the assumption that congestion is the only cause of packet drops, which holds only for wired networks but not for wireless networks.

Fading also impacts the performance of ad hoc routing protocols in finding a route from a source to destination because it weakens the connectivity of the network, which is required by the flooding (route discovery) mechanism, which finds a target by broadcasting a query packet to neighboring nodes.

1.1 Multiple-Input Multiple-Output Communications

Fortunately, new research in wireless communication can provide us with radio technology that can help to solve the problems caused by interference and fading. The principle technique we focus on is Multiple-Input-Multiple-Output (MIMO) communication, which uses multiple antennas at both the transmitter and receiver for spatial multiplexing (SM) and spatial diversity (SD) [5]. We will present the details of these two physical layer techniques for MIMO in Chapter 2.

SM has generally been used to increase the capacity of a MIMO link by transmitting independent data streams in the same time slot and frequency band simultaneously from each transmit antenna, and differentiating multiple data streams at the receiver using channel information about each propagation path [6, 7]. Other than increasing the capacity of a link, SM can also mitigate interference from neighboring nodes by differentiating interference from the intended data stream. For spatial multiplexing to increase the capacity of a link or mitigate interference, the rank of the channel matrix between the transmitter and receiver has to be a full column rank. In reality, however, due to insufficient antenna spacing or scatterers, the fades of the propagation paths between the transmit and receive antennas might be correlated and thus this fading correlation leads to degradation of the link capacity [5, 8].

In contrast to SM, the purpose of SD is to increase the diversity order of a MIMO link to mitigate fading by coding a signal across space and time so that a receiver can receive the replicas of the signal transmitted over independent fading paths and combine those signals constructively to achieve a diversity gain [9, 10].

1.2 Cross-layer MAC Design

In general, a MAC protocol is used to allocate shared medium resources to multiple users. For example, nodes using a CSMA/CA based MAC protocol share time resources with each other by hearing other node's transmissions. As physical layer communication technologies advance and provide a variety of transmission modes that could improve the performance of a link or a network in many respects, more sophisticated MAC protocols have been developed to control and to utilize those capabilities of flexible physical layers.

For example, we are able to control the transmission rate of a physical layer by using various coding rates and signal constellations to improve the average throughput of a link [11], or transmission power to increase the spatial reusability and thus increase the network capacity or to minimize the power consumption of the network [12, 13]. Moreover, by controlling the direction of a transmission with directional and smart antenna technologies we are able to minimize the interference between neighboring nodes and thus increase the reusability of a network and consequently maximize the capacity of the network [14–18].

Similar to the above examples, MIMO provides another level of flexibility to a physical layer. When MIMO is used for spatial multiplexing, it can increase the capacity of a link or mitigate interference from neighboring nodes, whereas when MIMO is used for spatial diversity, it can mitigate fading and thus increase the reliability of a wireless link. Most MIMO research has been focused on improving a single link's capacity or reliability [6, 7, 9, 10]. To improve the performance of a whole network by addressing the previously mentioned problems, our claim is that we need to design a new MAC protocol that fully utilizes the flexible capabilities of MIMO focusing on the overall network performance rather than just the capacity or quality of a link. As we will describe in detail in Section 2.3, there is limited work on MAC protocols that utilizes MIMO technology [19–22].

1.3 Thesis

My thesis is:

Jointly designing a medium access control protocol with a multiple-input multiple-output physical layer scheme to address the problems of the MAC and higher layer protocols can improve overall network performance.

1.4 Goals and Approaches

Our goal is to show that we are able to address a number of problems that the MAC and higher layer protocols of wireless networks have by designing new MAC protocols jointly with a physical layer that employs MIMO communication technologies. Using the ns-2 network simulator [23], we validate our argument by implementing the proposed MAC protocols, conducting extensive simulations, and measuring the performance of the systems that employ the proposed MAC protocols.

Firstly, we propose a basic design for a MAC protocol, Mitigating Interference using Multiple Antennas MAC (MIMA-MAC), that mitigates interference from neighboring nodes by utilizing the spatial multiplexing capability of a MIMO physical layer and show that the proposed MAC protocol can solve the unsolved hidden node and unfairness problems that eventually degrade network performance in 802.11. We measure the throughput of the network and fairness between constant-bit-rate (CBR) traffic flows. The measured performance is compared with a 802.11 system that uses a single antenna over an ideal (orthogonal) channel and a Rayleigh fading channel [5]. The simulation results show that the MIMA-MAC system outperforms the 802.11 system in terms of both throughput and fairness.

Second, as an enhancement of the MIMA-MAC, we propose the Mitigating Interference using Multiple Antennas with Antenna Selection MAC (MIMA/AS-MAC), which selects a transmit antenna from the available antennas for a data

packet transmission to obtain diversity against fading as well as to suppress interference from neighboring transmitters. We use a zero-forcing (ZF) receiver [5] to obtain a lower bound on system performance. The antenna is selected that maximizes the post-processing signal-to-noise ratio (SNR) of the data packet that is *destined* for the receiver. The receiver estimates the channel by receiving a request-to-send (RTS) control packet from the transmitter and feeds back the selected antenna information to the transmitter using a clear-to-send (CTS) packet. Moreover, the protocol employs Alamouti encoding [9] for control packet transmission to increase the reliability of these transmissions using both transmit antennas. The performance is compared with that of the MIMA-MAC system both with and without Alamouti encoding for the control packet transmission and the 802.11-Alamouti system that uses the IEEE 802.11 MAC protocol with Alamouti encoding for both control and data packets. The simulation results show that the throughput of the MIMA/AS-MAC system is approximately 14% to 26% higher than that of the MIMA-MAC system and 15% to 60% higher than that of the 802.11-Alamouti system.

Third, based on the above two MAC protocol designs, we study the performance of TCP in a multi-hop wireless network. Since the MIMA-MAC can mitigate interference from neighboring nodes, it can also mitigate the self-generated interference of the TCP flow and thus improve TCP throughput. Unfortunately, the simulation results show that the MIMA-MAC is inefficient for small-sized packet transmission, such as TCP's acknowledgement packet, because its MAC frame size is fixed and large. Therefore, we propose an enhanced MAC protocol, TCP enhanced MIMA/AS-MAC, which further enhances the MIMA/AS-MAC by concatenating a small packet with a large packet and transmitting them in the same MAC frame so as to increase the efficiency of small packet transmission. The simulation results show that, when simulated over an ideal channel, we can achieve approximately 21% to 44% throughput gain by increasing the efficiency of small packet transmission.

Finally, we explore ways of designing cross-layer MAC protocols that control transmission modes to address the problems of a system using a reactive ad hoc routing protocol. Since a route request packet (RREQ) might fail to reach its destination due to packet drops when transmitted over a fading channel, it is a reasonable choice to use spatial diversity to increase the reliability of a link. Using spatial diversity for both broadcast and unicast packets, however, might be too conservative since unicast packets are generally large in size and thus it might be better to increase the capacity than to increase the reliability of a link for an unicast packet. Therefore, as a way of addressing this problem, we propose an aggressive MAC protocol, which uses spatial diversity for broadcast packet transmission and uses spatial multiplexing or antenna selection diversity with an adaptive modulation scheme based on the channel condition for unicast packet transmission. The simulation results show that by controlling transmission modes based on the type of packets and channel conditions, we can improve overall network performance.

The remainder of this document is organized as follows. In Chapter 2, we present background about the IEEE 802.11 MAC protocol and MIMO communications and related work. In Chapter 3, we present the MIMA-MAC, which addresses the unsolved hidden node and unfairness problems. In Chapter 4, we propose the MIMA/AS-MAC, which fully utilizes multiple antennas in the physical layer to mitigate fading as well as interference from neighboring nodes by employing antenna selection diversity. In Chapter 5, we extend our study to TCP and show the performance improvement using the proposed MAC protocols that exploits the capabilities of MIMO in the physical layer. Moreover, we explore ways to enhance the MIMA-MAC for small-sized packet transmissions. In Chapter 6, we further extend our study to routing protocols that suffer from fading during the route discovery process. Finally in Chapter 7, we present the contributions and conclusions.

Chapter 2

Background and Related Work

In this chapter, we present the background material that is needed to understand the remainder of the thesis as well as key related work. First, we present the basic operation of the conventional 802.11 MAC protocol and its problems. Next, we present the basics of MIMO communications; how it works, its requirements, and its capabilities. Finally, we present related work.

2.1 IEEE 802.11 MAC Protocol Overview

Though the IEEE 802.11 MAC protocol [2], which is a working example of a general Carrier Sense Multiple Access with Collision Avoidance (CSMA/CA) with Request-To-Send/Clear-To-Send (RTS/CTS) MAC protocol, is successful for access point based wireless networks, there is growing evidence that it does not work well for multi-hop wireless networks. To understand the related problems, we present the basic operation of a CSMA/CA and RTS/CTS based MAC protocol and its problems when used for a multi-hop wireless network.

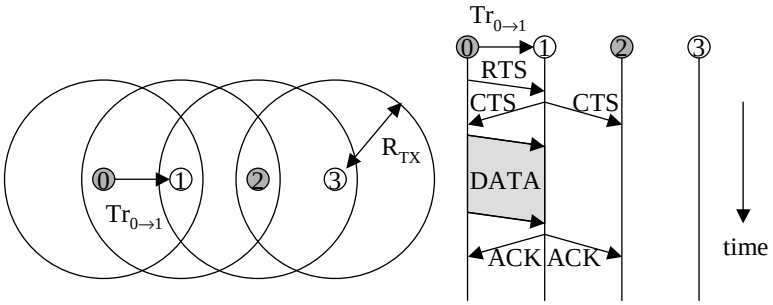

Figure 2.1: A linear topology wireless network consisting of four nodes (left) and the basic operation of the IEEE 802.11 MAC protocol (right). The circle around the node represents the transmission range, R_{TX}.

2.1.1 Basic operation

The design of the 802.11 MAC protocol is based on a CSMA/CA with RTS/CTS protocol [2]. Figure 2.1 illustrates the basic operation of the protocol for a wireless network consisting of four nodes. In the figure, the circles around the nodes represent the transmission range, R_{TX}, within which the nodes can receive and decode data successfully. In CSMA/CA, every node first senses the carrier before transmission. In general, the carrier sensing range is larger than the transmission range. If the channel is busy, the transmitter defers its transmission to avoid a collision. The carrier sensing mechanism, however, cannot prevent collisions if the node near the receiver is unable to sense the transmission from the transmitter but is close enough to the receiver that it can still interfere the reception at the receiver. In this case, the interfering node is said to be *hidden* from the transmitter. This is generally known as the *hidden node problem*. For example, in Figure 2.1, if we assume that node 2 cannot sense the unicast transmission from node 0 to node 1, node 2 is hidden from node 0 and can cause interference to node 1. To solve this problem, 802.11 employs a RTS/CTS protocol, which exchanges RTS and CTS control packets between the transmitter and receiver before a DATA packet transmission. The basic idea is to first acquire the *channel* ("clearing the floor") before the DATA

packet transmission by blocking the neighboring nodes that overhear the control packet transmissions [24]. The RTS and CTS each have network allocation vector (NAV) information, which indicates when the dialog between the transmitter and the receiver finishes. When nodes near the transmitter and receiver successfully decode the control packets and obtain the NAV information, those nodes will stay silent for the amount of time indicated in the NAV to avoid collision with the ongoing dialog. For example, consider a DATA transmission from node 0 to node 1. Since node 2 can decode the CTS transmitted from node 1, node 2 stays silent until the end of the dialog. Therefore, node 0 can transmit a DATA packet to node 1 without any interference from node 2, solving the hidden node problem. Finally, the receiver replies with an acknowledgement (ACK) packet back to the transmitter to indicate that it received the DATA packet successfully. One thing to notice in this example is that the transmission between node 0 and node 1 blocked a possible transmission between node 2 and node 3.

To understand our later results, we need a few additional details about the protocol. In the protocol, a node can actually only transmit a new packet if the channel is idle for a DCF Inter Frame Space (DIFS) interval, otherwise the node waits for the channel to be idle again. If the channel is busy and a node can decode the other node's transmission, the node again defers for a DIFS just after the end of the transmission. If, however, the node cannot decode but can sense the transmission, it defers for an Extended Inter Frame Space (EIFS) interval, which is much longer than a DIFS. An EIFS consists of a Short Inter Frame Space (SIFS), which is the time required between the packets in the same dialog, the time required for a ACK packet transmission, and a DIFS [2]. Moreover, to reduce the collisions between the nodes that try to access the channel after a DIFS or EIFS, the nodes generate and defer an additional random backoff period, which is determined by randomly choosing an interval within their contention window (CW). The size of

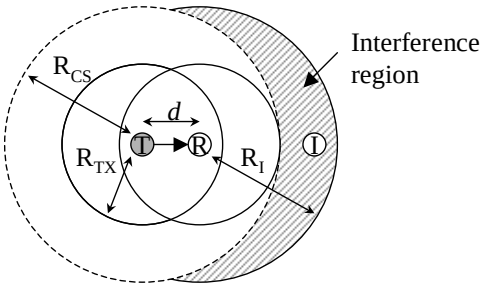

Figure 2.2: Illustration of the unsolved hidden node problem of the IEEE 802.11 MAC protocol. The shaded area represents the interference region that CSMA/CA and the RTS/CTS protocol cannot cover. The interferer, node I, is hidden from the transmitter, node T, and interferes with the receiver, node R.

the CW is increased to double the previous size for every unsuccessful transmission until it reaches its maximum value, CW_{max}.

2.1.2 The unsolved hidden node problem

Though the CSMA/CA and RTS/CTS protocols provide the major functionality for a wireless network to share the channel resource, in practice, an aspect of the hidden node problem still remains unsolved and causes performance degradation [3, 4]. Consider a wireless network consisting of three nodes as shown in Figure 2.2. In the figure, node T, node R, and node I denote the transmitter, the receiver, and the interferer, respectively, and R_{CS} and R_I denote the carrier sensing range and the interference range respectively, where R_{CS} is the range within which the nodes can sense the transmission from the transmitter and R_I is the range within which the interferer causes interference to the receiver [4]. R_{TX} and R_{CS} are measured from the transmitter, whereas R_I is measured from the receiver. R_I varies depending on the signal-to-interference ratio (SIR) threshold, $SIR_{Threshold}$, the path-loss exponent, n, and the distance between the transmitter and receiver, d. $SIR_{Threshold}$ is the minimum required SIR for the receiver to decode the packet successfully in the presence of the interference assuming that the noise power at the receiver is

negligible. R_I is derived in [4] as

$$R_I = \sqrt[n]{SIR_{Threshold}} \cdot d. \tag{2.1}$$

In Figure 2.2, the following assumptions are made for R_{TX}, R_{CS}, and R_I. Typically, R_{CS} is larger than R_{TX} since the received power required at a node for sensing the transmission from a transmitter is much lower than that required for correctly receiving the transmission. We assume that $R_{CS} \approx 2R_{TX}$ based on the AT&T WaveLAN wireless LAN card modelled in ns-2 [23] and on [25] showing that, for an access-point based network, the ideal relation between R_{CS} and R_{TX} is $R_{CS} = 2R_{TX}$. Moreover, in case of $SIR_{Threshold} = 10$dB and $n = 2$ for the free space propagation model [26], from (2.1) R_I becomes approximately $3.16d$. If d is small, which means that the transmitter and receiver are close, R_I becomes small and if d is large, which means that the receiver is close to the edge of R_{TX}, R_I becomes large. For this example, we assume that $R_I \approx R_{CS}$, which is possible by choosing $d \approx R_{CS}/3.16$.

With these assumptions, we can find a region, in which interfering nodes are still *hidden* from the transmitter. We denote this region as the *interference region* [4] (the shaded area in Figure 2.2). When the transmitter, node T, starts to transmit, the nodes that are within R_{CS} of node T defer their transmission until the end of the transmission according to the carrier sensing mechanism and when the receiver, node R, replies with a CTS, the nodes within R_{TX} of node R defer their transmission until the end of the dialog between node T and node R according to the RTS/CTS protocol. The nodes that are out of the region covered by the CSMA/CA and RTS/CTS protocol but within R_I of the receiver, however, can only sense the CTS transmission, and will try to access the channel after deferring an EIFS and an additional random backoff period of time. Therefore, if the nodes that are in the interference range access the channel before the end of the transmission from node

T, a collision will occur at node R. Thus, in practice, the hidden node problem still remains. We will illustrate this problem in more detail in Section 3.5.

2.1.3 Key problems

Interference from neighboring nodes, which is rooted in the unsolved hidden node problem, incurs two serious problems: the *unfairness* problem and the *extreme throughput degradation* (ETD) problem. We first present the network topology and traffic configurations in which the unfairness and ETD problems are frequently observed and then explain the unfairness and ETD problems in detail.

Network topology and traffic configurations

Consider the path that a data flow takes in a multi-hop wireless network. In general, it will be a zig-zag of hops connecting source to destination. It is likely that the path will be an approximation of the shortest possible path, such as the routes found by popular ad hoc routing protocols [27,28]. To achieve the shortest path each hop will tend to be as long as possible, which unfortunately also results in maximizing the interference range. We are concerned with the effects of interference, which means the distances between a transmitter, a receiver, and a possible interferer are crucial, but the angle formed between them is not. Thus, as in [3], we can approximate this zig-zag path as a linear one.

There could be two basic scenarios for multi-hop wireless networks: same direction traffic (SDT) and opposite direction traffic (ODT). After discovering the route to the destination, the source starts to inject data packets into the network. The intermediate nodes along the route will try to forward data packets to the destination in the same direction. Thus, the transmissions from the nodes along the route form *same direction traffic* as shown in Figure 2.3. Moreover, consider a reliable data transmission protocol such as the transport control protocol (TCP),

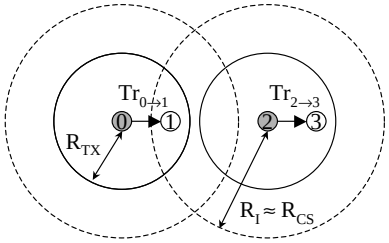

Figure 2.3: The same direction traffic (SDT) scenario. The two traffic flows, $Tr_{0\rightarrow1}$ and $Tr_{2\rightarrow3}$, transmit data from node 0 to node 1 and from node 2 to node 3 respectively. The two traffic sources, node 0 and node 2, are out of each other's R_{CS}, but node 2 is within the R_I of node 1.

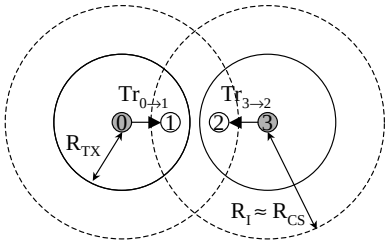

Figure 2.4: The opposite direction traffic (ODT) scenario. The two traffic flows, $Tr_{0\rightarrow1}$ and $Tr_{3\rightarrow2}$, transmit data from node 0 to node 1 and from node 3 to node 2 respectively. The two traffic sources, node 0 and node 3, are out of each other's R_{CS}. Both node 0 and node 3, however, are within the R_I of node 2 and node 1, respectively.

which has ACK packets sent from the destination. Since the ACK and data packets have opposite directions, these two traffic flows form *opposite direction traffic* (ODT) as shown in Figure 2.4. Since they arise from flows of data, we expect that these two scenarios will be common in multi-hop wireless networks. As we will illustrate in the following sections, unfairness and ETD are frequently observed in the SDT and ODT scenarios, respectively. These scenarios will be used throughout the simulations for performance evaluation and comparison.

The unfairness problem

The unfairness problem is observed in a network when one traffic flow dominates the channel resource, and thereby one traffic flow has much higher throughput than any other. We can observe this problem in the SDT scenario shown in Figure 2.3. In the network, there are two traffic flows with the same direction, one from node 0 to node 1, $Tr_{0\rightarrow1}$, and the other from node 2 to node 3, $Tr_{2\rightarrow3}$. In this scenario, we again assume that $R_{CS} \approx R_I \approx 2R_{TX}$. To show the extreme case of the unfairness problem, the network is configured such that the two transmitters, node 0 and node 2, cannot sense each other's transmission and one of the two receivers, node 1, can sense but cannot decode the transmission from the other traffic's transmitter, node 2. Since, the two transmitters cannot sense each other's transmission, one can commence its transmission even when the other transmitter is in the middle of transmission. Unfortunately, when both transmitters try to access the channel simultaneously, the packet transmitted from node 2 will successfully received at node 3 without any collision but the packet transmitted from node 0 will collide with the packet transmitted from node 2 at node 1. This is because node 2 is within R_I of node 1 whereas node 0 is out of R_I of node 3. This makes the throughput of $Tr_{2\rightarrow3}$ higher than that of $Tr_{0\rightarrow1}$, which results in unfairness between the two flows. As we will cover in more detail in Chapter 3, unfairness can also arise without interference

from hidden nodes due to the side effects of the carrier sensing mechanism and transmitters having unequal information about transmissions in the network.

Moreover, the unfairness gets worse if we assume that both flows fully consume the channel resource by transmitting large data packets at the maximum data rate for the following reasons. Since the channel is fully consumed by $Tr_{2\rightarrow 3}$, which continuously causes interference at node 1, all the packets transmitted from node 0 to node 1 collide with packets from node 2. Furthermore, the transmission failure experienced by node 0 continuously increases the size of the CW of node 0 [29], which further lowers its chance to access the channel. Therefore, while node 2 is transmitting to its destination, node 0 cannot access the channel, whereas node 2 can always access the channel regardless of the transmission from node 0, which results in extreme unfairness between the neighboring two flows.

The extreme throughput degradation problem

The extreme throughput degradation (ETD) problem is observed in a wireless network when two neighboring traffic flows have opposite directions and the sources of the two flows cannot sense each other's transmission but one's transmission can interfere with the other's data reception and vice versa. This implies that the source of one traffic flow acts as an *interferer* to the receiver of the other traffic flow. For example, in the ODT scenario shown in Figure 2.4, suppose node 0 initially transmits a packet to node 1. When node 3 transmits a packet to node 2 before the end of the transmission from node 0, it will interfere with the ongoing data transmission from node 0 to node 1 and will prevent node 1 from receiving the packets from node 0. At the same time, since the packet from node 0 also causes interference to node 2, the packet sent from node 3 to node 2 will also be dropped. To resolve the contention between the two flows, both transmitters back off by increasing their CWs. If, however, one transmitter tries to access the channel when the other transmitter

is transmitting a RTS or DATA packet, both transmissions will fail and thus will again increase the CWs of both transmitters. Therefore, if the CW is not sufficiently large, collisions will continuously occur and consequently lower the throughput of both flows. Furthermore, if the maximum possible defer time, which is defined as the maximum backoff time determined by CW_{max} plus DIFS (or EIFS), is shorter than the time required for the RTS-CTS-DATA-ACK exchange, which is possible when the DATA packet is sufficiently large, the transmitters cannot resolve collisions because the deferred transmitter will try to access the channel before the end of the dialog of the other traffic flow, and this causes packet drops at both receivers. Therefore, in the worst case of the ODT scenario, if the size of the DATA packet is sufficiently large, the network suffers from extremely low throughput performance.

2.2 Multiple-Input Multiple-Output (MIMO) Communications Overview

As shown in the previous section, CSMA/CA and RTS/CTS based MAC protocols suffer from performance degradation caused by interference from neighboring nodes. To solve these problems, we propose to use a flexible physical layer technology that provides interference mitigation capability. Recent research on wireless communications has shown that using multiple antennas on both the transmitter and receiver over a rich-scattering channel can increase the capacity and/or the reliability of a wireless link [6, 7, 10]. Two major techniques that exploit such capabilities are spatial multiplexing (SM) and spatial diversity (SD) [5]. SM increases the capacity of the multiple-input-multiple-output (MIMO) link by transmitting independent data streams simultaneously from each transmit antenna and differentiating two data streams at the receiver by employing a number of space-time interference cancellation algorithms [5]. On the other hand, SD schemes such as space-time trellis coding

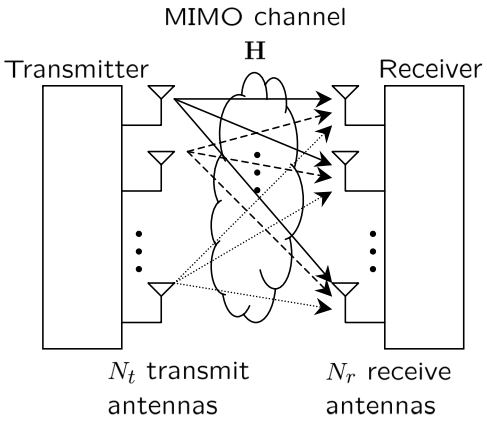

Figure 2.5: A basic diagram of a MIMO communication system with N_t transmit antennas and N_r receive antennas.

(STTC) [10] and space-time block coding (STBC) [9] transmit carefully space-time coded data across multiple antennas and time in order to reduce the probability of error over a fading channel by increasing the diversity order of a link. The diversity order is defined as the magnitude of the slope of the error rate versus the signal-to-noise (SNR) curve on a log-log scale [5, 30].

2.2.1 Spatial multiplexing

Spatial multiplexing transmits independent data streams from the transmit antennas simultaneously using the same carrier frequency. If transmit antennas are spaced sufficiently far apart and if there are rich scatterers with no line-of-sight (LOS) between the transmit and receive antennas, each data stream experiences independent fading, which serves as a unique "signature" for each propagation path between a pair of transmit and receive antennas [31]. The receiver estimates the signatures (or channel responses) of the propagation pathes from known transmitted training signals. The different signatures of the data streams make it possible to differentiate the simultaneously transmitted data streams by employing a number of interference cancellation algorithms. In the following, we will briefly show how we can differen-

tiate multiple independent data streams using an appropriate receiver design with a number of interference cancellation algorithms and how well they perform.

Consider a wireless communication system as illustrated in Figure 2.5 equipped with N_t transmit and N_r receive antennas, transmitting data over a rich scatterers with no LOS and a flat-fading (narrowband) MIMO channel $\mathbf{H}$, where $\mathbf{H}$ is a $N_r \times N_t$ channel matrix composed of N_t channel vectors $\mathbf{H}$=$[\mathbf{h}_1\ \mathbf{h}_2\ \cdots\ \mathbf{h}_{N_t}]$ and $\mathbf{h}_i = [h_{1i}\ h_{2i}\ \cdots\ h_{N_r i}]^T$ is the channel vector representing the propagation channel between the i^{th} transmit antenna and the N_r receive antennas, where ^{T} denotes transpose. The channel gain of the propagation path for a rich-scattering channel with no LOS is usually assumed to be Rayleigh distributed [32, 33], which means that each entry of the channel matrix is an uncorrelated complex Gaussian random variable with zero mean and a variance of one, i.e. $\mathcal{CN}(0, 1)$. In this example, the transmitter transmits N_t independent data streams, $x_1, x_2, \cdots, x_{N_t}$, from N_t transmit antennas, simultaneously, over a MIMO channel $\mathbf{H}$. At the receiver, each receive antenna receives N_t multiple data streams. Thus, we can express the received $N_r \times 1$ signal vector $\mathbf{y} = [y_1\ y_2\ \cdots\ y_{N_r}]^T$ in a discrete-time signal model for one observation as

$$\mathbf{y} = \sqrt{\frac{E_s}{N_t}}\mathbf{H}\mathbf{x} + \mathbf{n} \tag{2.2}$$

where, $\mathbf{x} = [x_1\ x_2\ \cdots\ x_{N_t}]^T$ is $N_t \times 1$ transmit signal vector, $\mathbf{n} = [n_1\ n_2\ \cdots\ n_{N_r}]^T$ is the $N_r \times 1$ noise vector, n_i is a zero mean circularly symmetric complex Gaussian random variable with variance N_0, and E_s/N_t is the average transmit energy per symbol period per antenna.

Assuming that the channel matrix $\mathbf{H}$ is perfectly known to the receiver, we can separate simultaneously received N_t data streams at the receiver by employing a maximum-likelihood (ML) receiver or linear receivers such as the zero-forcing (ZF) and minimum mean-square error (MMSE) receivers [5].

The ML receiver is the optimal receiver in the sense of minimizing error probability but also has high decoding complexity. The ML receiver searches for the transmitted signal vector $\mathbf{x}$ for all possible candidates that satisfies (2.3). In other words, the ML receiver is searching for a vector that is closest to the transmitted signal vector.

$$\hat{\mathbf{x}} = \arg\min_{\mathbf{x}} \left\| \mathbf{y} - \sqrt{\frac{E_s}{N_t}}\mathbf{H}\mathbf{x} \right\|^2 . \tag{2.3}$$

As a practical solution, we can reduce the decoding complexity by using a linear filter that can separate multiple data streams and decode each data stream separately. A ZF receiver is one of the simplest nontrivial receivers but worst performing linear decoding scheme due to its noise enhancement problem [5]. It simply inverts the channel matrix $\mathbf{H}$ and multiplies it by the received signal vector $\mathbf{y}$. The output of the ZF receiver is obtained by multiplying the received signal vector $\mathbf{y}$ with the ZF linear matrix filter $\mathbf{G}_{ZF} = \sqrt{\frac{N_t}{E_s}}\mathbf{H}^{\dagger}$, where † denotes pseudo inverse. Thus, the output of the ZF receiver $\mathbf{y}_{ZF}$ can be expressed as

$$\begin{aligned} \mathbf{y}_{ZF} &= \mathbf{G}_{ZF}\mathbf{y} \\ &= \mathbf{G}_{ZF}\sqrt{\frac{E_s}{N_t}}\mathbf{H}\mathbf{x} + \mathbf{G}_{ZF}\mathbf{n} \\ &= \mathbf{H}^{\dagger}\mathbf{H}\mathbf{x} + \sqrt{\frac{N_t}{E_s}}\mathbf{H}^{\dagger}\mathbf{n} \\ &= \mathbf{x} + \sqrt{\frac{N_t}{E_s}}\mathbf{H}^{\dagger}\mathbf{n}. \end{aligned} \tag{2.4}$$

Equation (2.4) shows the received signal separated from each other. The noise, however, is correlated across the channel. From (2.4), since the noise power of the k th data stream is $\frac{N_t}{\rho}[(\mathbf{H}^H\mathbf{H})^{-1}]_{k,k}$, where $\rho = \frac{E_s}{N_0}$, we can express the post-

processing signal-to-noise ratio (SNR) of the k^{th} data stream, η_k as [5, 34]

$$\eta_k = \frac{\rho}{N_t} \frac{1}{[(\mathbf{H}^H\mathbf{H})^{-1}]_{k,k}}. \tag{2.5}$$

The ZF receiver performs poorly when the channel gain is low (e.g. deep fading), which results in noise enhancement because as the channel gain decreases, the denominator of (2.5) increases. We will use the ZF receiver in Chapter 3 and Chapter 4 to obtain a lower bound on system performance.

As an enhancement, the MMSE receiver reduces the noise enhancement by selecting a linear matrix filter $\mathbf{G}_{\text{MMSE}}$ that minimizes the total error. As shown in [5], the linear matrix filter that minimizes the total error can be found from the following equation

$$\mathbf{G}_{\text{MMSE}} = \arg\min_{\mathbf{G}} \mathcal{E}\left\{\|\mathbf{G}\mathbf{y} - \mathbf{x}\|_F^2\right\} \tag{2.6}$$

where, the expectation $\mathcal{E}\{\cdot\}$ is taken over the signal and noise. Using the orthogonality principle, $\mathcal{E}\left\{(\mathbf{G}\mathbf{y} - \mathbf{x})\mathbf{y}^H\right\} = \mathbf{0}_{N_t,N_r}$, $\mathbf{G}_{\text{MMSE}}$ is derived as

$$\mathbf{G}_{\text{MMSE}} = \sqrt{\frac{N_t}{E_s}}\left(\mathbf{H}^H\mathbf{H} + \frac{N_t}{\rho}\mathbf{I}_{N_t}\right)^{-1}\mathbf{H}^H. \tag{2.7}$$

Thus, the output of the MMSE receiver $\mathbf{y}_{\text{MMSE}}$ can be expressed as

$$\begin{aligned} \mathbf{y}_{\text{MMSE}} &= \mathbf{G}_{\text{MMSE}}\mathbf{y} \\ &= \mathbf{G}_{\text{MMSE}}\sqrt{\frac{E_s}{N_t}}\mathbf{H}\mathbf{x} + \mathbf{G}_{\text{MMSE}}\mathbf{n}. \end{aligned} \tag{2.8}$$

Therefore, from (2.7) and (2.8), the post-processing SNR of the k th data stream for the MMSE receiver can be expressed as [5, 34]

$$\eta_k = \frac{1}{[(\frac{\rho}{N_t}\mathbf{H}^H\mathbf{H} + \mathbf{I}_{N_t})^{-1}]_{k,k}} - 1. \tag{2.9}$$

The above result shows that at low SNR region the MMSE receiver mitigates noise enhancement and outperforms the ZF receiver.

2.2.2 Spatial diversity

Another ability of MIMO communications is to make a channel more reliable. Prior to the transmission, the data stream must be carefully space-time coded so that the replicas of the data stream traverse different channels, which enables the receiver to gain spatial diversity by receiving different versions of the same data stream. We will use spatial diversity in our MAC design to mitigate fading in Chapter 4 and Chapter 6.

Alamouti encoding

Among various space-time coding schemes, we present the well known Alamouti encoding scheme [9], which is a simple transmit diversity scheme for a transmitter with two antennas that achieves full diversity order without any knowledge of the channel at the transmitter. In the following, we will briefly show how Alamouti encoding works and how well it performs.

The Alamouti encoding scheme converts a MIMO channel $\mathbf{H}$ into an effective orthogonal MIMO channel $\mathbf{H}_{eff}$ that satisfies $\mathbf{H}_{eff}^{H}\mathbf{H}_{eff} = \|\mathbf{H}\|_F^2\,\mathbf{I}_2$, where $\|\mathbf{H}\|_F^2$ is the squared Frobenius norm of $\mathbf{H}$ and $\mathbf{I}_2$ is 2×2 identity matrix, by coding two different symbols across two antennas and two symbol periods in the following manner. Figure 2.6 illustrates a two antenna MIMO system with a 2×2 channel matrix $\mathbf{H}$ defined as

$$\mathbf{H} = \begin{bmatrix} h_{11} & h_{12} \\ h_{21} & h_{22} \end{bmatrix}. \tag{2.10}$$

The transmitter first transmits two different symbols x_1 and x_2 during the first

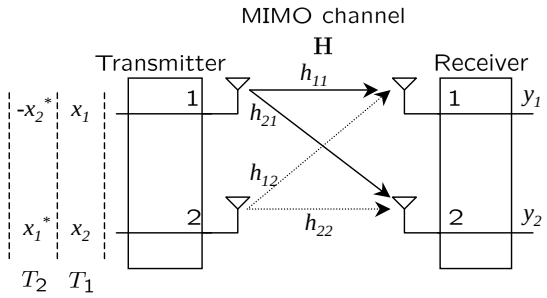

Figure 2.6: A basic diagram of the Alamouti encoding scheme for 2×2 MIMO system.

symbol period (T_1) from the first and second transmit antennas, respectively. In the second symbol period T_2, the same two symbols, x_1 and x_2, are encoded to x_1^* and $-x_2^*$, respectively, where * is conjugate. x_1^* is then transmitted from the "second" transmit antenna and $-x_2^*$ is transmitted from the "first" transmit antenna, which is why this scheme is called "space-time" coding. Since, Alamouti encoding transmits two symbols in two symbol periods, the transmission rate is just one symbol per symbol period, which does not increase the capacity of the MIMO link. We, however, can achieve diversity gain by constructing the received signals as follows. For the first symbol period, the received signal vector $\mathbf{y}_1$ can be expressed as

$$\mathbf{y}_1 = \sqrt{\frac{E_s}{2}} \begin{bmatrix} h_{11} & h_{12} \\ h_{21} & h_{22} \end{bmatrix} \begin{bmatrix} x_1 \\ x_2 \end{bmatrix} + \begin{bmatrix} n_1 \\ n_2 \end{bmatrix} \tag{2.11}$$

where n_1 and n_2 are zero mean circularly symmetric complex Gaussian random variable with variance N_0. For the second symbol period, the received signal vector $\mathbf{y}_2$ can be expressed as

$$\mathbf{y}_2 = \sqrt{\frac{E_s}{2}} \begin{bmatrix} h_{11} & h_{12} \\ h_{21} & h_{22} \end{bmatrix} \begin{bmatrix} -x_2^* \\ x_1^* \end{bmatrix} + \begin{bmatrix} n_3 \\ n_4 \end{bmatrix} \tag{2.12}$$

where n_3 and n_4 are zero mean circularly symmetric complex Gaussian random

variable with variance N_0. The receiver then stacks the two received signal vectors $\mathbf{y_1}$ and $\mathbf{y_2^*}$ and forms a new vector $\mathbf{y}$ to convert the channel $\mathbf{H}$ into $\mathbf{H}_{eff}$ as

$$\begin{aligned}\mathbf{y} = \begin{bmatrix} \mathbf{y}_1 \\ \mathbf{y}_2^* \end{bmatrix} &= \sqrt{\frac{E_s}{2}} \begin{bmatrix} h_{11} & h_{12} \\ h_{21} & h_{22} \\ h_{12}^* & -h_{11}^* \\ h_{22}^* & -h_{21}^* \end{bmatrix} \begin{bmatrix} x_1 \\ x_2 \end{bmatrix} + \begin{bmatrix} n_1 \\ n_2 \\ n_3^* \\ n_4^* \end{bmatrix} \\ &= \sqrt{\frac{E_s}{2}} \mathbf{H}_{eff}\mathbf{x} + \mathbf{n} \end{aligned} \tag{2.13}$$

where, $\mathbf{x} = [x_1\ x_2]^T$ and $\mathbf{n} = [n_1\ n_2\ n_3\ n_4]^T$. The important thing to notice is that the converted channel $\mathbf{H}_{eff}$ is orthogonal, which satisfies $\mathbf{H}_{eff}^H\mathbf{H}_{eff} = \|\mathbf{H}\|_F^2\,\mathbf{I}_2 = (|h_{11}|^2+|h_{12}|^2+|h_{21}|^2+|h_{22}|^2)\mathbf{I}_2$. Therefore, we can differentiate the two transmitted symbols by multiplying (2.13) by $\mathbf{H}_{eff}^H$ as follows

$$\mathbf{H}_{eff}^H\mathbf{y} = \sqrt{\frac{E_s}{2}}\,\|\mathbf{H}\|_F^2\,\mathbf{I}_2\mathbf{x} + \tilde{\mathbf{n}} \tag{2.14}$$

where, $\tilde{\mathbf{n}} = \mathbf{H}_{eff}\mathbf{n}$. The post-processing SNR of both symbols are the same and can be derived as

$$\eta_{Alamouti} = \frac{\|\mathbf{H}\|_F^2\,\rho}{2} \tag{2.15}$$

where, $\rho = \frac{E_s}{N_0}$. Equation (2.15) shows that Alamouti encoding enables the receiver to combine all four propagation paths constructively, which provides full diversity order of four without channel knowledge at the transmitter [5].

2.3 Related work

Recently, designing a MAC protocol for the physical layer that uses directional antennas, adaptive (or smart) antennas, and MIMO techniques has drawn great interest. In [14], Ko and *et al.* have proposed a MAC protocol, Directional MAC (D-MAC), that exploits the leverage of directional antennas to improve ad hoc network capacity by allowing adjacent simultaneous transmissions without causing interference to each other. D-MAC, however, requires tracking the physical location of itself and neighboring nodes, which is not a trivial problem. This problem is also observed in [15]. In [16], Masipuri and *et al.* have proposed a MAC protocol for directional antennas that obtains the direction of a desired destination by exchanging RTS/CTS packets in omni-directional mode and transmitting a DATA packet in that direction using directional antennas. Though this protocol reduces interference caused during a DATA packet transmission, it still blocks nodes near the transmitter and receiver since RTS/CTS packets are transmitted in all directions and thus does not increase the capacity of the network. Moreover, in [17], directional antennas are employed for the purpose of a transmission range extension to reduce the number of hops to the destination rather than increasing spatial reuse of the wireless channel. When the topology of the network is aligned, the performance of the proposed protocol, however, degrades due to high directional interference. In contrast, since the proposed MIMA-MAC protocol transmits packets in omni-directional mode and mitigates interference by using the MIMO's spatial multiplexing capability, it neither requires physical locations of the transmitter and neighboring nodes nor blocks neighboring transmitters.

While directional antenna schemes use a number of predetermined beam patterns, adaptive antennas adapt their beam pattern either to mitigate interference from neighboring transmissions or to minimize interference to other neighboring nodes. In [18], Bellofiore and *et al.* have proposed a MAC protocol for adap-

tive antennas based on the RTS-CTS-DATA-ACK exchange style MAC with two additional transmitter and receiver training sequences before a DATA packet transmission to form a beam pattern that maximizes the SINR (signal to interference plus noise ratio) at the receiver. As long as neighboring transmissions have different directions with the constructed beam pattern, the neighboring nodes can simultaneously communicate with their destination without causing interference to the ongoing transmission. Since this approach also exchanges RTS/CTS control packets in omni-directional mode and transmits DATA packets in directional mode, as in [16], it also has the same problem of limiting the capacity of the network.

Although work on MAC protocols for a physical layer that uses MIMO techniques has been limited, in [19], Demirkol and Ingram have proposed an algorithm that determines the maximum number of independent data streams for each transmitter in an ad hoc network of interfering MIMO links. For the algorithm to work, it requires knowledge of the distance to the nearest receiver, with which the transmitter might interfere. Using this basic idea, in [20], Sundaresan and *et al.* have proposed a MAC protocol that exploits the interference mitigating capability of MIMO for ad hoc networks with MIMO links. The authors have first designed a centralized stream control medium access (SCMA) protocol and then extended this design into a distributed SCMA protocol. The distributed SCMA protocol still requires most of the information required for the centralized SCMA protocol to work and thus it has to share significant amounts of information with one-hop and two-hop neighbors. In contrast to the distributed SCMA protocol, the proposed MIMA-MAC protocol does not require such information sharing. In [21], Hu and Zhang proposed a MAC protocol, SD-MAC (spatial diversity MAC), which utilizes spatial diversity for four-way handshaking (i.e. RTS-CTS-DATA-ACK) only to increase the diversity order of a link. In [22], Park and *et al.* proposed a MAC protocol, SPACE-MAC, which utilizes multiple antennas for beamforming to mitigate interference from neighboring

nodes and allow simultaneous transmissions in the same contention floor. Weight vectors are exchanged during the RTS/CTS handshaking. This protocol however has the unsolved hidden node problem we mentioned earlier.

Chapter 3

Mitigating Interference Using Multiple Antennas MAC Design

In this chapter, we present a MAC protocol design, Mitigating Interference Using Multiple Antennas MAC (MIMA-MAC), that utilizes the capability of MIMO system to solve the unfairness and throughput degradation problems of conventional CSMA/CA and RTS/CTS based MAC protocols.

3.1 Basic Idea

Figure 3.1 shows how wireless networks can employ multiple antennas in two different ways. One simple and obvious way to use multiple antennas is simply increasing the capacity or reliability of the links in the network and employing the conventional 802.11 MAC protocol as shown in Figure 3.1(a). In this case, each link is configured as a $M_t \times M_r$ MIMO channel, where $M_r = M_t = 2$. For example, in Figure 3.1(a), node 0 transmits two independent data streams to its destination, node 1, using both antennas in the spatial multiplexing mode. Assuming that the receiver has perfect channel information and the MIMO channel is a full-rank channel, which

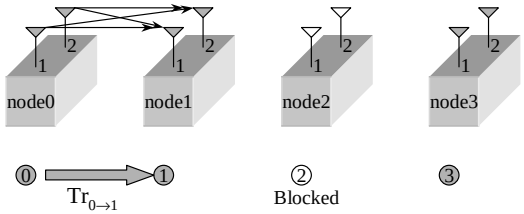

(a) The IEEE 802.11 MAC protocol

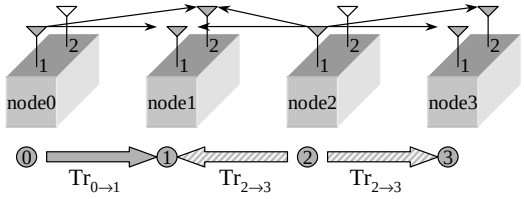

(b) The proposed MIMA-MAC protocol

Figure 3.1: Using multiple antennas in two different ways for an ad hoc network: (a) nodes using multiple antennas with the IEEE 802.11 MAC protocol simply to increase the performance of a single link, and (b) nodes using multiple antennas with the proposed MIMA-MAC protocol to mitigate the interference from the adjacent transmission to improve the performance of the network.

we will assume throughout this chapter, it can separate the two independent data streams successfully with two receive antennas and an interference cancellation algorithm, which increases the capacity of the link and thereby potentially increases the capacity of the network. This scheme, however, does not solve the unfairness and extreme throughput degradation (ETD) problems, since those problems are inherited from the 802.11-style MAC protocol.

In contrast to a MAC that employs multiple antennas to simply increase the performance of a single link, the proposed MIMA-MAC protocol employs multiple antennas to mitigate interference from the neighboring nodes to solve the unfairness and ETD problems. The basic idea of the proposed MIMA-MAC protocol is illustrated in Figure 3.1(b). In the MIMA-MAC protocol, the transmitters use one transmit antenna for data transmission and the receivers use two receive antennas to receive the two independent data streams. Thus, each link is configured as

1×2 single-input multiple-output (SIMO) channel. For example, in Figure 3.1(b), the transmitter of $Tr_{0\rightarrow1}$, node 0, only uses one of the two antennas for its data transmission and the receiver, node 1, uses both antennas for data reception. Since node 1 can receive and separate two independent data streams by employing a ZF or MMSE receiver, another adjacent transmitter, node 2, can transmit to its destination, node 3, using one transmit antenna without causing interference to node 1. Since the data stream from node 2 is destined to the other receiver node 3, it is considered to be interference to node 1. Therefore, unless the data stream from node 2 is destined to node 1, node 1 does not need to decode the data stream successfully but only need to differentiate it from the data stream from node 0. Thus, $Tr_{0\rightarrow1}$ and $Tr_{2\rightarrow3}$ can coexist in the network, which implies that fairness between the two traffic flows is guaranteed since neither blocks the other. Furthermore, since the receivers can receive the intended data stream in the presence of interference from the neighboring node, the ETD problem shown in Figure 2.4 is also resolved.

3.2 Protocol Design

We first present the basic requirements of the MIMA-MAC design. As shown in the previous subsection, M_t independent transmitters have to transmit independent data streams simultaneously and the receivers have to receive M_t independent data streams in the same time slot. Therefore, all the nodes that participate in the communication have to be *synchronized*, which is the weakness of the MIMA-MAC approach. We assume that all the nodes are synchronized, which is possible by employing the global positioning system (GPS) [35]. In [36], it is shown that GPS could provide a reference signal for time synchronization with an uncertainty of less than 20ns. It however might be infeasible to use GPS in an indoor environment because it requires a line-of-sight path between a node and a GPS satellite. In [37], Tang and Heath proposed a two step feedfoward solution for frequency offset and

timing synchronization for each transmit-receive antenna pair of a MIMO-OFDM (multiple-input multiple-output orthogonal frequency division multiplexing) system, which addresses the synchronization problem between the different transmit-receive antenna pairs. First, they estimate the frequency offset and timing based on training sequences and then correct the phase rotation and the timing of the data stream. Since the physical layer synchronization issue is out of our scope of research, we will not discuss this in further detail.

In order to provide the functionality that enables a node to receive M_t independent data streams from M_t independent transmitters simultaneously and to differentiate the received data streams successfully in a distributed manner, the MIMA-MAC protocol requires following basic structure:

- *Negotiation period*: Since the number of receive antennas, M_r, is fixed and limited, the number of independent data streams that the receiver can differentiate is also limited. Therefore, the nodes in the network have to negotiate with each other in a distributed manner and have to select the M_t transmitters satisfying $M_t \leq M_r$ so that the receiver can separate all the received data streams successfully.

- *Propagation channel estimation*: Since the receiver has to estimate the CSI of each propagation path from each transmit antenna to each receive antenna for data stream separation, there needs to be a number of periods in which a known training sequence is transmitted without any interference.

- *Simultaneous data transmission*: The channel between the M_t independent transmitters and the receiver with M_r receive antennas form M_t $(1 \times M_r)$ SIMO links. To make M_t $(1 \times M_r)$ SIMO links into an equivalent $M_t \times M_r$ MIMO link, the M_t independent data streams have to be transmitted in the same time slot.

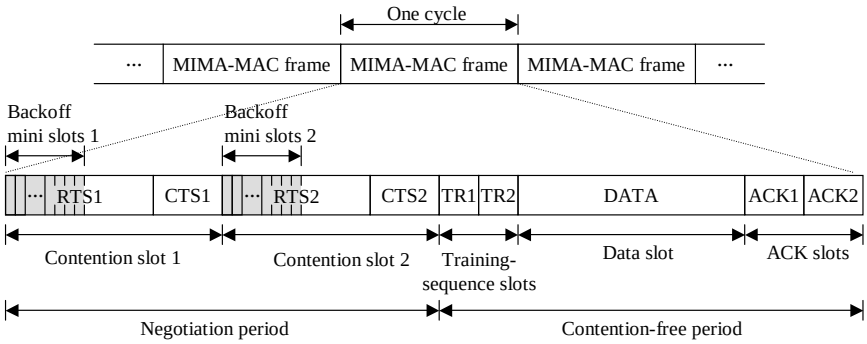

Figure 3.2: The basic structure of the proposed MIMA-MAC protocol.

- *Acknowledgment*: For reliable data transmission, there needs to be ACK packets sent from the receivers corresponding to the successfully received data packets.

The detailed structure of the MIMA-MAC protocol for the two antenna case, is illustrated in Figure 3.2. The MIMA-MAC protocol divides time into fixed size MIMA-MAC frame slots. The MIMA-MAC frame slot is divided into a *negotiation period* and a *contention-free period*. During the negotiation period, a number of transmitters contend with each other to acquire the channel resource. The negotiation period consist of two *contention* slots. The contention-free period consist of two *training-sequence* slots, a *data* slot, and two *acknowledgment* slots. The details of each time slot of the MIMA-MAC protocol are:

Contention slot

We extend the RTS/CTS structure of 802.11 for our contention slot design. There are two contention slots in a MIMA-MAC frame. Each contention slot is divided into a RTS and a CTS slot. To acquire the channel, a node that has data to send first transmits a RTS packet to its destination during the first RTS slot if the channel is idle. If the channel is busy, it defers and retries in the next contention slot. Upon receiving the RTS packet, the receiver replies with a CTS packet to the transmitter

during the CTS slot informing that the receiver is able to receive data from the transmitter. If, however, the RTS/CTS exchange fails during the first contention slot, the transmitter retries during the second contention slot. Only the transmitters that received CTS packets from their destinations during the contention slots are allowed to transmit their data packets in the data slot. Therefore, the number of contention slots limits the number of transmitters and thus the number of contention slots must be less than or equal to the number of receive antennas.

At the beginning of each RTS slot, all the nodes that have data to send will try to access the channel, and if they transmit at the same time, they will collide. To address this problem, we employ both *backoff* and *persistence* mechanisms similar to [38] as follows. Similar to the binary exponential backoff algorithm [2], which is employed in the 802.11 MAC, at the beginning of the RTS slot, we designed N backoff mini-slots to resolve the contention between the RTS packets. Since the size of a MIMA-MAC frame is fixed, the number of the backoff mini-slots is also fixed and has to be small in order to reduce the overhead of the backoff period but has to be large enough to resolve the contention. In our design, we use N=32 as is used for the minimum CW size in IEEE 802.11b [39]. The basic operation of the backoff algorithm is as follows. Provided that the node did not receive an ACK from its destination during the previous frame, which implies that the node had no data transmission or failed to transmit the data packet to its destination in the previous MIMA-MAC frame, the node that has data to transmit first randomly selects a mini-slot out of the N mini-slots and sends the RTS packet at the start of the selected mini-slot if the channel is idle. If, however, the node successfully received an ACK from its destination during the previous frame, the node transmits the RTS packet at the start of the *last* mini-slot, which forces the node to have the lowest priority among the transmitters and thus gives the other nodes a higher probability of accessing the channel. This is similar to the IEEE 802.11 MAC protocol, in

which a node that successfully received an ACK has to defer a DIFS period and one additional contention window period with the minimum CW [2].

If, however, the density of nodes is high, the fixed small number of backoff mini-slots is insufficient to resolve collisions. Therefore, we propose a simple *adaptive collision avoidance (ACA)* algorithm. The basic operation of the ACA algorithm is as follows. First, every node has its transmission (or persistence) probability p with the initial value of $p = 1$. If a node fails to exchange the RTS/CTS packets with its destination during one MIMA-MAC frame, the node decreases the transmission probability to half the previous value to decrease the channel access rate of the node. If, however, the node successfully exchanges RTS/CTS packets, the transmission probability is increased by α times the previous value, where $1 < \alpha < 2$. If α is too close to 1, the transmitter will track the contention in the network too slowly. On the other hand, if α is too close to 2, the transmitter will increase the transmission probability too fast, which might again cause contention in the network. In our design, we used $\alpha = 1.5$. This is similar to the TCP congestion control algorithm, which employs an additive-increase-multiplicative-decrease (AIMD) mechanism to adaptively control the congestion in a network [40].

In contrast to the high density case, if there is no contender near the transmitter or receiver, it would be better to transmit using both transmit antennas to increase the link capacity. This would be possible by competing in the second contention slot with a low priority when the transmitter succeeded in the first contention slot or by receiving information from the receiver about whether or not there is other transmission near the receiver.

Training-sequence slot

After the negotiation period, the selected transmitters have to transmit a known training sequence before the data transmission to provide the CSI of each propa-

gation path to the receiver. There are two training sequence slots, TR1 and TR2, in a MIMA-MAC frame. The training sequences must be transmitted without any interference so that the receiver can estimate the correct channel response of the propagation paths. Therefore, only one transmitter is allowed to transmit the training sequence during one training-sequence slot at a time. TR1 and TR2 are allocated to the transmitters that successfully exchanged RTS and CTS packets during the first and the second contention slots, respectively. Alternatively, we could also use a single training-sequence slot but use two orthogonal (or uncorrelated) training sequences, TS1 and TS2, in which case the contention slot determines which sequence. Therefore, the index of the contention slot that the transmitter used for the RTS/CTS control packet exchange determines which training sequence slot (or training sequence) it has to use for the training sequence transmission.

Data slot

After the training sequence period, the transmitters transmit their data packets in the data slot simultaneously. Since, the CSI of each propagation path is estimated during a training sequence slot, a receiver can separate two independent data packets by employing an interference cancellation algorithm such as a ZF receiver or a MMSE linear receiver [41]. If the post-processed signal to noise ratio (SNR) [5] of the data packet that is destined for the receiver is above the threshold-SNR that guarantees a certain level of bit error probability, the separated data packet can be decoded without error. Otherwise the data packet is discarded. Moreover, if the number of simultaneously received data packets is greater than the number of receive antennas, the receiver cannot separate the data packets correctly, which could be considered as "collision", and thus all the received packets are discarded.

Acknowledgment (ACK) slot

The ACK packet, which corresponds to the received data packet, is replied back to the transmitter to inform it that the receiver has received the data packet correctly. As shown in Figure 3.2, the two separate ACK slots, ACK1 and ACK2, accommodates the two ACK packets that corresponds to the two simultaneously transmitted data packets. ACK1 and ACK2 are allocated to the receivers that successfully exchanged the RTS/CTS packets in the first and second contention slots, respectively, similarly to the allocation scheme that we used for the training-sequence slots.

3.3 Operation

As an example, we describe the basic operation of the proposed MIMA-MAC protocol for the network shown in Figure 3.1(b), where node 0 transmits data to node 1, and node 2 transmits data to node 3, simultaneously. The transactions between the nodes are illustrated in Figure 3.3. In this scenario, we assume that the two transmitters, node 0 and node 2, transmit two RTS packets, RTSa and RTSb, almost at the same time, and the transmission from node 0 does not interfere node 3 due to the distance between the two nodes. Since node 1 is within the transmission range of node 0 and node 2, the two RTS packets will collide at node 1, whereas node 3 receives RTSb from node 2 without any interference from node 0. Therefore, node 2 and node 3 successfully exchange RTSb and CTSb in the first contention slot and stay silent in the second contention slot. In the second contention slot, node 0 and node 1 exchange RTSa and CTSa successfully. Thus, TR1 and ACK1 are allocated to node 2 and node 3, respectively, and TR2 and ACK2 are allocated to node 0 and node 1, respectively.

After the negotiation period, node 2 first transmits the training sequence to the receiver, node 3, during TR1. Node 3 estimates the CSI of the two propagation

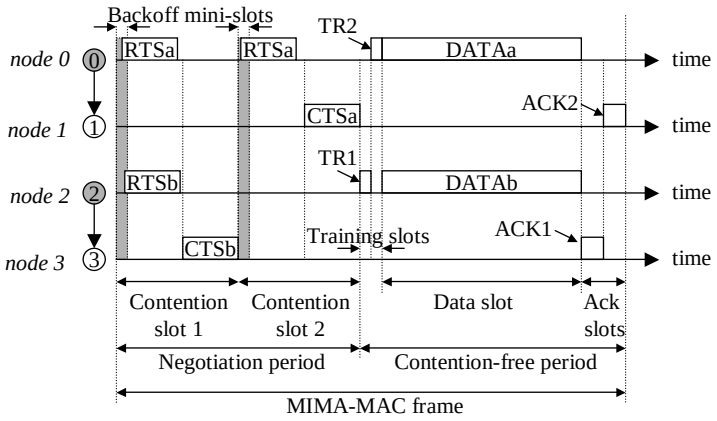

Figure 3.3: The time line of the proposed MIMA-MAC protocol for the ad hoc network consisting of four nodes.

paths between node 2 and node 3. At the same time, node 1 also receives the training sequence from node 2 and estimates the CSI of the two propagation paths between node 1 and node 2. Similarly, during TR2, node 0 transmits the training sequence and node 1 estimates the CSI of the propagation paths between node 0 and node 1. Therefore, after the two training-sequence slots, node 1 has obtained all the CSI of four paths from node 0 and node 2, which is required for separating the data packet from node 0 and the interference from node 2. After the training sequence period, the two transmitters transmit their data packets, DATAa and DATAb, simultaneously during the data slot period. Node 1 receives two independent data packets and separates the data packets using a ZF or MMSE receiver. Since node 3 is located far enough from node 0, node 3 receives DATAb without any or negligible interference. Therefore, both node 1 and node 3 receive data packets from node 0 and node 2 simultaneously without collision. After receiving the data packets, the corresponding ACK packets are replied back to the transmitters in the allocated ACK slots.

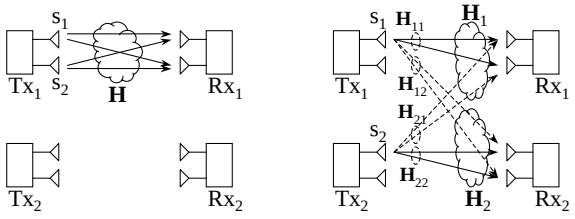

(a) 802.11 MAC (b) MIMA-MAC

Figure 3.4: Illustration of the 802.11 system and the MIMA-MAC system for $M_t = M_r = 2$.

3.4 Theoretical Analysis and Comparison

To evaluate the performance of the proposed MIMA-MAC protocol, we first analyze the theoretical capacity of the MIMA-MAC system and compare it with the system using an 802.11 style MAC with spatial multiplexing. We investigate the capacity of the network shown in Figure 3.4. The network consists of two transmitters each with M_t antennas and two receivers each with $M_r (\geq M_t)$ antennas. All the nodes are assumed to be within each other's carrier sensing range. In other words, all the nodes are within the same contention floor.

3.4.1 Spatial multiplexing + IEEE 802.11 style MAC

According to the CSMA/CA mechanism, in the 802.11 system, when one transmitter detects (or hears) the other node's transmission, it defers its transmission to avoid the possible collision. Therefore, in this network configuration, there can be only one active transmitter at a time and thus the aggregate transmit power of the network is limited to the transmit power of the single active transmitter.

For the network configuration shown in Figure 3.4(a), we can express the $M_r \times 1$ received signal vector $\mathbf{y}_1$ of the first receiver Rx_1 as

$$\mathbf{y}_1 = \sqrt{\frac{E_s}{M_t}}\mathbf{H}\mathbf{s} + \mathbf{n} \tag{3.1}$$

where, E_s is the signal energy, M_t is the number of transmit antennas, $\mathbf{H}$ is the $M_r \times M_t$ MIMO channel between the transmitter and receiver, $\mathbf{s} = [s_1, s_2, ..., s_{M_t}]^T$ is the $M_t \times 1$ signal vector, and $\mathbf{n} = [n_1, n_2, ..., n_{M_r}]^T$ is the $M_r \times 1$ zero mean circularly symmetric complex Gaussian (ZMCSCG) noise vector with the covariance matrix $\mathcal{E}[\mathbf{n}\mathbf{n}^H] = N_0\mathbf{I}_{M_r}$. ^{H} denotes the Hermitian. Assuming that the transmitter does not have channel information, we choose the transmission covariance matrix $\mathcal{E}[\mathbf{s}\mathbf{s}^H] = \mathbf{I}_{M_t}$ [5]. As shown in [5, 34] and also in Section 2.2, when we use a zero-forcing (ZF) receiver for interference cancellation, the k th data stream's post-processing signal-to-noise ratio (SNR) can be expressed as

$$\eta_k = \frac{\rho}{M_t} \frac{1}{[(\mathbf{H}^H\mathbf{H})^{-1}]_{kk}} \tag{3.2}$$

where, ρ is $\frac{E_s}{N_0}$.

Assuming that $\mathbf{H}$ has full column rank, i.e. rank($\mathbf{H}$)=M_t, the link between Tx_1 and Rx_1 is equivalent to M_t parallel channels each with η_k post-processing SNR. The ZF receiver first separates M_t data streams and then decodes each data stream independently. As Paulraj described in [5], since a packet is decoded correctly when the signal with the worst post-processing SNR is decoded correctly, if we assume that the transmitter does not have the channel information, the statistics of the system is governed by the worst post-processing SNR's statistics. In [34], Heath also showed that the performance of linear systems is governed by the smallest post-processing SNR. Therefore, the capacity of the system may be expressed as [5, 42]

$$C_{\text{SM}} = M_t \times \min_{k \in \{1,...,M_t\}} \{\log_2(1 + \eta_k)\}. \tag{3.3}$$

Notice that although there are two links (link Tx_1-Rx_1 and link Tx_2-Rx_2) in the network, we are only able to use one link at a time due to the mechanism of the 802.11 style MAC. This clearly shows that the network resources are not

fully utilized, since only half of the antennas and half of the transmit power of the network is being used at a time.

3.4.2 Spatial multiplexing + MIMA-MAC

Now we analyze the proposed MIMA-MAC system. Assuming that M_t is an even number and since the MIMA-MAC is designed to allow at most two active links in the same contention floor, the transmitters use only half the transmit antennas ($\frac{M_t}{2} \geq 1$) for data transmission and the receivers use all the M_r ($\geq M_t$) receive antennas. Therefore, in the MIMA-MAC system, we can have at most two simultaneous transmissions in the network at a time. Note that since there are two active transmitters in the same contention floor, if we assume that all the nodes have the same maximum transmit power, the aggregate transmit power of the network utilized by the MIMA-MAC system becomes double the aggregate transmit power of the network utilized by the 802.11 system.

For the network shown in Figure 3.4(b), the $M_r \times 1$ received signal vector $\mathbf{y}_i$ of the i th receiver Rx_i can be expressed as

$$\mathbf{y}_i = \sqrt{\frac{2E_s}{M_t}}\mathbf{H}_i\mathbf{s} + \mathbf{n}_i \tag{3.4}$$

where, $\mathbf{H}_i = [\mathbf{H}_{1i}\ \mathbf{H}_{2i}]$, $\mathbf{H}_{1i}$ is the $M_r \times \frac{M_t}{2}$ channel matrix between Tx_1 and Rx_i, $\mathbf{H}_{2i}$ is the $M_r \times \frac{M_t}{2}$ channel matrix between Tx_2 and Rx_i. The $M_t \times 1$ transmitted signal vector $\mathbf{s} = [\mathbf{s}_1^T\ \mathbf{s}_2^T]^T$, where $\mathbf{s}_i$ is the $\frac{M_t}{2} \times 1$ signal vector transmitted from the i th transmitter Tx_i, and $\mathbf{n}_i = [n_{i1}, n_{i2}, ..., n_{iM_r}]^T$ is the $M_r \times 1$ ZMCSCG noise vector at the i th receiver Rx_i, for $i \in \{1, 2\}$.

Notice that from (3.4) and (3.1), the aggregate transmit power of the proposed system is twice that of the 802.11 system. This is because, in the MIMA-MAC system, there could be two active transmitters each transmitting signals with its maximum transmit power using half of their transmit antennas, whereas in the

802.11 system, there could be only one active transmitter at a time using all of its transmit antennas.

Again, assuming that we are using a ZF receiver, the k th data stream's post-processing SNR at the i th receiver, $\eta_{i,k}$ can be expressed as

$$\eta_{i,k} = \frac{2\rho}{M_t} \frac{1}{[(\mathbf{H}_i^H \mathbf{H}_i)^{-1}]_{kk}} \tag{3.5}$$

where, $i \in \{1, 2\}$ and $k \in \{1, 2, ..., M_t\}$. For Rx_1, only the first half of the received data streams ($k = 1, 2, ..., \frac{M_t}{2}$) are destined for the receiver, and for Rx_2, only the second half of the data streams ($k = \frac{M_t}{2} + 1, ..., M_t$) are destined for the receiver. Therefore, similar to (3.3), assuming that $\mathbf{H}_i$ has full column rank, the attainable capacity of the network, C_{MIMA}, can be expressed as

$$\begin{aligned} C_{\mathrm{MIMA}} &= \underbrace{\frac{M_t}{2} \times \min_{k \in \{1, ..., \frac{M_t}{2}\}} \{\log_2(1 + \eta_{1,k})\}}_{\text{link Tx}_1\text{-Rx}_1} \\ &+ \underbrace{\frac{M_t}{2} \times \min_{k \in \{\frac{M_t}{2}+1, ..., M_t\}} \{\log_2(1 + \eta_{2,k})\}}_{\text{link Tx}_2\text{-Rx}_2}. \end{aligned} \tag{3.6}$$

The above result shows that the capacity of the network increases as the number of antennas increases. Moreover, the increased number of the simultaneous transmissions increases the aggregate transmit power of the network and eventually increases the network capacity. Furthermore, we may easily extend the above result (3.6) to the case where we allow $N(> 2)$ simultaneous transmissions by increasing the number of the contention slots of the MIMA-MAC. Assuming M_t is divisible by N, for N simultaneous transmissions the k th data stream's post-processing SNR at the i th receiver, $\eta_{i,k}(N)$ can be expressed as

$$\eta_{i,k}(N) = \frac{N\rho}{M_t} \frac{1}{[(\mathbf{H}_i^H \mathbf{H}_i)^{-1}]_{kk}} \tag{3.7}$$

where, $\mathbf{H}_i = [\mathbf{H}_{1i}... \mathbf{H}_{Ni}]$, $\mathbf{H}_{pi}$ is the $M_r \times \frac{M_t}{N}$ channel matrix between Tx_p and Rx_i, $1 \leq p \leq N$. The attainable capacity of the network, $C_{\mathrm{MIMA}}(N)$ can be expressed as

$$C_{\mathrm{MIMA}}(N) = \frac{M_t}{N} \sum_{i=1}^{N} \left\{ \min_{k \in \{\frac{M_t}{N}(i-1)+1 ... \frac{M_t}{N} i\}} \{\log_2(1 + \eta_{i,k}(N))\} \right\}. \tag{3.8}$$

3.4.3 Numerical results

Using the results derived above, we compare the ergodic capacity of the MIMA-MAC system with those of the 802.11 system by varying the received SNR, ρ, from 0dB to 30dB and by varying the number of antennas M_t=M_r= 2, 4, and 8.

We assume that all the neighboring transmitters and receivers are evenly spaced and thus the distance between Tx_2 and Rx_1 (or Tx_1 and Rx_2) is $\sqrt{2}$ times longer than the distance between Tx_1 and Rx_1. Assuming free-space propagation with a path-loss exponent of 2 [26], for Rx_1, the signal from Tx_2 (i.e. interference) has half the power of that from Tx_1.

We assume an uncorrelated Rayleigh fading channel. For the channel between Tx_1 and Rx_1 (or Tx_2 and Rx_2), each entry of the channel is assumed to be a ZMCSCG random variable with variance of 1, i.e. $\mathcal{CN}$(0,1). For the channel between Tx_1 and Rx_2 (or Tx_2 and Rx_1), taking the path-loss effect into account, each entry of the channel is assumed to be a ZMCSCG random variable with variance of $\frac{1}{2}$, i.e. $\mathcal{CN}(0, \frac{1}{2})$.

Figure 3.5 shows the comparison of the ergodic capacity of the MIMA-MAC system with that of the 802.11 system. For both systems, the ergodic capacity increases as ρ increases and as M_t and M_r increase. The results show that the MIMA-MAC system has higher spectral efficiency than the 802.11 system and the gain increases as M_t and M_r increase. For example, for M_t=M_r=2 and ρ=20dB, the ergodic capacity of the MIMA-MAC system is approximately 3 bits/sec/Hz higher than that of the 802.11 system. The gain increases to 5.1 bits/sec/Hz for

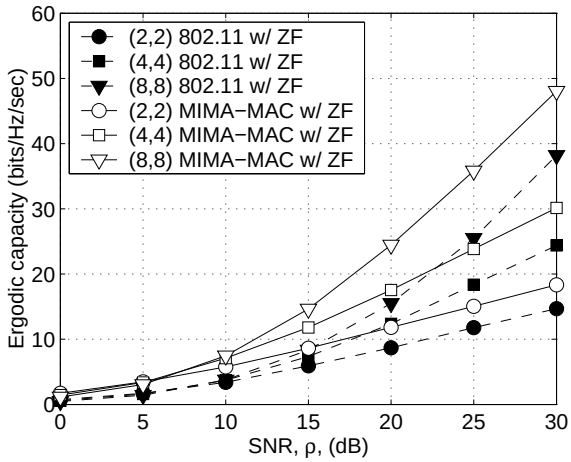

Figure 3.5: Comparison of erodic capacity of the 802.11 system and the MIMA-MAC system both with the zero-forcing (ZF) receiver. (M_t,M_r) indicates the number of transmit and receive antennas.

M_t=M_r=4 and to 9 bits/sec/Hz for M_t=M_r=8. As expected from (3.2) and (3.5), this is because the MIMA-MAC system has twice the active transmitters of the 802.11 system and since each transmitter of the MIMA-MAC system uses only half of its transmit antennas, it can transmit signals with twice the transmit power of the 802.11 system. The simulation results show that the systems using a ZF receiver suffers from low capacity in the low SNR region due to the noise enhancement of a ZF receiver. We can improve this by using MMSE receiver. Figure 3.6 shows the simulation results for the systems using an MMSE recever. The simulation results show that the performance of the systems in the low SNR region greatly improves by using the MMSE receiver.

3.5 Simulation Results and Performance Analysis

We implemented the MIMA-MAC protocol in the *ns-2* network simulator [23]. We measured the total throughput of a network and the fairness between two neighboring traffic flows. The performance of the MIMA-MAC system, which uses the

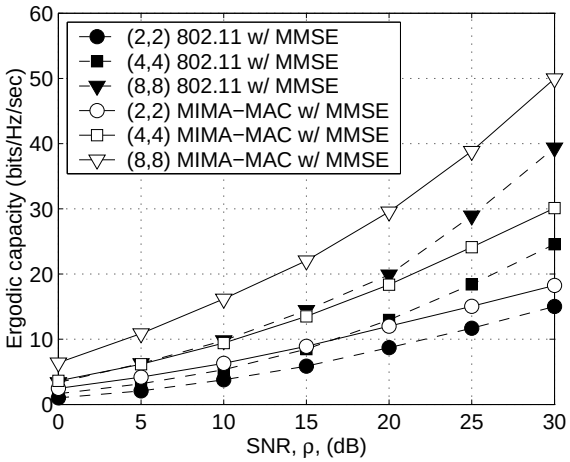

Figure 3.6: Comparison of erodic capacity of the 802.11 system and the MIMA-MAC system with an MMSE receiver. (M_t,M_r) indicates the number of transmit and receive antennas.

MIMA-MAC protocol with two antennas, is compared with that of the 802.11 system, which uses the IEEE 802.11 MAC protocol with a single antenna.

3.5.1 Simulation environment

First we discuss the simulation environment we used for our proposed cross-layer MAC design. We implemented our proposed MIMA-MAC design in ns-2 [23]. For the simulations, we assume that perfect channel knowledge can be obtained by transmitting training sequences to the receiver. The basic structure of the simulator is as follows.

When a node receives a packet, it first calculates the propagation path-loss between the transmitter and receiver and also generates a MIMO channel matrix between the two nodes. The packet has a pointer to the generated channel matrix so that the MAC protocol can use this channel matrix for determining whether simultaneously received packets can be separated successfully. For an uncorrelated Rayleigh fading channel simulation, each entry of the channel matrix is generated

from a ZMCSCG number generator. If the packet's received power is greater than the carrier sense threshold, the packet is forwarded to the MAC protocol for further processing; otherwise it is discarded.

Since the MIMA-MAC protocol is designed so that each phase of the protocol is synchronized with other nodes and the size of each time slot (e.g. RTS or CTS slot) is fixed, we use a slot-timer for each slot, which has a timeout value set to the MIMA-MAC frame period. When the slot-timer expires, the slot-timer restarts with the same timeout value so that it fires for every MIMA-MAC frame period and the MAC protocol checks whether it has any packets to send during this time slot. For example, when the RTS slot-timer fires at the start of each RTS slot, the protocol checks whether there is a RTS packet to transmit or not. This applies to all other slots.

When a packet is received at a node, in the MAC layer, the simulator first figures out in which time slot the packet has arrived. For example, it checks whether the packet is received in the control slot (e.g. RTS or CTS or ACK slot) or the DATA slot. If the packet is received during one of the control slots, it checks whether the receiver is in the idle state. If the receiver is in the idle state, the simulator starts a receive-timer that has a timeout value, which is determined by the size and the transmission rate of the packet; otherwise the receiver checks if the receiver is currently receiving another control packet. The receive-timer emulates the transmission time required for the packet transmission. If there is another control packet that is being received, the receiver compares the two packets' received power. If the packet which was received later has the received power much lower (e.g. 10dB lower) than that of the previously received control packet, the later packet is ignored and discarded; otherwise the two packets are assumed collide with each other and thus both packets are discarded. When there is no collision, the receiver waits until the receive-timer expires (waits until the packet reception is completed). When

the receive-timer expires, the receiver starts parsing the received packet and then processes the received packet according to the MAC protocol. For example, when a RTS packet is received and it's received power is above the reception threshold and it is destined for the receiver, the receiver starts to generate a CTS packet and waits for the CTS slot-timer to fire so that it can transmit the CTS packet to the transmitter.

If a packet is received in the DATA slot, the receiver counts the number of received data packets in the DATA slot. If the number of packets exceeds the number of the receive antennas, the receiver discards all the data packets received in the DATA slot. If there is only one packet received in the DATA slot, similar to the control packet process, the receiver sets the receive-timer and waits for the timer to expire. If, however, there are two data packets received in the DATA slot, first the receiver checks if the data packets are using different training-sequence slots. If they are using the same training-sequence slot, the receiver assumes that it does not have the correct channel information and thus cannot separate the simultaneously received data packets. Therefore, in this case, the receiver discards both data packets. When the data packets are using different training-sequence slots, the receiver tries to differentiate the data packets using a zero-forcing receiver. The receiver first retrieves the channel matrix from each of the data packets. Recall that the pointer to the channel matrix is in each packet. Using the result of the post-processing SNR of the ZF receiver [5], the receiver calculates the post-processing SNR of each data packet. If the calculated post-processing SNR is higher than the reception threshold, the data packet is forwarded to the upper layer of the protocol stack after checking the MAC address and generates an ACK packet with the destination address of the data packet's transmitter; otherwise the data packet is discarded.

When the transmitter receives an ACK packet destined for itself after sending a data packet to its destination, the transmitter clears its buffer, in which it stored

the transmitted data packet for retransmission. The MAC protocol also signals the queue at the upper layer, which buffers data packets to transmit, asking for another data packet to transmit in the next MAC frame. If the transmitter does not receive the ACK packet from the destination during the allocated ACK slot, the same data packet, which was transmitted earlier, is retransmitted in the next MAC frame.

3.5.2 Simulation setup

The following describes the setup we used for the simulations.

Channel model

In our simulations, we use two channel models: an *ideal* channel model and an *uncorrelated complex Gaussian* channel model [5], which is generally known as a *Rayleigh* fading channel model. We define an ideal channel as an orthogonal MIMO channel [5], which satisfies $\mathbf{H}\mathbf{H}^H = \mathbf{H}^H\mathbf{H} = c\mathbf{I}$, where $\mathbf{H}$ is a channel matrix between the two transmitters and receiver and c is a constant. For the ideal channel model, we use $c = 1$ to only consider the path-loss effect due to the distance between the nodes but no packet drops due to fading. Therefore, for the MIMA-MAC system, if CSI is perfectly known to the receiver, two independent data streams over an ideal channel are separated perfectly. The purpose of using an ideal channel is to investigate only the effect of interference from neighboring nodes on the performance of the system by excluding the effect of packet drops due to fading and detection schemes. A Rayleigh fading channel model is used in order to simulate the system over a more realistic environment. We assume rich scatters near the nodes and no line-of-sight (LOS) between the transmitter and receiver, which makes each entry of the Rayleigh fading channel matrix to be an uncorrelated complex Gaussian random variable with zero mean and variance of 1, i.e. $\mathcal{CN}(0, 1)$ [32, 33]. In this model, we also consider the path-loss due to the distance between the transmitter and receiver.

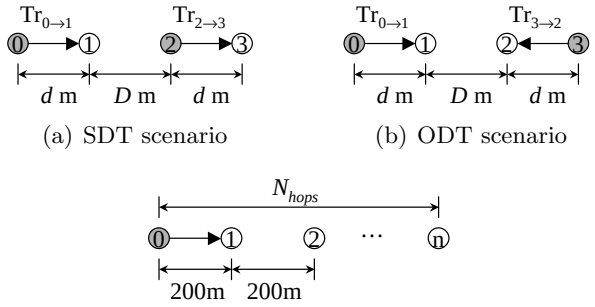

Figure 3.7: Network topology and traffic configurations.

Moreover, we assume that the channel is quasi-static and thus the channel response of the propagation path varies slowly over time and does not change within a packet.

Network configuration

Figure 3.7 shows the network and traffic configurations that were used for the simulations. We use three scenarios for the simulations: the same direction traffic (SDT) scenario, the opposite direction traffic (ODT) scenario, and the multi-hop SDT scenario as shown in Figure 3.7(a), Figure 3.7(b), and Figure 3.7(c), respectively. For the SDT and ODT scenarios, we measure the system performance by varying the distance D between the two nodes, node 1 and node 2, to investigate the effect of neighboring traffic flows on network performance. For an ideal channel model, the distance between the transmitter and receiver, d, is set to 200m, whereas for a Rayleigh fading channel model, d is set to 100m to increase the reliability of the link so that the effect of packet drops due to fading on the system performance is reduced. For the multi-hop SDT scenario, the throughput of the network is measured by varying the number of hops between the source and destination, N_{hops}, to investigate the effect of interference from neighboring nodes along the route to the destination. In the multi-hop SDT scenario, all the neighboring nodes are equally spaced by 200m.

Carrier frequency	2.4 GHz
Bandwidth	2 MHz
Data rate	1 Mbps
Transmit power	24.5 dBm
Reception threshold	-63.5 dBm
Carrier sensing threshold	-70.4 dBm
Signal-to-interference ratio threshold	10 dB
Number of antennas per node	2
Path-loss exponent	2
Transmission range	250 m
Carrier sensing range	550 m

Table 3.1: Physical layer parameters

Traffic model

We use the constant-bit-rate (CBR) traffic model for the simulations to show the impact of the MAC layer protocol on the performance of the network. In order to make the traffic flows fully consume the channel resource, the packet size and the packet interval of the CBR traffic are set to 2048 bytes and 20.5 msec respectively. This traffic model can be used for modelling traffic that has a large size of data for a long period of time such as image data streaming. To support CBR traffic, the user datagram protocol (UDP) is used in the transport layer, which excludes the effect of the complex dynamic of a transport layer protocol such as TCP on the system performance.

Physical layer parameters

The parameters of the physical layer are listed in Table 3.1. Most of these parameters are from the *ns-2* simulator, which is based on the IEEE 802.11b specification, except the number of antennas. Moreover, a ZF receiver, which has the worst performance, is used to obtain a lower bound on system performance. The transmission power is set to 24.5dBm and the path-loss exponent is set to 2. In order to make the

MIMA-MAC frame	20.788 msec
Contention slot	984 μsec
RTS slot	676 μsec
CTS slot	308 μsec
Training sequence slot	84 μsec
Data slot	18.036 msec
ACK slot	308 μsec
Number of backoff mini-slots	32
Mini-slot time	10 μsec
Overhead $(\frac{\text{Totalframe}-\text{Dataslot}}{\text{Totalframe}} \times 100)$ %	13.2%

Table 3.2: MIMA-MAC parameters

transmission range and the carrier sensing range to be 250m and 550m, respectively, the reception threshold and the carrier sensing threshold are set to -63.5dBm and -70.4dBm, respectively. The interference range is calculated from (2.1) with the parameters in Table 3.1. For d=100m, the interference range becomes 316m. Since ns-2 assumes that the receiver cannot sense a packet transmission if the transmitter is out of the carrier sensing range, when the interference range is larger than the carrier sensing range, the interference range is approximated to the carrier sensing range [23]. Therefore, for d=200, the interference range becomes 550m.

MIMA-MAC protocol parameters

The parameters for the MIMA-MAC protocol are listed in Table 3.2. The size of the RTS slot is determined by the sum of the total duration of the backoff mini-slots and the time required for transmitting a RTS packet at a data rate of 1Mbps. The number of backoff mini-slots is set to 32 and the duration of each mini-slot is set to $10\mu sec$ which makes the total duration of the backoff mini-slots $320\mu sec$. The RTS packet is 44 bytes long based on the IEEE 802.11b specification and thus it requires $352\mu sec$ to transmit the packet at 1Mbps. Considering $4\mu sec$ for a guard interval, the RTS slot becomes $676\mu sec$. Similarly, based on the size of the CTS

packet, which is 38 bytes long, it requires $308\mu sec$ to transmit the CTS packet with the guard interval ($4\mu sec$). This is also the case for the ACK slot. We assume that each training sequence slot is 10 bytes long, which equals to $80\mu sec$, so the training sequence slot becomes $84\mu sec$ long with the guard interval. To reduce the overhead of the negotiation period in a MIMA-MAC frame, the size of the data slot is set to 18.036msec. The overhead of the control packets and backoff mini-slots is approximately 13.2%. In the case of a 1Mbps transmission rate, approximately 2200 bytes of application data can be transmitted in a MIMA-MAC frame. The maximum backoff time is determined so that there could be only one RTS transmission in each RTS slot.

Routing protocol

To exclude the effect of a routing protocol to the system performance, we use static routing, which uses a fixed predetermined route for packet transmission, throughout the simulations in this chapter.

Performance metrics

The performance of the MIMA-MAC system is compared with that of the 802.11 system using two metrics: the *fairness* between the two traffic flows and the *total throughput* of the flows. Throughput is measured in bits/sec and fairness is measured by a new metric, the *fairness-ratio* (FR), which is defined as

$$FR = 1 - \frac{|Th_A - Th_B|}{Th_A + Th_B} \tag{3.9}$$

where Th_A and Th_B denote the throughput of $Tr_{0\rightarrow 1}$ and the throughput of $Tr_{2\rightarrow 3}$ for the SDT scenario (or $Tr_{3\rightarrow 2}$ in case of the ODT scenario) respectively. When two traffic flows are perfectly fair, FR becomes 1, whereas if the two traffic flows are extremely unfair, FR approaches 0.

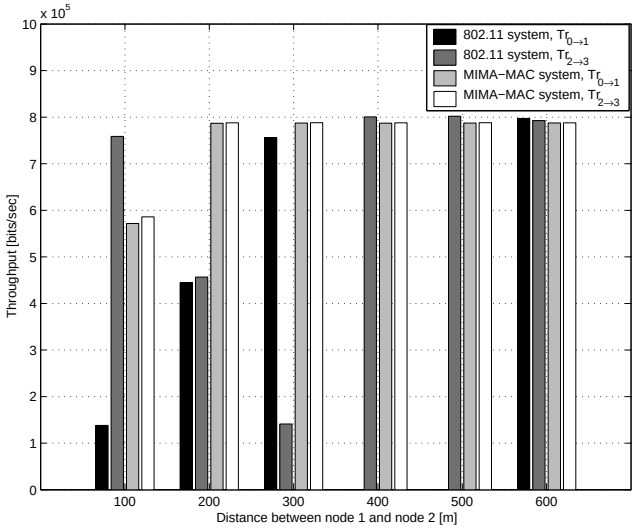

(a) Comparison of throughput

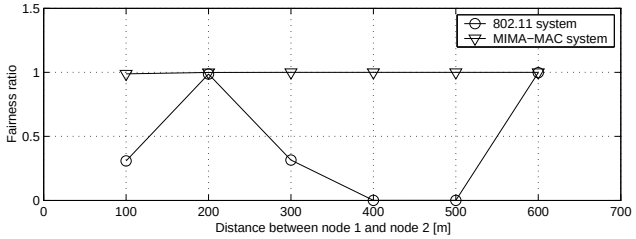

(b) Comparison of fairness-ratio

Figure 3.8: The performance comparison between the MIMA-MAC system and the 802.11 system over an ideal channel in the SDT scenario.

3.5.3 The SDT scenario

We first compare the throughput of the MIMA-MAC system and that of the 802.11 system over an ideal channel model and a Rayleigh fading channel model in the SDT scenario shown in Figure 3.7(a). The throughput of each traffic flow and the fairness between the two traffic flows are measured by varying the distance D from 100m to 600m.

D m	100	200	300	400	500	600
node: $0 \leftrightarrow 2$	C[a] /I[b]	C/I	C/I	O[c]	O	O
node: $0 \leftrightarrow 3$	C/I	O	O	O	O	O
node: $1 \leftrightarrow 2$	T[d]	T	C/I	C/I	C/I	O
node: $1 \leftrightarrow 3$	C/I	C/I	C/I	O	O	O

[a]C: The two nodes are within R_{CS} of each other.
[b]I: The two nodes are within R_I of each other.
[c]O: The two nodes are out of R_{CS} of each other.
[d]T: The two nodes are within R_{TX} of each other.

Table 3.3: Relation between the nodes in the SDT and ODT scenarios over an ideal channel (d=200m)

Ideal channel model

Figure 3.8 shows the simulation results over an ideal channel model in the SDT scenario. Figure 3.8(a) compares the throughput of each traffic flow of the MIMA-MAC system and that of the 802.11 system and Figure 3.8(b) compares the FR of both systems. The simulation results clearly show that the 802.11 system experiences severe unfairness between $Tr_{0\rightarrow1}$ and $Tr_{2\rightarrow3}$ in the case where D is close enough to cause interference to each other's communication, whereas the MIMA-MAC system guarantees fairness between the two traffic flows regardless of D. The FR of the MIMA-MAC system is approximately 1, which indicates that the MIMA-MAC system has perfect fairness between the two traffic flows in the SDT scenario. The throughput of the MIMA-MAC system is slightly degraded at D=100m because both transmitters try to resolve collisions during the negotiation period by decreasing the transmission probability p.

Because the exact explanation of why the 802.11 system performs poorly is not intuitive and depends on details of the interaction between the nodes, it is worth taking a closer look at these results. A key to detailed understanding is knowing within which of the possible regions, R_{TX}, R_{CS} and R_I, a pair of nodes fall, since this will determine how they interact. Table 3.3 summarizes these relationships over

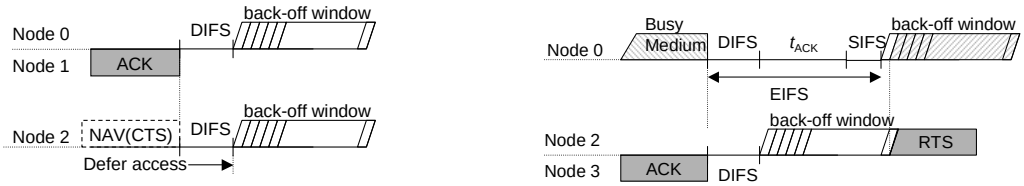

(a) After the transmission of Node 0

(b) After the transmission of Node 2

Figure 3.9: The SDT scenario, D=100m.

an ideal channel for D from 100m to 600m, where T, C and I denote that the two nodes are within R_{TX}, R_{CS}, and R_I of each other respectively, and O denotes that the two nodes are out of R_{CS}. Note that the relation between R_{TX}, R_{CS}, and R_I can be represented as $R_{TX} < R_{CS} \approx R_I$ from Table 3.1 and (2.1). Using Table 3.3, we analyze the simulation results by investigating which one of the two transmitters has a higher chance of accessing the channel for the two possible cases: after the end of a $Tr_{0\rightarrow1}$ transmission and after the end of a $Tr_{2\rightarrow3}$ transmission. The unfairness observed at D=100 and 300m is due to a side effect of the carrier sense mechanism and the design of 802.11, whereas the unfairness at D=400 and 500m is due to interference from the hidden node. We interpret the results for each distance as follows:

- *D=100m*: In this case, all the nodes can carrier sense each other's transmission and thus nodes will always defer to an active transmitter. As shown in Figure 3.9(a), one transmitter, node 2, can acquire NAV information for $Tr_{0\rightarrow1}$ by overhearing CTS packets from node 1 and thus it will defer its transmission until the end of the dialog between node 0 and node 1. This means that after a $Tr_{0\rightarrow1}$ finishes both node 0 and node 2 will have the same chance of acquiring the channel because both nodes will defer the same period of time which consists of a DIFS period and a CW period with the minimum size of the CW [2].

  The other transmitter (node 0), however, cannot decode CTS packets from

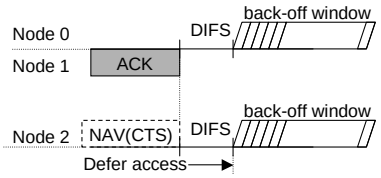

(a) After the transmission of Node 0

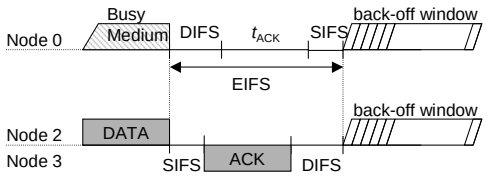

(b) After the transmission of Node 2

Figure 3.10: The SDT scenario, D=200m.

node 3 and thus does not know when $Tr_{2\rightarrow3}$ will finish. It, however, will carrier sense the ACK from node 3 when $Tr_{2\rightarrow3}$ finishes. Now the question is whether node 0 or node 2 has the greatest chance of accessing the channel next. According to the specification [2], node 0 can access the channel only after deferring an extended interframe space (EIFS) period and the CW period, while node 2 again tries to access the channel after deferring a DIFS period and the CW period as shown in Figure 3.9(b). Since an EIFS consists of a short interframe space (SIFS) period, the time required for an ACK packet transmission (t_{ACK}), and a DIFS period, it is much longer than a DIFS and thus node 2 has a better chance to access the channel than node 0. These two points account for the unfairness at D=100m shown in Figure 3.8, where $Tr_{2\rightarrow3}$ has higher throughput than $Tr_{0\rightarrow1}$.

- *D=200m*: As shown in Figure 3.10(a), for the $Tr_{0\rightarrow1}$ completing case the analysis is the same as for D=100 and thus there is no unfairness. For the $Tr_{2\rightarrow3}$ completing case the key change is that node 0 can no longer sense the transmission of the ACK from node 3. Therefore, as shown in Figure 3.10(b), node 0 starts to defer from the end of the DATA transmission from node 2 for an EIFS period followed by the CW period. Since EIFS consists of (SIFS+ACK+DIFS), the EIFS period of node 0 and the DIFS period of node 2 finish at the same time, and thus start to backoff at the same time for the CW period. Therefore, there is no unfairness at D=200m.

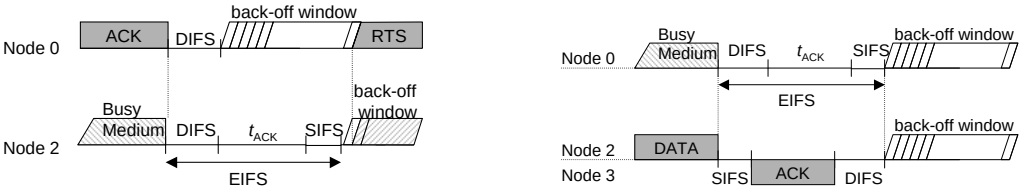

(a) After the transmission of Node 0 (b) After the transmission of Node 2

Figure 3.11: The SDT scenario, D=300m.

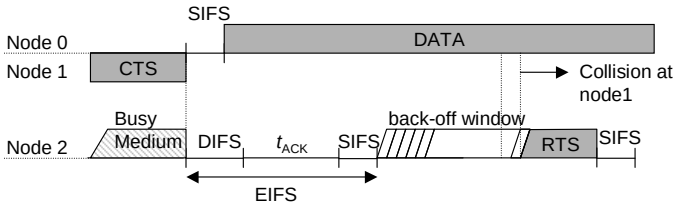

Figure 3.12: The SDT scenario, D=400m and 500m. Node 2 interferes the transmission between node 0 and node 1.

- *D=300m*: For the $Tr_{0\rightarrow1}$ completing case the key change is that now node 2 can no longer acquire NAV information for $Tr_{0\rightarrow1}$. Therefore, as shown in Figure 3.11(a), node 2 starts to defer from the end of the ACK transmission from node 1 and defers an EIFS period followed by the CW period, while node 0 tries to access the channel after deferring a DIFS period and the CW period. Since DIFS is much shorter than EIFS, node 0 has a higher chance of accessing the channel than node 2. As shown in Figure 3.11(b), for the $Tr_{2\rightarrow3}$ completing case the analysis is the same as for D=200 and thus both nodes can equally access the channel. Therefore, unfairness is observed at D=300m, where the throughput of $Tr_{0\rightarrow1}$ is higher than $Tr_{2\rightarrow3}$.

- *D=400m and 500m*: In this case, both node 0 and node 2 cannot carrier sense each other's transmission, and node 2 cannot acquire NAV information for $Tr_{0\rightarrow1}$. Node 2, however, can still interfere with the reception at node 1. For the $Tr_{0\rightarrow1}$ completing case, as shown in Figure 3.12, node 2 can transmit while node 0 is in the middle of a DATA transmission and thus cause interference

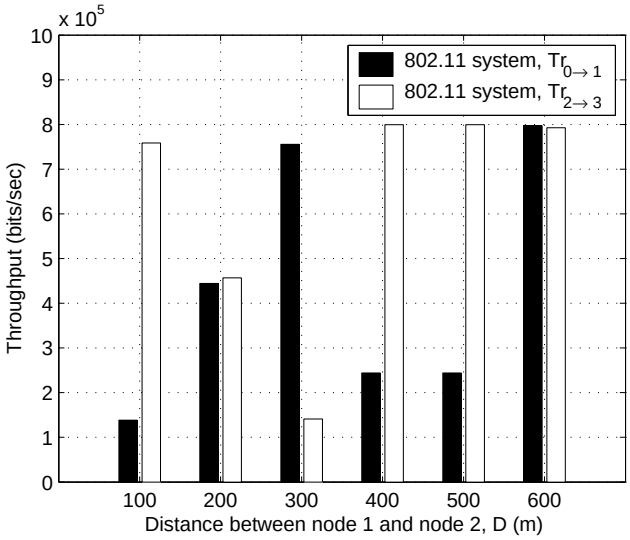

Figure 3.13: The throughput of the 802.11 system over an ideal channel in the SDT scenario for $\mathrm{SIR}_{\mathrm{threshold}} \leq$6dB and carrier sensing threshold = -70.4dBm.

at node 1. Node 3, however, receives the transmission from node 2 without interference. For the $Tr_{2\rightarrow 3}$ completing case, node 0 cannot acquire the channel due to the interference from node 2 at node 1. Thus, node 2 acquires the channel regardless of the transmission from node 0. This causes severe unfairness at D=400m and 500m and thus $Tr_{2\rightarrow 3}$ dominates the channel.

- *D=600m*: In this case, $Tr_{0\rightarrow 1}$ and $Tr_{2\rightarrow 3}$ do not interfere with each other. Therefore, both $Tr_{0\rightarrow 1}$ and $Tr_{2\rightarrow 3}$ can achieve their maximum throughput and can gain fairness. Since the MIMA-MAC system transmits packets with a single antenna, the throughput of the MIMA-MAC system is close to that of the 802.11 system.

Suppose we decrease $\mathrm{SIR}_{\mathrm{threshold}}$ to 6dB, which makes the receiver more robust to neighboring interference than the previous case ($\mathrm{SIR}_{\mathrm{threshold}}$ = 10dB). We will maintain the carrier sensing threshold to have a carrier sensing range of 550m. Figure 3.13 shows the simulation results for the lowered $\mathrm{SIR}_{\mathrm{threshold}}$. For

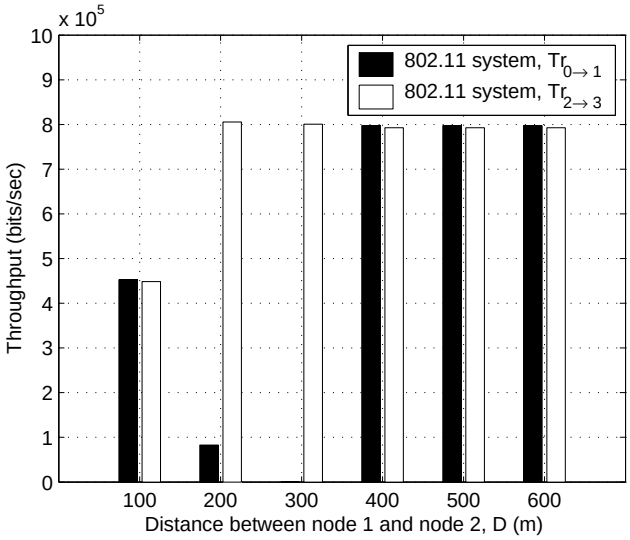

Figure 3.14: The throughput of the 802.11 system over an ideal channel in the SDT scenario for $\text{SIR}_{\text{threshold}}$ $\leq$6dB and carrier sensing threshold = -67.4dBm.

D=100m to D=300m, the results are the same as the previous case. For D=400m and 500m, the throughput of $Tr_{0\rightarrow 1}$, however, increases and is higher than the case of $\text{SIR}_{\text{threshold}}$=10dB. This is because when there is a transmission from node 0 to node 1, the transmission from node 2 no longer interferes with the data reception at node 1. The throughput, however, does not increase significantly since when there is a packet transmission from node 2, node 1 can still sense the transmission and if a packet (e.g. RTS) from node 0 is received after the synchronization period (128μsec for IEEE 802.11b [39]) of the packet from node 2, which is likely the case, node 1 is unable to receive the packet from node 0 [43], which prevents node 0 from accessing the channel [1]. This example shows that a low $\text{SIR}_{\text{Threshold}}$ improves the fairness for D=400m and 500m, but does not eliminate the unfairness problem due to the large carrier sensing range.

Now suppose we shrink the carrier sensing range from 550m to approximately

[1] In ns-2, this is approximated as follows: when the stronger packet (from node 0) arrives at the receiver (node 1) later than the weaker packet (from node 2), they are considered a collision.

390m by increasing the carrier sensing threshold by 3dB and leaving $\text{SIR}_{\text{Threshold}}$ at 6dB. Figure 3.14 shows the simulation results. For D=400m and 500m, both flows can fully access the channel without any interference from each other because now node 1 cannot sense the transmission from node 2 and thus can receive data from node 0 regardless of the transmission from node 2. For D=200m and 300m, $Tr_{0\rightarrow 1}$, however, experiences severe throughput degradation due to the shrunk carrier sensing range. For D=200m, the analysis is the same as for the $Tr_{0\rightarrow 1}$ completing case shown in Figure 3.10(a) and there is no unfairness in accessing the channel. When node 2 is transmitting, node 0, however, cannot sense the transmission since they are out of each other's carrier sensing range and thus node 0 will try to access the channel resulting in collision at node 1, which degrades the throughput of $Tr_{0\rightarrow 1}$. For D=300m, the analysis is the same as the cases of D=400m and 500m of the 802.11 system with the carrier sensing range of 550m and $\text{SIR}_{\text{Threshold}}$=10dB, which are shown in Figure 3.8(a), and thus $Tr_{0\rightarrow 1}$ experiences throughput degradation due to interference. Similarly, the fairness observed in the case of D=100m can be explained with the same argument we used previously for the D=200m case of the 802.11 system with the carrier sensing range of 550m and $\text{SIR}_{\text{Threshold}}$=10dB, which is shown in Figure 3.10, where both flows can access the channel fairly. This example shows that although shrinking the carrier sensing range and lowering $\text{SIR}_{\text{Threshold}}$ (using a transmission scheme which is robust to interference) might address the unfairness problem for D=400m and 500m, it might cause the unfairness problem for D=200m and exacerbate the unfairness problem for 300m, which were not observed in the large carrier sensing range (=550m) case.

Rayleigh fading channel model

Figure 3.15 shows the simulation results over a Rayleigh fading channel in the SDT scenario. The throughput and FR of the MIMA-MAC system and that of

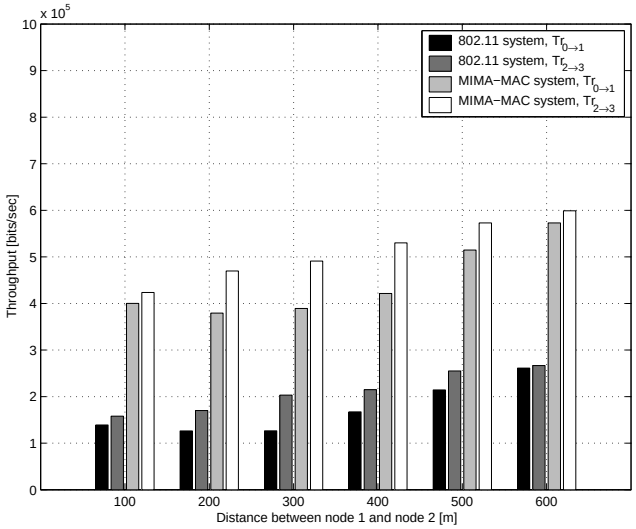

(a) Comparison of throughput

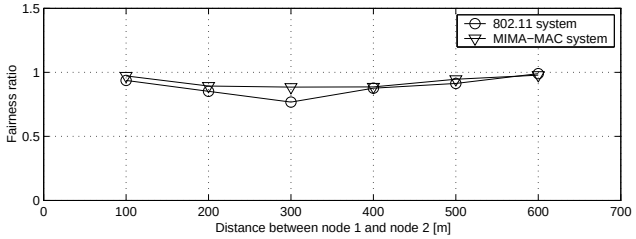

(b) Comparison of fairness-ratio

Figure 3.15: The performance comparison between the MIMA-MAC system and the 802.11 system over a Rayleigh fading channel in the SDT scenario.

the 802.11 system are compared in Figure 3.15(a) and Figure 3.15(b), respectively. Figure 3.15(a) clearly shows that the MIMA-MAC system outperforms the 802.11 system by more than a factor of 2 when there is neighboring interference. The unfairness of the 802.11 system, however, is not so severe as it was in the ideal case, and slight unfairness is observed in the MIMA-MAC system.

A detailed explanation of the simulation results is possible by looking at the key difference between the ideal channel case and the Rayleigh channel case. Firstly, d is decreased from 200m to 100m to increase the reliability of the link and thus R_I

D m	100	200	300	400	500	600
node: $0 \leftrightarrow 2$	$\approx$T	C/$\approx$I	$\approx$C	$\approx$C	O	O
node: $0 \leftrightarrow 3$	C	C	$\approx$C	O	O	O
node: $1 \leftrightarrow 2$	T	$\approx$T	C/$\approx$I	C	$\approx$C	O
node: $1 \leftrightarrow 3$	$\approx$T	C/$\approx$I	$\approx$C	$\approx$C	O	O

Table 3.4: Relation between the nodes in the SDT and ODT scenarios over a Rayleigh fading channel (d=100m)

shrinks to approximately 316m. Because R_{CS} and R_{TX} are independent of d, the relation between the ranges becomes $R_{TX} < R_I < R_{CS}$. Another important point that affects the simulation results is that, since the channel varies over time, R_{TX}, R_{CS} and R_I also vary over time. Therefore, if the two nodes are close to the edge of the range, the relation between the two nodes also varies over time. For example, if a receiver is at the edge of R_{TX}, when it experiences deep fading, the receiver is no longer within R_{TX} and thus will drop the packet from the transmitter. Therefore, we say that the receiver is *approximately* within R_{TX} and this is expressed in Table 3.4 with a symbol $\approx$. Based on these differences, the relation between the nodes of $Tr_{0\rightarrow1}$ and $Tr_{2\rightarrow3}$ over a Rayleigh fading channel can be summarized as Table 3.4, and the simulation results can be interpreted using this table as follows.

As shown in Figure 3.15, the unfairness of the 802.11 system is less severe than the ideal channel case because the relation between the nodes varies over time and this change can make an unfavorable network configuration into a favorable one. For example, consider the D=200m case. When there is no fading between node 1 and node 2, node 2 has a higher chance to access the channel than node 0 because node 2 can obtain NAV information for $Tr_{0\rightarrow1}$ from node 1, whereas node 0 cannot. When there is deep fading between node 1 and node 2, node 2, however, fails to acquire the NAV information and thus gives both transmitters the same chance to access the channel, which increases fairness. For the D=300m case, the unfairness gets worse because there is higher chance for node 0 and node 2 to become out of

each other's R_{CS} and node 2 to interfere with node 1. This corresponds to the ideal channel case at D=400, 500m. For D=400m and 500m, node 2 is out of R_I of node 1 and thus there is a little chance of interference from node 2, which improves the fairness between the two traffic flows. Since node 1 can still sense the transmission from node 2, when node 2 is transmitting, node 1, however, has to stay silent, which gives node 2 a greater chance to access the channel than node 0. For D=600m, the two traffic flows are separated and thus fairness is guaranteed.

The reason for the slight unfairness experienced in the MIMA-MAC system is that the receiver of $Tr_{0\rightarrow1}$, node 1, at which two data packets are arriving simultaneously, has to separate the two traffic flows using a ZF receiver. Unfortunately the ZF receiver increases the noise power during the detection process and consequently decreases the post-processed SNR, which leads to packet drops. Thus, the throughput of $Tr_{0\rightarrow1}$ is decreased. At the receiver of $Tr_{2\rightarrow3}$ (node 3), there, however, is no such interference to separate or there is very weak interference, if any, due to the distance between the interferer, node 0, and node 3. Therefore, the throughput of $Tr_{2\rightarrow3}$ is higher than that of $Tr_{0\rightarrow1}$.

Although fading reduces the unfairness of the 802.11 system, it still degrades the throughput of the system, whereas the MIMA-MAC system is able to mitigate fading by employing a diversity scheme that uses two receive antennas. In our implementation, when there is only one packet to receive, we employ selection combining (SC) diversity [44], which selects the receive antenna that has the maximum SNR. Therefore, the MIMA-MAC system outperforms the 802.11 system even when there is no interference between the two traffic flows.

If the 802.11 system employed a diversity scheme that mitigates fading, we can expect a throughput increase due to the reduction in packet drops. Now the variation of R_{TX}, R_{CS} and R_I, however, will become smaller and the relation between the nodes will be fixed and thus the unfairness problem will become worse

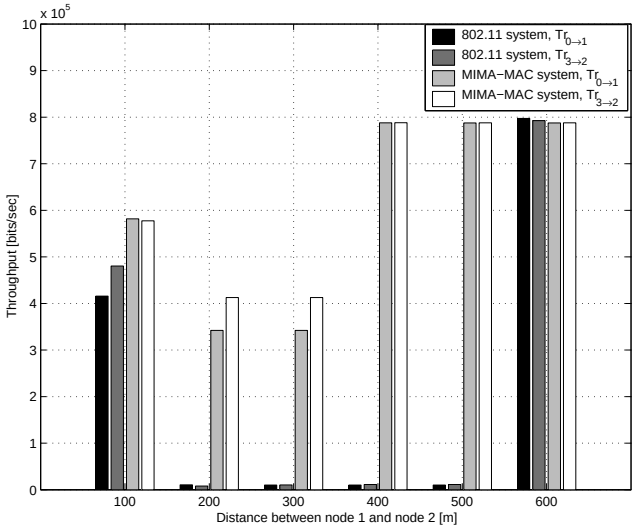

(a) Comparison of throughput

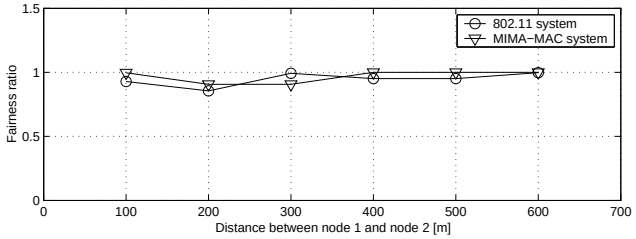

(b) Comparison of fairness-ratio

Figure 3.16: The performance comparison between the MIMA-MAC system and the 802.11 system over an ideal channel in the ODT scenario.

similar to that of the ideal channel case. We will show this in the simulation part of Chapter 4.

3.5.4 The ODT scenario

In this subsection, the performance of the MIMA-MAC system is compared with that of the 802.11 system for the ODT scenario shown in Figure 3.7(b). Simulations are performed over an ideal channel and a Rayleigh fading channel and the performance of both systems is measured by varying D from 100m to 600m.

Ideal channel model

Figure 3.16 shows the performance comparison between the MIMA-MAC system and the 802.11 system over an ideal channel in the ODT scenario. The results show that when the two traffic flows are close enough to interfere with each other's communication, the 802.11 system experiences extreme throughput degradation, whereas the MIMA-MAC system does not. The MIMA-MAC system, however, experiences throughput degradation when $D \leq 300$ because both transmitters are within R_I of each other's receiver and thus may have collisions between RTS packets at both receivers. These collisions are resolved by decreasing the transmission probability of each transmitter, which consequently lowers the throughput of both traffic flows. When D=100m, both transmitters can sense each other's transmission and thus a collision occurs between the RTS packets only when the two transmitters choose the same mini-slot in the contention slot, whereas when D=200, 300m, neither transmitter can sense the other's transmission and thus a collision occurs every time both transmitters try to send RTS packets in the same contention slot, which causes more collisions than in case of D=100m. Therefore, the transmitters have higher transmission probability when D=100m than when D=200, 300m. This directly affects the throughput of the system and thus the network throughput is higher when D=100m than when D=200, 300m. The simulation results also show that a certain level of fairness can be guaranteed for both systems because of the *symmetric* configuration of the network and traffic, which makes both transmitters have the same level of the information of the network and makes both receivers experience the same amount of the interference from neighboring transmission.

Using Table 3.3, the details of the simulation results and the reason for the extreme throughput degradation of the 802.11 system can be explained as follows:

- *D=100m*: In this case, all the nodes can carrier sense each other's transmission. Moreover, since the two traffic flows are symmetric, both transmitters

are within R_I of each other's receiver and do not have NAV information for each other's dialog, which means that both transmitters have no advantage over each other. Therefore, a certain level of throughput and fairness can be guaranteed.

- *D=200m and 300m*: The key difference is that both transmitters, node 0 and node 3, can no longer sense each other's transmission but can still interfere each other's communication, which turns out to be the worst case for the ODT scenario. Therefore, node 0 can commence its transmission during the transmission of node 3 and vice versa, which result in collisions at both receivers (node 1 and node 2). Since we assumed that the channel is fully consumed by both transmitters and the packet size is sufficiently large, these collisions will continue and thus ETD is observed.

- *D=400m and 500m*: In this case, the transmissions from both node 0 and node 3 no longer interferes with each other's RTS or DATA reception. The CTS and ACK packets from the receiver of one traffic flow, however, can still interfere with the reception of the RTS and DATA packets at the receiver of the other traffic flow and vice versa. Therefore, ETD is again observed.

- *D=600m*: In this case, the two traffic flows are separated and can achieve their maximum throughput.

Rayleigh fading channel model

Figure 3.17 shows the performance comparison between the 802.11 system and the MIMA-MAC system over a Rayleigh fading channel in the ODT scenario. The figure shows that the 802.11 system does not experience the severe ETD that was observed in the ideal channel case because R_{TX}, R_{CS} and R_I vary dynamically over time due to fading. The 802.11 system, however, still suffers from interference when the two

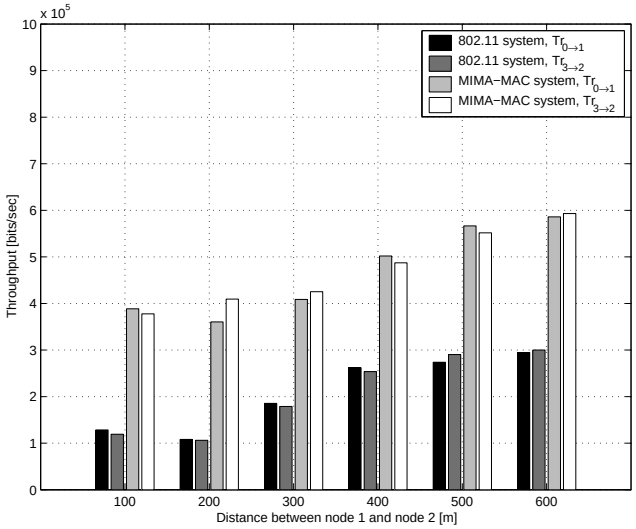

(a) Comparison of throughput

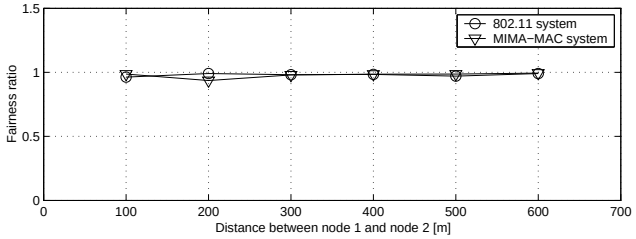

(b) Comparison of fairness-ratio

Figure 3.17: The performance comparison between the MIMA-MAC system and the 802.11 system over a Rayleigh fading channel in the ODT scenario.

traffic flows are close enough. Figure 3.17(b) shows that both systems guarantee fairness as in the ideal channel case. Recall that d=100m and thus R_I is shrunk to 316m.

The simulation results show that when D=200m, which corresponds to D=200m and 300m for the ideal channel case, the MIMA-MAC system outperforms the 802.11 system by more than a factor of 3 in terms of total network throughput. When D=300m, which corresponds to D=400m and 500m for the ideal channel case, only interference between node 1 and node 2 exists as shown in Table 3.4 and thus the

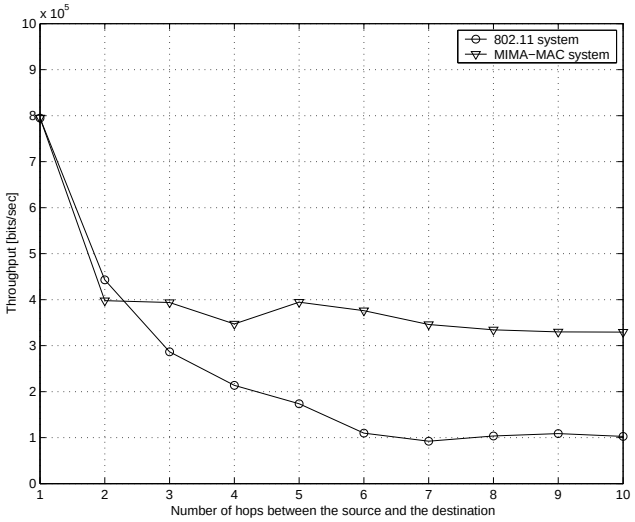

Figure 3.18: The throughput comparison between the MIMA-MAC system and the 802.11 system for a *multi-hop* linear topology network over an ideal channel. A single CBR traffic is transmitted from source to destination.

MIMA-MAC system outperforms the 802.11 system by a factor of 2. When $D \geq$ 400m the two traffic flows become gradually separated and the performance degradation due to the interference becomes smaller. As shown in the SDT scenario, the 802.11 system, however, suffers from fading, whereas the MIMA-MAC system does not by employing SC diversity. Therefore, the MIMA-MAC system outperforms the 802.11 system in terms of total network throughput when $D \geq$ 400m as well.

3.5.5 The multi-hop SDT scenario

Now consider a multi-hop network with a linear topology, in which all the nodes are equally spaced by 200m as shown in Figure 3.7(c) and a single CBR traffic flow is transmitted from node 0 (source) to node n (destination) over an ideal channel model. We again assume that $R_{CS} \approx 2R_{TX}$ and $R_{TX} < R_{CS} \approx R_I$. We can consider the SDT scenario as the building block of the multi-hop network with a CBR traffic flow. In this subsection, we investigate only the impact of the interference from the

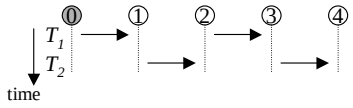

(a) The MIMA-MAC system

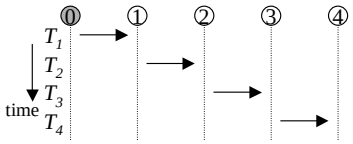

(b) The 802.11 system

Figure 3.19: An example of an ideal CBR traffic flow in a four-hop linear topology network. (a) The CBR transmission using the MIMA-MAC protocol. Two transmissions can coexist in the network. The transmitter only needs to wait for the next-hop node to forward the packet to its destination. (b) The CBR transmission using the IEEE 802.11 MAC protocol. Only one transmission can exist in the network at a time. The transmitter must wait until the data packet reaches its destination.

neighboring nodes on the multi-hop network excluding the effect of fading.

In Figure 3.18, the throughput of the MIMA-MAC system is compared with that of a 802.11 system. The simulation results show that as the number of hops increases, the MIMA-MAC system outperforms the 802.11 system. More interestingly, when $N_{hops} > 6$, the MIMA-MAC system outperforms the 802.11 system by a factor of 3. The performance gain comes from the fact that the proposed MIMA-MAC protocol can mitigate interference from neighboring nodes. In the MIMA-MAC system, two transmissions can coexist if they are at least one hop apart. When N_{hops}=1, the source can continuously transmit data to its destination. Since we are assuming that a node cannot receive and transmit at the same time, when $N_{hops} \geq$2, the source has to wait for the next-hop to forward the received data to its next-hop destination as shown in Figure 3.19(a) and thus the throughput is reduced to half. Since the two adjacent flows need to be separated by just one hop, the throughput of the MIMA-MAC system starts to stabilize at N_{hops}=2. In contrast to the MIMA-MAC system, in the 802.11 system, two transmitters cannot successfully deliver packets

at the same time when they are within three hops. Therefore, when $N_{hops} \leq 4$, there can be only one transmission in the network at a time. As shown in Figure 3.18, in the case of $N_{hops}=4$, the throughput of the 802.11 system is one forth that of a single link. This is because the source can transmit a new data packet without collision only when the previous data packet reaches the destination as shown in Figure 3.19(b). For $N_{hops} > 4$, there can be more than one transmission in the network at a time. Because the nodes are not perfectly scheduled, the throughput, however, is less than 1/4 of the maximum throughput. For $N_{hops}=10$, the throughput of the 802.11 system is approximately 102Kbps. The important thing to note in this simulation is that the interference from neighboring nodes is generated by the CBR traffic itself and thus the performance of the 802.11 system is degraded by *self-interference*, whereas the MIMA-MAC system mitigates such interference. In [45], Holland also showed this self-interference problem but without taking the unsolved hidden node problem into account.

3.6 Overcoming Spatial Fading Correlation

In this section, we describe intuitively how our MIMA-MAC approach can mitigate fading correlation and improve overall network performance.

3.6.1 Spatial fading correlation

In a real communication environment, the fades between the propagation paths may not be independent due to insufficient spacing between antennas or insufficient scatterers around the transmitter or receiver [5, 8]. It is shown in [5, 8, 46] that the channel capacity decreases as the correlation increases. This is because as the correlation between the fades of the pairs of transmit-receive antennas increases, it gets harder for the receiver to distinguish received signals from each other and thus gets harder to decode the signals correctly.

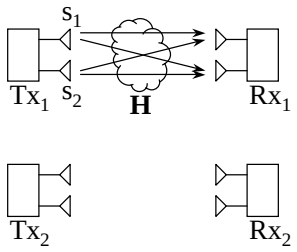

Figure 3.20: Illustration of the 802.11 system for $M_t = M_r = 2$.

3.6.2 Impact of fading correlations on network performance

Now consider a wireless network using the conventional IEEE 802.11 MAC protocol and MIMO in a layered fashion and assume that the links between the nodes experience fading correlation. How would this ill-conditioned MIMO channel affect the network performance? The answer to this question is straight forward. Since the layers are designed independently, 802.11 does not know whether its physical layer (PHY) is using multiple antennas or not. The MAC layer only receives decoded MAC frames from the physical layer. Therefore, if the channel between the transmitter and receiver is favorable to spatial multiplexing, the link can provide multiple parallel channels and the receiver can differentiate independent data streams transmitted from the transmit antennas successfully and thus we can increase the overall network performance. If, however, the channel is ill-conditioned then it becomes hard for the receiver to differentiate simultaneously transmitted data streams and thus the network performance degrades. For example, consider a network with four nodes each with two antennas as shown in Figure 3.20 assuming that all the nodes are in the same contention floor. Since the network is using 802.11, there could be only one active transmission. For this example, we assume that the active transmission is from Tx_1 to Rx_1. If the channel between Tx_1 and Rx_1 is an idealistic i.i.d. Rayleigh fading channel, we can improve the network performance by transmitting independent data streams from the two transmit antennas and differentiating the

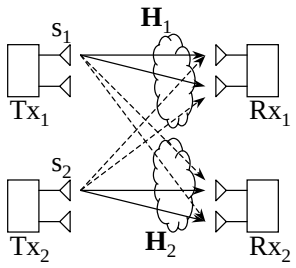

Figure 3.21: Illustration of the MIMA-MAC system for $M_t = M_r = 2$.

data streams at the receiver successfully. If, however, the channel suffers from fading correlation, it becomes hard for the receiver to differentiate the two data streams transmitted from the two transmit antennas successfully. Therefore, the network performance degrades. Since the network is using a layered approach, the problem in the PHY due to the correlated fading channel cannot be addressed or alleviated by the MAC or other layers but could only be addressed by the PHY itself. One possible PHY solution for mitigating fading correlation is to increase the distance between the neighboring antennas on the same node so as to increase the difference between the propagation paths between the transmitter and receiver. This, however, might be infeasible to increase the spacing between the antennas to the point where fading correlation is mitigated due to the limited size of a node.

3.6.3 Mitigating fading correlations using the MIMA-MAC

Consider a network shown in Figure 3.21. Since the MIMA-MAC system enables two simultaneous transmissions in the same contention floor, the two transmitters can transmit data streams to their destinations simultaneously. The receiver will receive the data streams from the two different transmitters, which are generally located at different and independent locations. Therefore, the propagation paths between the two transmitters and the receiver will be independent of each other most of the time. For example, suppose there are spatial fading correlations between the

propagation paths between a transmitter-receiver pair. In case of the 802.11 system, since a transmitter uses two transmit antennas placed closely to each other (e.g. half the wavelength of a transmitted signal), the array responses become similar to each other and thus the 802.11 system cannot separate the simultaneously received data streams successfully due to the fading correlation. In contrast to the 802.11 system, in case of the MIMA-MAC system, the two transmitters located at different locations transmit their data each using only one of the two antennas. Therefore, the effective distance between the two transmit antennas equals the distance between the two transmitters. Since the fading correlation decreases as the distance between the transmit antennas increases for a certain range of distance, the increased effective distance between the transmit antennas mitigates the spatial fading correlation.

Chapter 4

Mitigating Interference Using Multiple Antennas with Antenna Selection Diversity MAC Design

In this chapter, we propose an enhancement to the MIMA-MAC protocol, Mitigating Interference using Multiple Antennas with Antenna Selection (MIMA/AS-MAC) to fully utilize the MIMO physical layer's capabilities. The MAC protocol is extended not only to increase fairness and capacity but also to increase the diversity of a link to mitigate fading.

4.1 Basic Idea

The proposed MIMA/AS-MAC protocol enables the network to use all the transmit and receive antennas to increase the throughput and fairness of the network not only by mitigating interference from neighboring nodes but also by mitigating fading.

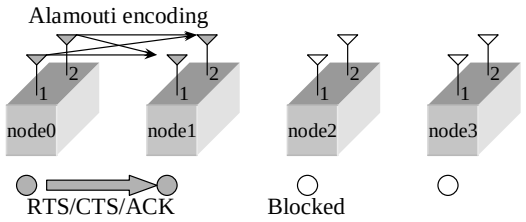

(a) A control packet transmission

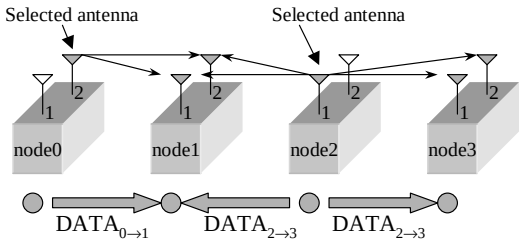

(b) A data packet transmission

Figure 4.1: The basic concept of the proposed MIMA/AS-MAC protocol for a control packet and a data packet transmission. The active antennas are colored in gray.

In MIMA-MAC, the transmitters use a single fixed antenna and the receiver uses multiple antennas allowing the receiver to suppress interference thanks to space-time processing. Since the protocol uses multiple antennas for spatial multiplexing and employs a zero-forcing (ZF) linear receiver [41], which only provides $N_r - N_t + 1$ order diversity [5], where N_t is the number of transmit antennas (i.e. the number of the transmitted data streams) and N_r is the number of receive antennas, when $N_t = N_r$, the diversity order becomes 1 and thus the MIMA-MAC system suffers from fading more than systems with higher diversity.

To improve the ability to mitigate fading, we propose to use space-time block coding (STBC) for control packet transmission and antenna selection (AS) diversity [47] for data transmission. AS diversity selects N_s antennas from N_t transmit antennas. For a network consisting of nodes with two antennas (i.e. $N_t = N_r = 2$), which we will use throughout the following sections, we use Alamouti encoding [9] for

control packet transmission and AS to select a single antenna for data transmission. As shown in Figure 4.1(a), when either of the transmitters are contending with each other to acquire the channel during the negotiation period or the receivers are replying with ACK packets back to the transmitters, they use both transmit antennas and use Alamouti encoding to exploit spatial diversity. In the data slot, the transmitters does not use Alamouti encoding, since all the transmitters must use a single transmit antenna for data transmission and the receiver has to differentiate multiple data streams that they have received from the different transmitters. Though, Naguib *et al.* proposed a combined interference suppression and maximum-likelihood (ML) decoding scheme for STBC in [48], using this scheme limits the maximum symbol rate of the data packet transmission to 1, which cannot increase the capacity of the link by increasing the number of antennas. Thus, as shown in Figure 4.1(b), we propose to use AS diversity, which uses N_s=1 transmit antennas that is selected from the possible N_t=2 transmit antennas for a data packet transmission to increase the post-processing SNR of the packet. The symbol rate of a data packet transmission is easily increased by increasing $N_s > 1$ for N_t and $N_r > 2$. The receiver selects the transmit antenna based on the estimated channel information, which is obtained during control packet reception, and feeds back the selected antenna information to the transmitter. The receiver selects the antenna that maximizes the post-processing SNR of the data packet that is *destined* for the receiver to minimize the bit-error-rate (BER).

4.2 Protocol Design

The basic frame structure of the MIMA/AS-MAC protocol is almost the same as that of the MIMA-MAC protocol. The main difference between the two protocols is that the MIMA/AS-MAC protocol is using Alamouti encoding for control packets such as RTS, CTS, and ACK packets and AS diversity for a data packet, whereas

the MIMA-MAC protocol does not. To support such diversity schemes, we designed the MIMA/AS-MAC protocol as follows:

- To provide Alamouti encoding for control packets, the receiver must know the channel information for all the propagation paths from the transmit antennas to the receive antennas. Thus, two additional training sequence slots for every transmit antenna are placed just before the transmission of each control packet. The receiver uses the channel information for antenna selection as well as control packet detection.

- To provide AS diversity for the data packet transmission, the receiver selects the transmit antenna based on its antenna selection criterion, which selects the transmit antenna that provides the best chance to receive the data packet successfully, and feeds back the selected antenna information (the index of the selected antenna) to the transmitter. This information is conveyed in the CTS packet. In the case of the transmitter with N_t antennas, we need only $\log_2 N_t$ bits to represent the selected antenna, which is much smaller than the number of bits required to send full channel information back to the transmitter. The transmitter then uses the information in the CTS packet to select the transmit antenna for data packet transmission.

4.3 Antenna Selection Criterion

In the MIMA/AS-MAC system, the receiver receives multiple data packets that may or may not be destined for the receiver from multiple transmitters. Since, only the packets that are destined for the receiver are relevant, other packets that have different destination addresses are discarded regardless of the post-processing SNR. Thus, the receiver measures the channel by receiving training sequence associated with the RTS control packet from the intended transmitter and selects the intended

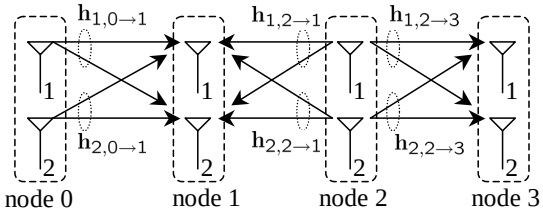

Figure 4.2: Illustration of the channel vectors between the transmitters (node 0 and node 2) and receivers (node 1 and node 3).

transmitter's antenna such that it can receive the data packet from the transmitter with the maximum post-processing SNR. The selected transmit antenna information is then conveyed in a CTS packet and replied to the transmitter. Since the bit error rate and capacity are a function of the post-processing SNR, this should ensure improved error rate for a fixed data rate or ensure improved throughput for a fixed error rate by increasing the data rate.

The antenna selection criterion for the MIMA/AS-MAC protocol is derived as follows. Figure 4.2 illustrates the channel vectors between the transmit and receive antennas. In this example, we assume that node 0 and node 2 transmit data packets to their destination, node 1 and node 3, respectively. We assume that the transmission from node 2 interferes with node 1, but the transmission from node 0 does not interfere with node 3 due to the distance between the two nodes. Let $\mathbf{h}_{i,x\to y}$ denote a (2×1) channel vector from i^{th} transmit antenna of node x to two receive antennas of node y. We assume that each entry of the channel vector is an uncorrelated complex Gaussian random variable with mean 0 and variance 1, $\mathcal{CN}(0,1)$. Since both transmitters are transmitting their data packets simultaneously, the channel matrix $\mathbf{H}_k^{(i,j)}$ between the receiver, node k, and the i^{th} transmit antenna of node 0 and the j^{th} transmit antenna of node 2 can be expressed as $\mathbf{H}_k^{(i,j)} = [\mathbf{h}_{i,0\to k}\ \mathbf{h}_{j,2\to k}]$. Using the ZF receiver, the l^{th} post-processing SNR of the

two multiplexed data packets over a channel matrix $\mathbf{H}_k^{(i,j)}$ can be expressed as [47]

$$SNR_l = \frac{\rho}{[\mathbf{H}_k^{(i,j)H}\mathbf{H}_k^{(i,j)}]_{ll}^{-1}} \tag{4.1}$$

where, ^{H} denotes the Hermitian, $\rho = \frac{E_s}{N_0}$ denotes the received SNR, E_s is the received symbol energy, and N_0 is noise power at the receiver. Notice that the received SNR ρ is not divided by N_t transmit antennas, since every transmitter is using one antenna with its maximum transmit power.

The receiver, node 1, selects the transmit antenna that node 0 has to use based on the channel matrix $\mathbf{H}_1^{(i,j)} = [\mathbf{h}_{i,0\to1}\ \mathbf{h}_{j,2\to1}]$. Since, the data packet received from node 2 is considered as interference, node 1 is only interested in decoding the data packet from node 0. Therefore, for a given neighboring channel vector, $\mathbf{h}_{j,2\to1}$, the antenna selection criterion that maximizes SNR_1 (the post-processing SNR of the data packet from node 0), regardless of SNR_2 (the post-processing SNR of the data packet from node 2) is equivalent to searching for the transmit antenna s_{opt} for all i that minimizes $[\mathbf{H}_1^{(i,j)H}\mathbf{H}_1^{(i,j)}]_{11}^{-1}$ for a given $\mathbf{h}_{j,2\to1}$ and can be expressed as

$$\begin{aligned} s_{opt} &= \arg\min_{i\in\{1,2\}} [\mathbf{H}_1^{(i,j)H}\mathbf{H}_1^{(i,j)}]_{11}^{-1} \\ &= \arg\min_{i\in\{1,2\}} \begin{bmatrix} \mathbf{h}_{i,0\to1}^H\mathbf{h}_{i,0\to1} & \mathbf{h}_{i,0\to1}^H\mathbf{h}_{j,2\to1} \\ \mathbf{h}_{j,2\to1}^H\mathbf{h}_{i,0\to1} & \mathbf{h}_{j,2\to1}^H\mathbf{h}_{j,2\to1} \end{bmatrix}_{11}^{-1} \\ &= \arg\max_{i\in\{1,2\}} \left\{ \|\mathbf{h}_{i,0\to1}\|_F^2 - \frac{|\mathbf{h}_{j,2\to1}^H\mathbf{h}_{i,0\to1}|^2}{\|\mathbf{h}_{j,2\to1}\|_F^2} \right\}. \end{aligned} \tag{4.2}$$

Therefore, the optimal antenna selection in terms of the post-processing SNR of the data packet from node 1 is equivalent to finding the transmit antenna s_{opt} that maximizes the optimum antenna selection metric, $m_{i,opt}$,

$$m_{i,opt} = \|\mathbf{h}_{i,0\to1}\|_F^2 - \frac{|\mathbf{h}_{j,2\to1}^H\mathbf{h}_{i,0\to1}|^2}{\|\mathbf{h}_{j,2\to1}\|_F^2}. \tag{4.3}$$

Unfortunately, there is a difficulty using the neighboring channel information, $\mathbf{h}_{j,2\rightarrow 1}$, for the optimum antenna selection because $\mathbf{h}_{j,2\rightarrow 1}$ itself has to be the channel between the receiver and the *optimum* transmit antenna of the neighboring transmitter that considered the interference from its neighboring transmitters during the antenna selection process. If both receivers hear each other's transmission, one cannot select the optimum transmit antenna in a distributed manner, since one's decision may affect the other's antenna selection, and vice versa. In other words, it might be hard for both receivers to make the optimum antenna selection at the same time.

Thus, we propose to use a suboptimal antenna selection metric, $m_{i,subopt}$, that does not use the channel information between the neighboring node and the receiver as follows

$$m_{i,subopt} = \|\mathbf{h}_{i,0\rightarrow 1}\|_F^2. \tag{4.4}$$

When the receiver uses $m_{i,subopt}$ as an antenna selection metric, it makes a decision error for the following two cases:

1. $\mathcal{E}_1 = \{m_{1,subopt} > m_{2,subopt}, m_{1,opt} < m_{2,opt}\}$
2. $\mathcal{E}_2 = \{m_{1,subopt} < m_{2,subopt}, m_{1,opt} > m_{2,opt}\}$

We estimated the decision error probability, $P_{error} = P\{\mathcal{E}_1\} + P\{\mathcal{E}_1\}$, by using Monte Carlo simulation. We generated 10,000 pair of channel matrices for the channel between node 0 and node 1 and the channel between node 1 and node 2, and counted the number of the error events $\mathcal{E}_1$ and $\mathcal{E}_2$. The estimated P_{error} is approximately 0.25, which means that using $m_{i,subopt}$ for the antenna selection metric guarantees approximately 75% of the optimal antenna selection for a given $\mathbf{h}_{j,2\rightarrow 1}$. Therefore, it is reasonable to use $m_{i,subopt}$ as an antenna selection metric and use the suboptimal antenna selection criterion that chooses the transmit antenna, s_{subopt}, that

maximizes $m_{i,subopt}$ for all $i \in \{1, 2\}$ as follows

$$s_{subopt} = \arg \max_{i \in \{1,2\}} \|\mathbf{h}_{i,0\rightarrow 1}\|_F^2. \tag{4.5}$$

4.4 Simulation Results

We implemented the proposed MIMA/AS-MAC protocol using ns-2. We compare the performance of the MIMA/AS-MAC system with that of the MIMA-MAC system both with and without Alamouti encoding for a control packet transmission and that of the 802.11-Alamouti system that uses the IEEE 802.11 MAC protocol with Alamouti encoding for both control and data packets. All the systems use two antennas. The systems are also compared with the 802.11 system with a single antenna.

4.4.1 Simulation setup

We use a linear topology network consisting of four nodes with two antennas as shown in Figure 4.1. The distance between node 0 (or node 2) and node 1 (or node 3), d=100m, and we measure the performance by varying the distance between the receiver (node 1) and the neighboring transmitter (node 2), D, from 100m to 600m. We use two constant-bit-rate (CBR) traffic flows just as we used in the same direction traffic (SDT) simulations and the same physical layer parameters presented in Section 3.5.2. We use a Rayleigh fading channel model to show the effect of the increased diversity order of the proposed MIMA/AS-MAC system. Each entry of the channel vectors is assumed to be $\mathcal{CN}(0, 1)$. We assume that the channel is quasi-static and thus fixed within a RTS-CTS-DATA-ACK exchange.

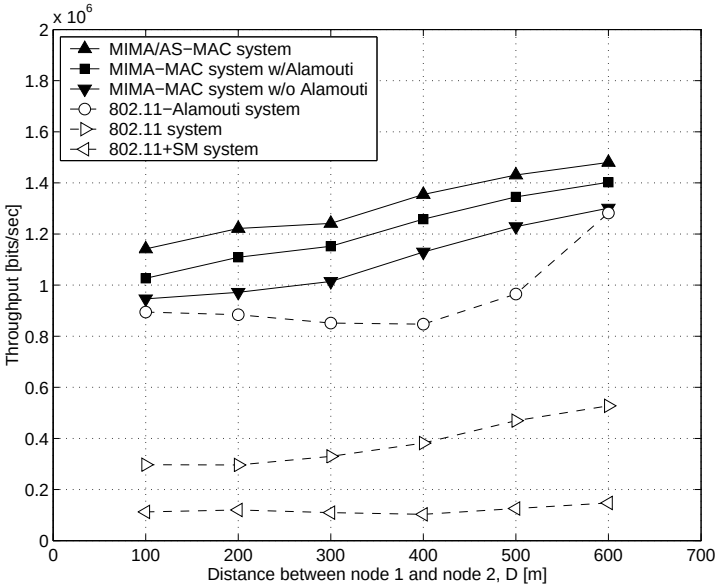

Figure 4.3: Comparison of total network throughput.

4.4.2 Performance evaluation

Again, the performance of the systems are measured in two ways: the total throughput of the network and the fairness between the two traffic flows in the network. The total throughput is measured by adding all the CBR packets that reached their destination successfully and dividing it by the simulation time, and fairness is measured using the fairness-ratio (FR) shown in (3.9).

Figure 4.3 shows the total throughput comparison between the proposed MIMA/AS-MAC system and the other five systems. To show the effect of the neighboring transmission (interference), the total throughput is measured by varying D from 100m to 600m. The results clearly show that the MIMA/AS-MAC system outperforms the MIMA-MAC system with and without Alamouti encoding for control packet transmission by approximately 6% to 11% and 14% to 26%, respectively. The antenna selection diversity and Alamouti encoding employed in the MIMA/AS-MAC system reduces the packet drops that are caused by fading. More-

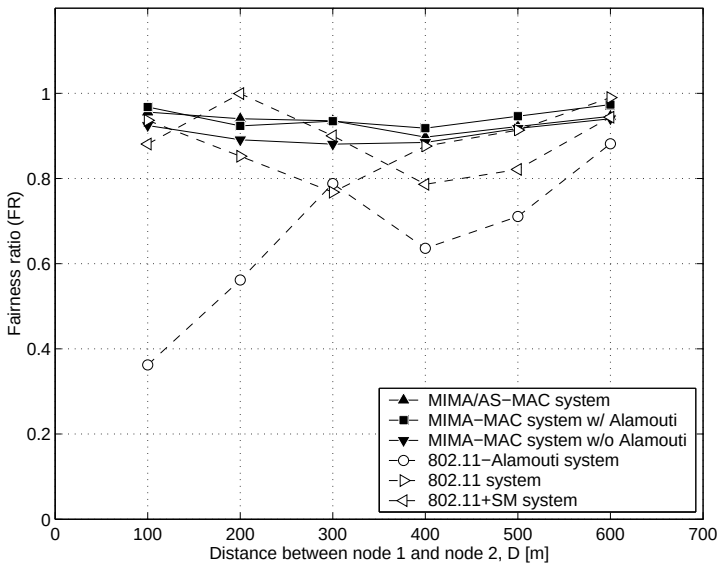

Figure 4.4: Comparison of fairness ratio.

over, the MIMA/AS-MAC system gains approximately 15% to 60% of throughput increase over the 802.11-Alamouti system. This is because, when $D \leq 500$m, one of the two traffic flows of the 802.11-Alamouti system suffers from a neighboring transmission that blocks or interferes with the transmission, whereas the MIMA/AS-MAC system and the MIMA-MAC system are designed to mitigate neighboring interference. The 802.11-Alamouti system, however, mitigates fading and thus has higher throughput than the 802.11 system with a single antenna by a factor of 2 to 3. The throughput of the 802.11 system using spatial multiplexing (802.11+SM) is even lower than that of the 802.11 system with a single antenna. This is because, for the 802.11+SM system, only half of the total transmit power is allocated to each transmit antenna and it is using a ZF receiver and data streams are uncoded and thus each data stream's received SNR becomes lower than that of the 802.11 system with a single antenna [5].

Figure 4.4 compares the fairness of the two traffic flows between the MIMA/AS-MAC system and the other five systems. The results show that the FR of the

MIMA/AS-MAC system is closer to 1 than that of the MIMA-MAC system when $D \leq 300$m. Fairness is improved since antenna selection diversity increases the post-processing SNR of the data packet received at node 1, which eventually increases the throughput of the traffic flow from node 0 to node 1. The improvement, however, decreases as interference between the traffic flows decreases. For $D \geq 400$m, the FR of the MIMA/AS-MAC system is lower than that of the MIMA-MAC system with Alamouti encoding because of the discrepancy between the channel over which the control packets are transmitted using Alamouti encoding and the channel over which the data packets are transmitted using AS diversity. It is shown in [5] that the post-processing SNR of Alamouti encoding is less than or equal to that of AS diversity when the selected channel (antenna) has the largest channel gain. The impact of using different transmission modes for different types of packets on the system performance could be explained as follows. Consider a case where the RTS packets from the two different transmitters node 0 and node 2 do not collide at the receiver node 1, which makes the two transmitters think that there are no neighboring interferers. Assuming that both transmitters used the first contention slot to exchange RTS/CTS packets with their destination, they will use the same training-sequence slot for their training-sequence transmission. Each transmitter will send the training-sequence from their selected antenna, which might have higher SNR than the RTS/CTS transmission, which uses Alamouti encoding. Therefore, even though there was no collision during the RTS/CTS exchange, the training-sequence transmission from node 2 might interfere with the training-sequence transmission from node 0 and prevent the receiver node 1 from correct channel estimation, which is required for differentiating the two simultaneous DATA transmissions from node 0 and node 2. This increases the packet drops at node 1 and thus the traffic flow from node 2 to node 3 has higher throughput than the traffic from node 0 to node 1.

As we have discussed in Chapter 3, the results also show that although the

802.11-Alamouti system gains a throughput improvement by employing Alamouti encoding, it suffers from unfairness due to interference from the neighboring traffic flow. This is because as we employ Alamouti encoding, the channel is stabilized and thus shows the similar unfairness that we saw in the ideal channel case in Section 3.5.3. When D=300m, the 802.11-Alamouti system provides a certain level of fairness because most of the time both transmitters have the same level of information about the network and experience the same level of interference. When D=600m, the two flows are almost separated and thus provides a certain level of fairness. For the 802.11 system using a single antenna and the 802.11+SM system, the packet drops due to fading dominate the systems' performance and thus the results do not show severe unfairness due to neighboring interference.

Chapter 5

Improving TCP Performance Using Multiple Antennas

In the previous chapters we proposed two MAC protocols, MIMA-MAC and MIMA/AS-MAC, that exploit the capabilities of MIMO communication schemes to mitigate interference from neighboring nodes and fading. In this chapter, we extend our study to investigate ways to solve the problems of higher layer protocols by designing MAC protocols that use MIMO. We start by investigating the impact of MIMA-MAC on the performance of TCP transmission for multi-hop wireless networks. Then we propose a MAC protocol, TCP enhanced MIMA/AS-MAC protocol that further improves the efficiency of the MIMA/AS-MAC protocol for small packet transmission.

5.1 Introduction

The Transport Control Protocol (TCP) is the most widely used connection oriented transport layer protocol and provides reliable communication for various applications such as FTP (File Transport Protocol), Telnet, SSH (Secure Shell), HTTP

(Hyper Text Transfer Protocol) and SMTP (Simple Mail Transfer Protocol). The important features of TCP are reliable data transmission and an adaptive congestion control mechanism that adaptively controls the number of packets that a source can send to its destination without causing congestion in the network. An important assumption that the designers of TCP made is that the channel over which TCP is operating is "lossless", which means that there will be no packet drops during transmission and thus assumes that congestion is the only cause of packet drops in the network. Therefore, when TCP detects a packet drop, it perceives this as congestion in the network and thus decreases the transmission rate to alleviate the congestion.

Although TCP is extremely successful in "wired" networks, it suffers from significant performance degradation in "wireless" networks. The key reason is that the assumption made by TCP no longer holds for wireless networking environments because wireless links are unreliable and thus packets are dropped not only due to congestion but also due to fading and interference during transmission over a wireless link. Since TCP cannot tell whether the packet drops are caused by congestion or a "bad" channel, the source of a TCP connection will also back off and increase the timeout value for a retransmission even though the packet drop was caused by a bad channel, which will only degrade the throughput of TCP without solving any problem.

A number of solutions have been proposed to address the problem of TCP over wireless [49–52]. The proposed solutions are mostly studied for one-hop wireless environments: a mobile host connected to a fixed network through a wireless link. One way to solve this problem is explicitly notifying the source of the TCP connection that there is congestion in the network by using an Explicit Congestion Notification (ECN) mechanism [52]. This enables the source to differentiate the cause of packet drops: congestion or a bad channel. Another way to deal with

this problem is concealing the packet drops due to a bad channel from TCP [49]. These approaches, however, do not eliminate the sources of the problem: *fading* and *interference*.

In [3], Xu and Saadawi showed the effect of interference from adjacent nodes on TCP throughput for multi-hop wireless networks. They showed that the IEEE 802.11 MAC does not work well for a multi-hop wireless network because it does not perfectly solve the hidden node problem, which eventually results in TCP throughput degradation. In [53], Stamoulis and Al-Dhahir showed that we can greatly improve the throughput of TCP by mitigating fading. They employed a MIMO scheme with a space-time block coding (STBC) that exploits spatial diversity. Although STBC solves the problem caused by fading, the problems caused by interference still remain unsolved.

As we have shown in Chapter 3, our proposed MIMA-MAC protocol is able to mitigate interference from neighboring nodes and thus could be a solution to the throughput degradation problem of TCP that was observed in [3]. Therefore, in this chapter, we will first demonstrate that we can improve TCP throughput for multi-hop wireless networks by employing the MIMA-MAC and show the significant impact of interference from neighboring nodes on TCP performance.

The MIMA-MAC, however, is inefficient for transmitting small packets such as the TCP acknowledgement (TCP-ACK) control packets because a TCP-ACK is much smaller than the size of a fixed MIMA-MAC frame. Since MIMA/AS-MAC is based on MIMA-MAC, this is also the case for MIMA/AS-MAC. Therefore, in this chapter, we further enhance the MIMA/AS-MAC to solve this inefficiency problem. We propose a TCP enhanced MIMA/AS-MAC protocol that can transmit small packets without wasting significant resources.

The remaining part of this chapter is organized as follows. In Section 5.2 we present the details of key problems that cause TCP throughput degradation. In

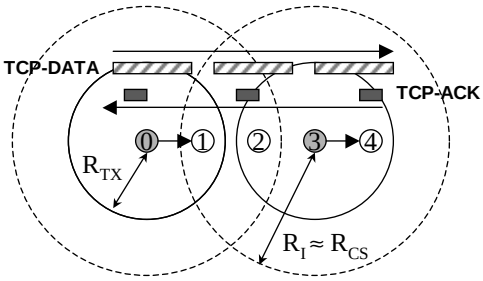

Figure 5.1: The effect of the interference from the neighboring node. A wireless network consisting of five nodes with a single TCP connection from node 0 to node 4.

Section 5.3 we demonstrate the impact of interference on the TCP throughput and show the performance improvement with MIMA-MAC. In Section 5.4 we propose an enhanced MAC protocol that increases the efficiency of the MIMA/AS-MAC protocol. Finally, to validate our design, in Section 5.5, we present simulation results.

5.2 Key Problems

In this section we present the key problems of TCP over multi-hop wireless networks caused by interference from neighboring nodes. We first explain the effect of interference from neighboring nodes in detail. Then we describe another problem that arises from using the MIMA-MAC as a solution to the interference problem.

5.2.1 Interference from neighboring nodes

Consider a wireless network using the IEEE 802.11 MAC in DCF mode shown in Figure 5.1. In the network, we assume that the only traffic is a single TCP connection from the source (node 0) to destination (node 4). Though there is only a single TCP connection between the source and destination, we are able to observe packets from node 0 dropped at node 1 due to the interference from node 3 if node 0 and node 3 transmit simultaneously. This is because node 0 and node 3 are out of each other's

carrier sensing range, R_{CS}, and thus they can transmit whenever they want to, but since node 3 is within the interference range, R_I, of node 1, this leads to a collision at node 1. To make matters worse, when node 3 transmits a 'large' data packet to node 4, node 0 will continuously fail to access the channel during this period of time because the large data packet from node 3 collides with the RTS packets being transmitted from node 0 at node 1. Not surprisingly, the continuous packet loss causes a serious problem to TCP performance. The MAC protocol interprets this as a link failure and does two things: first it discards the data packet it was trying to send from its buffer and second it reports a link failure to the routing protocol indicating that this link is no longer available. The packet drop eventually triggers the TCP congestion mechanism, which then decreases the TCP transmission rate to at most half the previous value. As we will discuss in more detail in Chapter 6, when the routing protocol such as AODV [27] or DSR [28] detects a link failure, it generates a route-error packet (RERR) that notifies the nodes along the route about the link failure. The nodes that receive the RERR update their routing table or cache by marking or deleting the corresponding route information so that it is not used in the future. When it comes to the retransmission of the dropped packet, the source will try to recover the route to the destination by broadcasting a new route discovery packet. This might take some time depending on the number of hops to the destination and eventually this route rediscovery overhead will further degrade TCP throughput.

5.2.2 Inefficiency of the MIMA-MAC for small packets

Though the MIMA-MAC can mitigate interference from neighboring nodes, it is inefficient for transmitting a packet that is much smaller than the data slot of a MIMA-MAC frame. For example, consider a TCP connection from the source to destination with only a single data flow from the source to destination. Though

the TCP connection is a single traffic flow, we can easily realize that there are two opposite and asymmetric traffic flows in the connection: TCP-DATA traffic flows from the source to destination and TCP-ACK traffic flows from the destination to source. Moreover, the size of a TCP-ACK is much smaller than that of a TCP-DATA. For example, the size of a TCP-ACK is 20 bytes and the default size of a TCP-DATA is 512 bytes and it could (and should) be set to a larger value during the establishment stage of a TCP connection. For example, in case of the 802.11 MAC, it can convey up to 2312 bytes of payload data [2], which makes the maximum size of TCP-DATA nearly 2300 bytes. Assuming 20 bytes of IP header and considering a preamble (16 bytes), a Physical Layer Convergence Procedure (PLCP) header (6 bytes), a MAC header (34 bytes), and frame check sequence (FCS) (4 bytes) based on the IEEE 802.11b specification [39] with a transmission rate of 1 Mbps, a TCP-ACK transmission utilizes approximately 100 bytes of a MIMA-MAC frame's `data-slot`, which is approximately 2200 bytes long. Thus when the intermediate nodes along the route forward TCP-ACKs to the source, only a small part ($\approx 4.5\%$) of the fixed-size `data-slot` is utilized and the rest of it is wasted, which consequently decreases the throughput of TCP. This motivates our design of an enhanced MIMA-MAC protocol.

In the following sections, we first compare the performance of the MIMA-MAC system and that of the conventional 802.11 system for a linear topology network using ns-2 to show the TCP throughput gain we can achieve by mitigating interference from neighboring nodes. Then, to improve the efficiency of the MIMA-MAC for a small packet transmission, we propose a TCP enhanced MIMA-MAC protocol and compare its TCP performance with that of the MIMA-MAC system by ns-2 simulations.

5.3 Improving TCP Using MIMA-MAC

Interference from neighboring nodes significantly degrades TCP throughput. One thing to note is that the interference is generated not only by other traffic flows but more critically by the TCP traffic flow itself, which means that a single TCP connection in a multi-hop wireless network will always have this throughput degradation problem due to neighboring interference even in the absence of other traffic. Therefore, we first demonstrate how we can improve TCP performance for multi-hop wireless networks using MIMA-MAC.

5.3.1 Mitigating self-interference using MIMA-MAC

We can view the interference problem that we have described in Section 5.2 as the SDT (same direction traffic) scenario that we have already discussed in Chapter 3 and thus we can solve this problem by employing MIMA-MAC and increase TCP throughput for multi-hop wireless networks.

To validate our argument, we conducted preliminary simulations with the *ns-2* network simulator for linear topology networks by varying the number of hops between the source and destination. We measure the TCP throughput of the MIMA-MAC system with two antennas and compare it with that of the 802.11 system with a single antenna to show the performance improvement gained by mitigating interference from neighboring nodes.

5.3.2 Simulation setup

We use the following simulation setup for measuring the TCP throughput of the MIMA-MAC system and that of the 802.11 system.

Network topology We use a multi-hop linear (chain) topology network shown in Figure 5.1 for the simulations to show the impact of interference on TCP perfor-

mance. Since we set the transmission range to 250m, we place all the nodes equally spaced by 200m so that when the source transmits a packet to its destination, the packet can reach its final destination only by going through all the intermediate nodes between the source and destination. The throughput of a single TCP connection is measured by varying the number of hops between the source and destination from 1 to 15.

Channel model For this simulation, we use an *ideal* channel model, which is defined to be an orthogonal MIMO channel [5] that has only the path-loss effect, but no fading. We assume that for the MIMA-MAC system, if the channel information is perfectly known at the receiver, two independent data streams are separated perfectly. The purpose of using an ideal channel is to investigate only the effect of the interference from neighboring nodes on the TCP performance by excluding the effect of the packet drops due to fading and detection schemes.

Physical and MAC layer parameters For the simulations of an ideal channel model, we use the same physical and MAC layer parameters that we used in Section 3.5.2.

Traffic model We use TCP and the File Transfer Protocol (FTP) for the transport layer and application layer, respectively. The packet size of the TCP connection is set to 2048 bytes. We use delayed ACKs [40] with the interval between TCP-ACKs set to 100msec to reduce the number of TCP-ACKs replied from the destination. We simulate a single TCP connection between the source and destination for 120sec.

5.3.3 Simulation results

Figure 5.2 shows the simulation results. We simulated both systems by varying the number of hops, N_{hops}, from 1 to 15. In this simulation, we investigate the impact

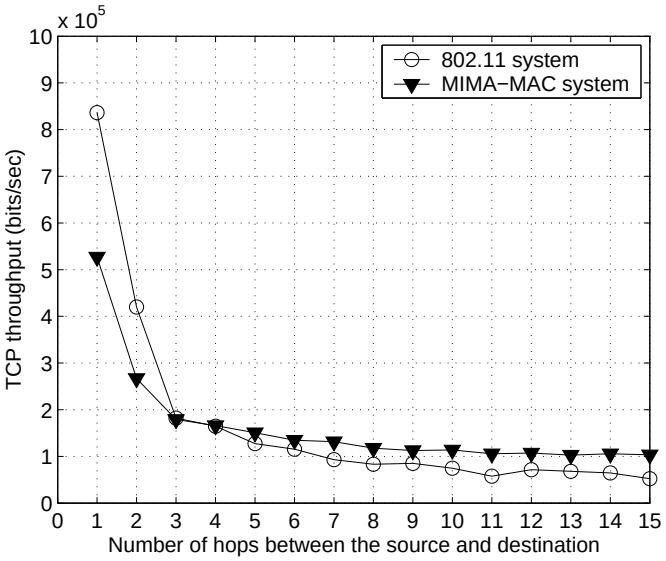

Figure 5.2: TCP throughput comparison between the 802.11 system and the MIMA-MAC system over an ideal channel.

of *interference* from neighboring nodes on the TCP throughput. The simulation results show that in the case where $N_{hops} < 3$, the 802.11 system outperforms the MIMA-MAC system. When N_{hops}=3 and 4, both systems have approximately the same throughput, and when $N_{hops} > 4$, the MIMA-MAC system starts to outperform the 802.11 system, which shows a throughput improvement when interference is mitigated by the MIMA-MAC. For $N_{hops} > 4$, the throughput of the MIMA-MAC system is approximately 16.8% to 97.9% higher than that of the 802.11 system. The intuition underlying these results is as follows: for the 802.11 system, when $N_{hops} < 3$, there are no packet drops due to interference from neighboring nodes because potential interferers are within each other's carrier sensing range, which prevents simultaneous transmissions. For the MIMA-MAC system, when $N_{hops} < 3$, it cannot take advantage of transmitting multiple TCP-DATA packets simultaneously because we are assuming that a node cannot transmit and receive at the same time. Moreover, since the ACK packet of TCP is much smaller than the `data-slot` of

the MIMA-MAC protocol, which is fixed in size, the MIMA-MAC protocol is less efficient than the 802.11 MAC protocol in transmitting TCP-ACKs. Therefore, in this region, the 802.11 system outperforms the MIMA-MAC system. As the number of hops increases to $N_{hops} > 4$, the 802.11 system suffers from packet drops due to interference from neighboring nodes. This is because the 802.11 MAC does not solve the hidden node problem perfectly. As we described in Section 5.2.1, this causes link failures and thus triggers the route rediscovery and lowers TCP's transmission rate. The MIMA-MAC system, however, does not suffer from interference from neighboring nodes because it is designed to mitigate such interference. Therefore, in this case, the MIMA-MAC system outperforms the 802.11 system despite MIMA-MAC's inefficiency in transmitting TCP-ACKs.

The reason for the rapid throughput degradation in case of $N_{hops} \leq 4$ for the 802.11 system can be explained with the similar argument we have used in Section 3.5.5 for CBR traffic model simulations. Similar to the CBR case, when N_{hops}=4, the TCP throughput is less than $\frac{1}{4}$ of the one-hop case because only one transmission can exist in the network at a time in order to provide collision free transmissions. If there are more than one transmission in the network, they will collide with each other and trigger TCP to lower its transmission rate. Therefore, the transmission rate will be maintained such that there is only one transmission in the network at a time. Different from the CBR case, however, now we have TCP-ACKs transmitted to the source from the destination in the opposite direction of TCP-DATA packets. As we have shown in Section 2.1.3, to TCP-DATA transmission, TCP-ACKs are another source of interference, which might increase collisions in the network and thus decreases the TCP throughput even more. Therefore, the performance of TCP is lower than the CBR case. For $N_{hops} > 4$, multiple transmissions can take place simultaneously and thus the TCP throughput is not so significantly degraded as N_{hops} increases as for $N_{hops} \leq 4$ case.

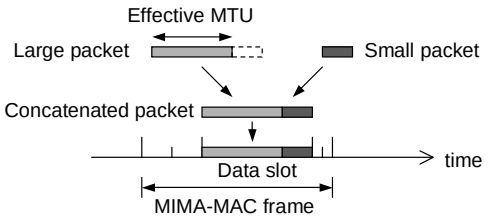

Figure 5.3: The basic idea of the TCP enhanced MIMA/AS-MAC protocol.

5.4 The TCP Enhanced MIMA/AS-MAC Design

The simulation results in the previous section clearly show that the MIMA-MAC system performs suboptimally when it has small packets to transmit. Since the MIMA/AS-MAC is based on the MIMA-MAC, it also has the same inefficiency problem. Therefore, in this section, we propose an enhanced MAC protocol, TCP enhanced MIMA/AS-MAC, which improves the efficiency of the MIMA/AS-MAC protocol for small packet transmissions.

5.4.1 Basic idea

Our goal is to enhance the MIMA/AS-MAC protocol to make it more efficient for transmitting small packets without wasting the data-slot of a MIMA-MAC frame. Our basic idea is whenever possible to transmit a small packet together with a large packet in the same data-slot. This is illustrated in Figure 5.3. We concatenate two packets when the packets satisfy the following conditions:

- **Size**: The size of the concatenated packet must be less than or equal to that of the data-slot.
- **Destination**: Both small and large packets have the same destination or when the packets have different destinations but the corresponding destinations can reply with an acknowledgement of packet reception.

We describe the details of the protocol in the following subsection.

5.4.2 TCP enhanced MIMA/AS-MAC protocol

We make the following modifications to the original MIMA/AS-MAC protocol to improve the efficiency of small packet transmission:

Effective MTU

To ensure that the size of the concatenated packet does not exceed that of the data-slot, instead of using actual maximum transmission unit (MTU) of the network, we use an effective MTU that is smaller than the actual MTU, so that the higher layer protocol hands down packets that can always be concatenated with a small packet when there is one. The size of the effective MTU is determined by subtracting the size of the small packet (around 100 bytes) from the actual MTU as

$$\texttt{sizeof}(\text{MTU}_{effective}) \leq \texttt{sizeof}(\text{MTU}_{actual}) - \texttt{sizeof}(\text{small packet}) \qquad (5.1)$$

where, $\text{MTU}_{effective}$ is the effective MTU, MTU_{actual} is the actual MTU of the network, and $\texttt{sizeof}(\cdot)$ returns the size in bytes. As we described in Section 5.2.2, the size of a TCP-ACK packet is 20 bytes and the default size of a TCP-DATA is 512 bytes and generally set to a larger value. Assuming the size of the small packets (including a MAC header, Physical Layer Convergence Procedure (PLCP) header, and preamble) to be 100 bytes based on the size of a TCP-ACK packet (40 bytes including IP header of 20 bytes) and that of the `data-slot` to be approximately 2200 bytes, the efficiency loss is approximately 4.5%. Since the maximum MTU size of the 802.11 based wireless ethernet is 2312 bytes [2], we might expect data packets with size close to this value from real traffic.

Multiple packet concatenation

To make sure that all the data packets are replied to with ACKs from their destinations, we concatenate the small packet to the large packet when the destinations of the both packets are the same or when their destinations are different from each other but the transmitter overhears a CTS transmission (not destined for the transmitter but for the other transmitter) from the small packet's destination, which implies that its destination is able to reply with an ACK. Therefore, to know whether or not the CTS is from the small packet's destination, we add a source address field to the CTS packet.

Batched acknowledgement

When the receiver receives multiple data packets from multiple transmitters, one from the intended transmitter with which it exchanged RTS/CTS control packets and the other from the unintended neighboring transmitter with which it did not, and if they are all destined for the receiver, it passes them up to the upper layer protocol and acknowledges the transmissions by replying with a single ACK packet with the multiple source addresses of the successfully received data packets as batched acknowledgments. For this purpose we add an additional destination address field to the ACK packet. For example, when the receiver receives two data packets from A and B simultaneously, the receiver replies with ACK(A,B) to node A and node B informing that it has received the packets successfully from A and B.

5.4.3 Operation

To make the proposed protocol clear, in Figure 5.4, we describe the operation of the protocol with an example of a simple wireless network. The network consists of four nodes each with two antennas and has a linear topology. Suppose a single TCP connection is established between the source (node 0) and destination (node 3), and

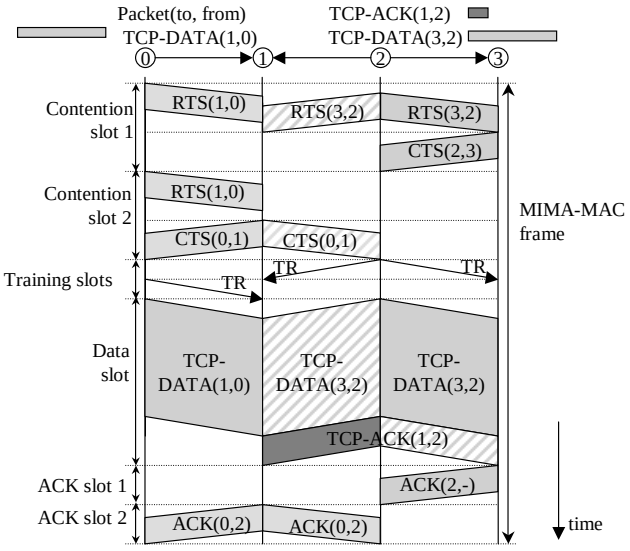

Figure 5.4: The operation of the TCP enhanced MIMA-MAC protocol for a simple four node linear network. For the ACK(a,b) packet, a and b denote the two different destination addresses. For all the other packets, (a,b) denotes the destination address a and the source address b of the packet.

node 0 and node 2 have TCP-DATA packets, TCP-DATA(1,0) and TCP-DATA(3,2), to transmit to the next-hop destinations, node 1 and node 3, respectively, where $Packet(a,b)$ denotes a packet with the destination address a and the source address b except for ACK packets. Notice that the size of TCP-DATA packets are limited to the effective MTU which is smaller than the size of the data-slot. Moreover, we assume that node 2 has a TCP-ACK(1,2), to transmit to node 1, which is opposite to the direction of the TCP-DATA flow. The two transmitters first contend with each other to acquire the channel for the TCP-DATA transmissions. During the negotiation period, node 2 and node 0 acquire the channel in the first and second contention slots, respectively. After transmitting the training sequence during the training-sequence slots, node 0 transmits TCP-DATA(1,0) to node 1 in the data slot. Since node 2 has a TCP-ACK to transmit to node 1 and it overheard a CTS transmission from node 1, the TCP-ACK is concatenated with TCP-DATA(3,2)

and transmitted in the same data slot, in which TCP-DATA(1,0) is transmitted. Since, node 1 has two receive antennas, it can receive TCP-DATA(1,0) from node 0 and both the TCP-DATA(1,2) and TCP-ACK(1,2) from node 2, simultaneously. Node 1 replies with a batched acknowledgement, ACK(0,2), where (a,b) denotes two destination addresses, indicating that it has received two data packets from the two transmitters, node 0 and node 2. Node 3 replies with ACK(2,-) indicating that it has received a single data packet from node 2.

When we add another TCP connection from node 3 to node 0 ($TCP_{3\rightarrow0}$), the TCP-DATA packets of $TCP_{3\rightarrow0}$ will have the same destination with the TCP-ACK packets of the TCP connection from node 0 to node 3 ($TCP_{0\rightarrow3}$). Therefore, now the TCP-ACK packets of $TCP_{0\rightarrow3}$ can be concatenated with the TCP-DATA packets of $TCP_{3\rightarrow0}$ and can be transmitted in the same data slot. Similarly, the TCP-ACK packets of $TCP_{3\rightarrow0}$ are concatenated with the TCP-DATA packets of $TCP_{0\rightarrow3}$.

5.4.4 Performance

We first evaluate the performance of the proposed MAC protocol over an ideal channel to see the effect of the packet concatenation on TCP performance. We use the same simulation setup that we used for the MIMA-MAC system and the 802.11 system in Section 5.3 and add the TCP performance of the TCP enhanced MIMA/AS-MAC system on to the previous results shown in Figure 5.2. Figure 5.5 compares the TCP performance of the TCP enhanced MIMA/AS-MAC system with that of the MIMA-MAC system and the 802.11 system. The simulation results show that when the number of hops between the source and destination (N_{hops}) is one or two, the performance of the TCP enhanced MIMA/AS-MAC system is similar to that of the MIMA-MAC system. This is because when N_{hops}=1, there are only the source node that transmits TCP-DATAs and the destination node that replies

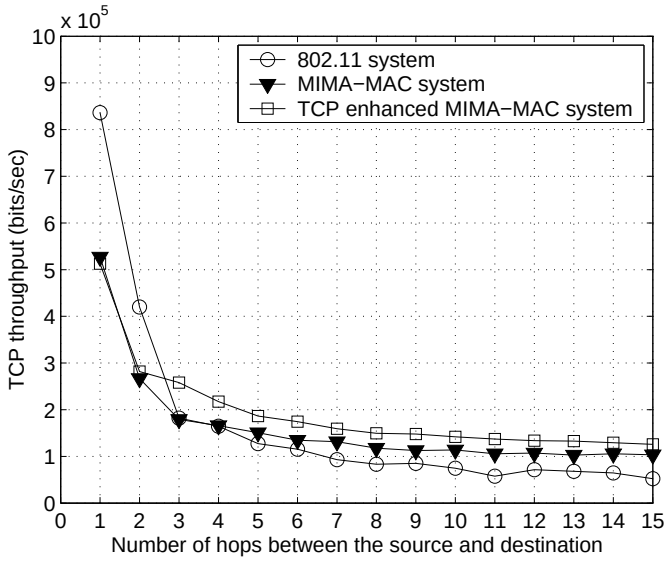

Figure 5.5: TCP throughput comparison for a linear topology network with a single TCP connection.

with TCP-ACKs and thus one cannot increase the system performance by concatenating a TCP-DATA and a TCP-ACK. When N_{hops}=2, there is one intermediate node between the source and destination, which can concatenate a TCP-DATA and a TCP-ACK and thus the TCP enhanced MIMA/AS-MAC system outperforms the MIMA-MAC system by approximately 6%. For $N_{hops} > 2$, the TCP enhanced MIMA/AS-MAC system gains approximately 21% to 44% of throughput improvement over the MIMA-MAC system. The simulation results show that the performance of the TCP enhanced MIMA/AS-MAC system is improved by increasing the efficiency of a small packet transmission.

5.5 Simulation in More Realistic Environments

In this section, we evaluate the TCP enhanced MIMA/AS-MAC system in more realistic environments. We simulate the TCP enhanced MIMA/AS-MAC system over a Rayleigh fading channel and use an MMSE receiver to differentiate the received

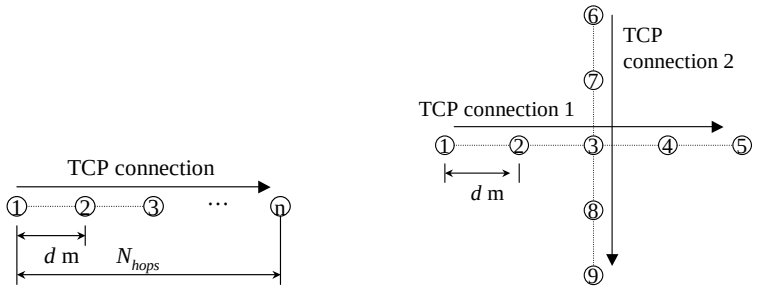

(a) Linear topology (b) Cross topology

Figure 5.6: The network configurations for the simulation. (d=140m)

signals. We also measure the performance of the TCP enhanced MIMA/AS-MAC system using an idealistic perfect receiver to show the upper bound of system performance. We compare the throughput of the TCP enhanced MIMA/AS-MAC system with that of the MIMA/AS-MAC system to show the performance gain we can achieve by increasing the efficiency of a small packet transmission and compare with that of the 802.11 system with Alamouti encoding (802.11-Alamouti) to see the performance gain over the conventional MAC protocol. We also measure TCP performance by turning off the link failure report (LFR) function in the MAC layer, which reports a link failure to the routing protocol, to see the effect of a link failure due to neighboring interference, which triggers a route rediscovery and an ARP (address resolution protocol) request. In our simulations, we assume that all the nodes are using two antennas.

5.5.1 Simulation setup

We use the following simulation setup:

Network configuration

We use two types of network topologies as shown in Figure 5.6: i) a linear topology and ii) a cross topology. For the linear topology network, we vary the number of

hops (N_{hops}) from 2 to 10. The nodes are evenly spaced and the distance between the neighboring nodes is set to 140m so that the next-hop of a packet becomes the closest adjacent node for a Rayleigh fading channel. As a more generalized network topology, we use the cross topology network, which consists of two 4-hop linear topology networks crossing each other's center node to show the effect of one TCP traffic flow crossing the another TCP flow.

Traffic model

We use TCP and the File Transfer Protocol (FTP) for the transport layer and application layer, respectively. The packet size of the TCP connection is set to 2048 bytes for both the 802.11 system and the MIMA/MAC system. The effective MTU of the proposed system is set to 2100 bytes (the actual MTU is 2200 bytes). Considering the IP and TCP headers, we set the packet size of TCP for the proposed system to be 2040 bytes. We simulate two types of TCP traffic models: i) a single TCP connection from source to destination and ii) two TCP connections, one from source to destination and the other from the destination to source. We add an additional TCP connection in the reverse direction to see how this might help the TCP enhanced MIMA/AS-MAC system during the packet concatenation process. Each of the TCP connections is an independent TCP connection and so any packet concatenation happens at the MAC layer.

Channel model

We use a Rayleigh fading channel model. Each entry of the channel matrix or vector is a zero mean circularly symmetric complex Gaussian random variable with variance of 1, $\mathcal{CN}(0,1)$. We also assume that channel varies very slowly and thus is fixed within a RTS-CTS-DATA-ACK exchange.

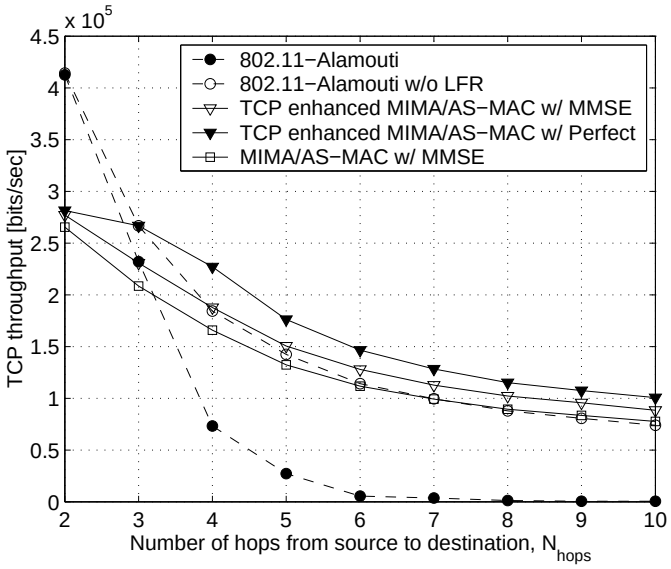

Figure 5.7: TCP throughput comparison for a linear topology network with a single TCP connection.

Physical layer parameters

Based on the the IEEE 802.11b implementation of ns-2, the transmit power is set to 24.5dBm. The carrier frequency is set to 2.4GHz and the data rate is set to 1Mbps. Assuming free space propagation, the path-loss exponent is set to 2. The reception threshold is set to -63.5dBm and the carrier sense threshold is set to -70.4dBm so that in an AWGN channel model the transmission range is 250m and the carrier sensing range is 550m.

5.5.2 Evaluation

We evaluate the performance of the proposed system by measuring TCP throughput. We evaluate the proposed system for i) the linear topology network with one TCP connection, ii) the linear topology network with two TCP connections, iii) the cross topology network with two TCP connections, and iv) the cross topology network with four TCP connections.

Linear topology network with one TCP connection

We first compare the TCP throughput of the proposed system with that of the 802.11-Alamouti system and that of the MIMA/AS-MAC system for the linear topology network with a single TCP connection. Figure 5.7 shows the simulation results. We also simulate the 802.11-Alamouti system (dashed lines) without the link failure report (LFR) to the upper layer routing protocol (here we used AODV) to see the effect of the route rediscovery on TCP throughput. All other systems are using the link failure report function as a default. For the MIMA/AS-MAC system and the TCP enhanced MIMA/AS-MAC system, we use an MMSE receiver. Moreover, to show the upper bound of the system performance, we also simulate the TCP enhanced MIMA/AS-MAC system using a perfect receiver that separates two simultaneously received data packets without error as long as the receiver has correct channel information.

The simulation results show that the proposed system with the MMSE receiver outperforms the MIMA/AS-MAC system by approximately 4% to 15%. The throughput improvement of the proposed system comes from the increased efficiency of the small packet transmission. The improvement, however, is not so significant because when there is only one TCP connection, we can only satisfy one of the two conditions for the packet concatenation we described in Section 5.4.2, which is when a transmitter overhears TCP-ACK's destination transmitting a CTS.

For the 802.11-Alamouti system, TCP throughput gets extremely low when $N_{hops} \geq 4$. The primary reason for this is because the neighboring node's transmission, which the CSMA/CA mechanism cannot prevent, interferes the other node's transmission and eventually causes a link failure. This triggers route rediscovery and degrades the throughput of the system. To make matters worse, transmission failures of the address resolution protocol (ARP) [54] request packet (ARP-REQUEST) also degrade the system performance. Figure 5.8 illustrates a snap shot of packet

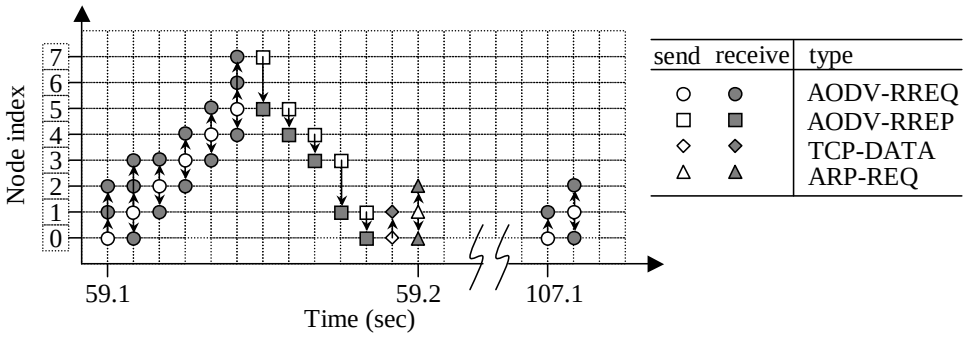

Figure 5.8: Illustration of the ARP request failure problem. The figure illustrates a snap shot of packet transactions in a linear topology network with 8 nodes. The discovered route is 0–1–3–4–5–7.

transactions between the nodes in a linear topology network with 8 nodes. Suppose the network has experienced a link breakage and is trying to discover a route to the destination again. As shown in the figure, node 0 floods a RREQ packet (drawn as a circle) and it is received by node 1 and node 2. The nodes that received the RREQ packet rebroadcast it unless the RREQ packet is destined for themselves. Since we are using a Rayleigh fading channel, how far (e.g. one or two hops) the RREQ packet can reach varies from time to time. After receiving the RREQ packet, the destination, node 7, replies with a RREP packet (drawn in a square). Since AODV selects the route with the minimum number of hops from the source to destination, for this example, the discovered route is "node 0 → node 1 → node 3 → node 4 → node 5 → node 7". Then node 0 transmits a TCP-DATA packet (drawn in a diamond) to its next hop, node 1. When node 1 receives the TCP-DATA packet, according to its routing table, it tries to forward the packet to its next hop, node 3. Unfortunately, if node 1 does not have the MAC address of node 3, which is the case for this example, node 1 has to discover the MAC address (hardware address) by broadcasting an ARP-REQUEST packet (drawn in a triangle). Although the RREQ packet successfully reached node 3 during the route discovery process, this time, due to a bad channel condition, the ARP-REQUEST packet fails to reach

node 3 and thus node 1 is unable acquire the MAC address and consequently node 1 cannot send the TCP-DATA packet to its next hop, node 3. Since, ARP does not retry to acquire the MAC address, the transmission is blocked for a long time and again triggers the route rediscovery process from the source, node 0. For an ideal channel case, which we have shown in Figure 5.2, the ARP-REQUEST transmission failure problem is not observed due to the static channel condition.

Moreover, we measure the performance of the 802.11-Alamouti system by disabling the link failure report function and compare it with the TCP enhanced MIMA/AS-MAC system, which can mitigate interference from neighboring nodes. The proposed system with the MMSE receiver outperforms the 802.11-Alamouti system without LFR by approximately 2% to 20% for $N_{hops} \geq 4$. This is because the proposed system suppresses interference from neighboring nodes and improves the efficiency of the small packet transmission. When we compare the 802.11-Alamouti without LFR with the MIMA/AS-MAC system, which is inefficient for small packets, both systems show similar performance. This is because, for the 802.11-Alamouti system without LFR, the transmission rate of TCP is lowered to the point where the TCP packets are separated far enough so that they do not interfere each other's transmission and the MAC protocol does not report a link failure to the routing protocol, which reduces the overhead of a route rediscovery. Therefore, the performance degradation of the 802.11-Alamouti system without LFR is not so significant as the 802.11-Alamouti system with LFR and thus comparable to the performance of the MIMA/AS-MAC system, which suffers from the inefficiency of small packet transmission. When we use the perfect receiver for the proposed system, the throughput improvement is approximately 23% to 36% over the 802.11-Alamouti system for $N_{hops} \geq 4$. When $N_{hops} < 4$, there however is no or little interference from the neighboring nodes to suppress and since the 802.11-Alamouti system's efficiency for transmitting small packets is higher than that of the proposed system, the 802.11

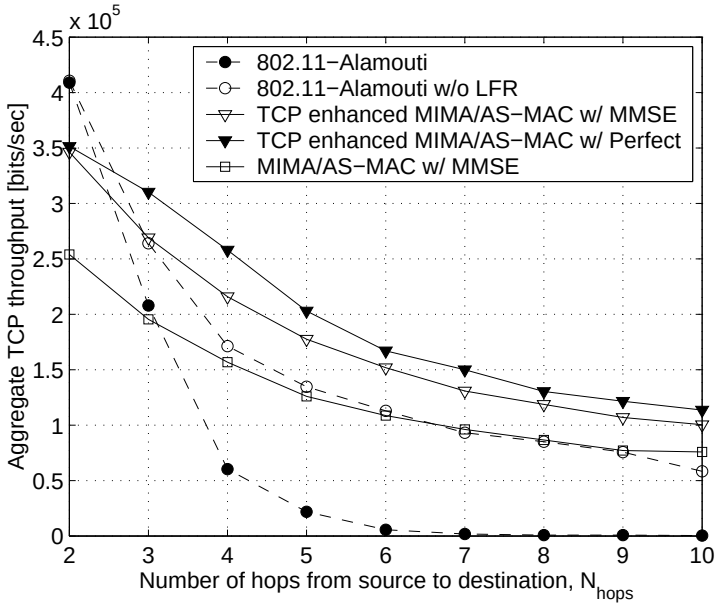

Figure 5.9: Aggregate TCP throughput comparison for a linear topology network with two TCP connections: one from the source to destination and the other from the destination to source.

system without LFR outperforms the proposed system.

Linear topology network with two TCP connections

Now, we add an additional TCP connection from the destination to source and compare the aggregate TCP throughput of the proposed system with that of the MIMA/AS-MAC system with the MMSE receiver and the 802.11-Alamouti system with and without LFR. The simulation results are shown in Figure 5.9. The performance of the proposed system with MMSE outperforms that of the MIMA/AS-MAC system with the MMSE receiver by approximately 32% to 41% and outperforms that of the 802.11-Alamouti system without LFR by approximately 26% to 72% for $N_{hops} \geq 4$. Moreover, by using the perfect receiver, the proposed system outperforms the 802.11-Alamouti without LFR by 51% to 95% for $N_{hops} \geq 4$. In this scenario, the performance improvement of the proposed system is greater than the previous single

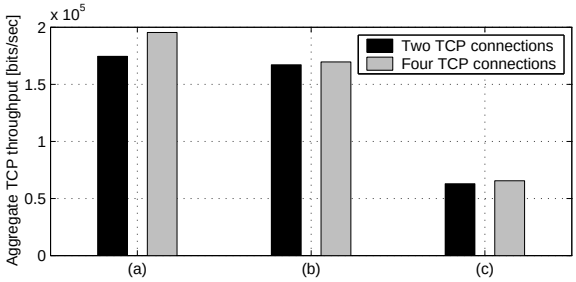

Figure 5.10: The aggregate TCP throughput comparison for the cross topology network with 9 nodes: (a) TCP enhanced MIMA/AS-MAC, (b) 802.11-Alamouti without LFR, and (c) 802.11-Alamouti.

TCP connection scenario. This is because, the reverse TCP-DATA flow from the destination to source helps increase the channel utilization by more compactly packing the channel with both TCP-DATAs and TCP-ACKs than the previous single TCP connection scenario. Recall that the TCP enhanced MIMA/AS-MAC can concatenate two packets when their destinations are the same. Therefore, when there is the reverse TCP-DATA flow, the TCP enhanced MIMA/AS-MAC system can concatenate the TCP-ACKs of the forward TCP-DATA flow with the reverse TCP-DATAs and vice versa, which improves the resource utilization. The results show that the aggregate TCP throughput of the MIMA/AS-MAC system, which cannot concatenate multiple packets, and that of the 802.11-Alamouti systems, which are already fully utilizing the channel resource, are similar or slightly lower than those of the single TCP connection scenario because the two TCP connections have to share the channel resource with each other.

Cross topology network with two TCP connections

We now evaluate the TCP enhanced MIMA/AS-MAC system for the cross topology network with 9 nodes shown in Figure 5.6(b). We first simulate the system over the network with two TCP connections: one from node 1 to node 5 and the other from node 6 to node 9. We measure the TCP throughput of each TCP connection.

Number of TCP connections	2	4
TCP enhanced MIMA/AS-MAC	0.98	0.93
802.11-Alamouti	0.99	0.84
802.11-Alamouti w/o LFR	0.84	0.61

Table 5.1: Comparison of Jain's fairness indexes for the cross topology network

The TCP enhanced MIMA/AS-MAC system is compared with the 802.11-Alamouti systems with and without LFR. The simulation results are shown in Figure 5.10. The results show that the aggregate TCP throughput of the TCP enhanced MIMA/AS-MAC system is close to the TCP throughput measured over the linear topology network with a single TCP connection shown in Figure 5.7. This is because for the cross topology network case, node 3 is responsible for delivering both of the TCP flows and thus it becomes a bottleneck of the network and limits the performance of the network. Therefore, the aggregate TCP throughput of the cross topology network does not exceed the TCP throughput of the linear topology network case. This is also the case for the 802.11-Alamouti systems and the results show that the aggregate TCP throughput is similar to that of the linear topology network case.

We also compare the fairness of the systems by comparing the throughput of two TCP flows. The fairness of the two TCP flows is measured by Jain's fairness index [55]. We use Jain's fairness index instead of the fairness ratio (FR) we used in (3.9) because Jain's fairness index can be used for multiple traffic flows whereas the fairness ratio is limited to only two traffic flows. We measure the fairness of more than two traffic flows for the four TCP connection case. Table 5.1 shows the comparison of the three systems' fairness for the cross topology network. Jain's fairness index ranges from 0 to 1, where the index value 1 indicates perfect fairness. The results show that the TCP enhanced MIMA/AS-MAC system and the 802.11-Alamouti system without LFR result in a fairness index close to one, which indicates that the two TCP connections provide similar throughput. The fairness index of the 802.11-Alamouti system with LFR, however, is approximately 0.84, which indicates

that one TCP connection has higher throughput than the other. This is because the 802.11-Alamouti system with LFR suffers from the unsolved hidden node problem and might cause a link failure, which triggers a route rediscovery. In the cross topology network, either self interference or interference from the other TCP flow causes a link failure. When a node has data to send over this link, it tries to recover a route by flooding a route request packet. Since there is another TCP traffic crossing the route to the destination, it might interfere the flooding and thus the route rediscovery might fail, which degrades the throughput of the TCP connection. Therefore, one TCP connection has higher throughput than the other TCP connection and as a result the 802.11 system with LFR has lower fairness index than the other two systems.

Cross topology network with four TCP connections

Now we add two additional TCP connections for the cross topology network, one from node 5 to node 1 and the other from node 9 to node 6. Figure 5.10 compares the aggregate TCP throughput of the three systems. Similar to the linear topology case with a reverse direction traffic flow, for the TCP enhanced MIMA/AS-MAC, adding a reverse direction TCP flow helps increase the channel utilization and increases the aggregate TCP throughput. Due to the bottleneck node at the center of the network (i.e. node 3), the performance however does not exceed that of the linear topology case. For the 802.11-Alamouti systems, since they are already fully utilizing the channel resources, the performance is almost the same as that of the cross topology network with two TCP connections. Table 5.1 shows the comparison of the Jain's fairness index of the three systems for the cross topology network with four TCP connections. The results show that the 802.11-Alamouti system suffers from unfairness due to the route rediscovery process we described in the cross topology network with two TCP connection case.

Chapter 6

Designing a MAC for Ad Hoc Routing Protocols Using Multiple Antennas

In the previous chapters, we have focused on designing MAC protocols that address the problems of conventional MACs and TCP by utilizing MIMO technologies to mitigate neighboring interference and fading and by selecting a transmission mode based on the types of MAC packets inside the MAC design. As a prelude to our future work, in this final study, we demonstrate how we can address other higher layer problems by controlling the transmission mode based on the type of higher layer packets. As an example, we show that we can improve the performance of a system that uses reactive ad hoc routing protocols by using different transmission modes for the route discovery phase, which uses broadcast packet transmission for a target discovery, and actual data transmission, which uses unicast packet transmission.

6.1 Background

In this section, we present background material for the following sections. We first present an overview of flooding and ad hoc routing protocols. Then, we present the key differences between broadcast and unicast packet transmissions.

6.1.1 Flooding

In a wireless network, flooding is a basic operation for target discovery [56]. A source floods query packets into the network to search for a destination (target). Since the source does not know how to reach the destination or even whether the destination exists or not, the query packet is broadcast. The source broadcasts the query packet to neighboring nodes and the neighboring nodes re-broadcast the query packet to their neighboring nodes hoping that it will propagate through the network and eventually reach its intended destination successfully. When the query packet reaches the destination, it usually replies with a unicast packet informing the source of its existence and/or route information from the source to destination. If the purpose of target discovery was to find a route to the destination such as in ad hoc routing protocols [27, 28], the source will use the replied route information and transmit unicast data packets along the route so discovered. Sensor networks also use flooding for discovering sensors with particular data and drawing the discovered data to the source [57]. Service discovery is another example that employs flooding for searching for a particular service in a network [58]. A node that has the requested service responds with a service reply to the source and the source uses the service. Here we observe a communication pattern that uses "broadcast" packet transmissions for target discovery and "unicast" packet transmissions for actual data packet transmissions. In the next subsection, we present an overview of ad hoc routing protocols as a typical example.

6.1.2 Ad hoc routing protocols

Ad hoc networks consist of mobile nodes communicating over a wireless channel without any infrastructure. Since, the topology of a wireless ad hoc network changes frequently due to the mobility of nodes and fluctuation of the channel, maintaining correct route information in the network is a great challenge.

Two of the best known ad hoc routing protocols, which discover a route from a source to destination in an on-demand (reactive) fashion, are Dynamic Source Routing (DSR) [28] and Ad-hoc On-demand Distance Vector (AODV) [27]. Both routing protocols search for a route to the destination only when they have data to send, and they do not maintain routes to all possible destinations in order to reduce routing overhead. The key difference between the two routing protocols is that DSR is based on a source routing protocol, which means that the full route information from the source to destination is in the data packet itself, whereas AODV maintains the next-hop information to the destination in the routing tables of intermediate nodes along the route and the data packet does not carry the full route but only the destination address.

Although, DSR and AODV are different in a number of aspects [59,60], both protocols consist of two common operations: *route discovery* and *route maintenance*.

Route discovery Reactive ad hoc routing protocols discover a route from a source to destination by "flooding" a broadcast control packet, which is called a route-request (RREQ) packet, to its neighboring nodes. When the RREQ packet finally reaches its destination, the destination replies with a route-reply (RREP) packet along the reverse route to the source with the route information. When the query fails, which is implicitly detected by a route-discovery timeout, the source retries with an increased route-discovery timeout assuming that the target might be located farther away from the source.

Route maintenance Because of node mobility and varying channel conditions, ad hoc networks frequently experience link failures. To cope with the changes in network topology, ad hoc routing protocols have to provide a route maintenance capability that maintains the route between the source and destination in case of link failures. In general, the node that detected a link failure generates a route-error (RERR) packet and notifies the nodes along the reverse route of the link failure. The nodes that received the RERR update their cache (or routing table) by marking or deleting the invalid route information so that the route is not used in the future.

6.1.3 Comparison of MAC layer broadcasting and unicasting

As shown in Table 6.1.3, there are a number of different characteristics between MAC layer broadcast and unicast packet transmission, which indicates that we might need to use different transmission modes for the different type of packets adaptively to improve network performance. A fundamental difference between broadcast and unicast packets is that while a broadcast packet is destined to all the neighboring nodes, a unicast packet is only destined to one particular destination. In general, when a receiver successfully receives a broadcast packet, it does not reply with any acknowledgement, whereas when it receives a unicast packet, it replies with an acknowledgement packet informing the receiver that it received the unicast packet correctly. Therefore, the transmitter knows whether or not the transmission was successful only for unicast packet transmissions and thus can use a retransmission scheme to increase the reliability of a link only for these packets. Moreover, usually, a broadcast packet is used for control or query purposes and thus its packet size is small, whereas a unicast packet is used for delivering actual data with relatively large size compared to the broadcast packet. Since the broadcast packet is mostly for control or queries, the transmitter sends out broadcast packets less frequently than data packets. To improve overall network performance, we need to take these

	Broadcast	Unicast
Destination	unspecified	specified
Content	control/query	data
Size	small	large
Feedback	no	yes
Retransmission	no	yes
Frequency	low	high

Table 6.1: Comparison of MAC layer broadcast and unicast packet transmissions

differences into account and control the transmission modes in the physical layer.

6.2 Key Problems

In this section, we present the key problems of broadcast packet transmission over wireless fading channels and their impact on ad hoc routing protocols.

6.2.1 Broadcast packet transmissions over a fading channel

For a wireless channel that has only the path-loss effect, a successful broadcast packet transmission is guaranteed if the distance between the transmitter and receiver is sufficiently close. In reality, wireless channels suffer from fading, which causes packet drops. Therefore, if we want to have the same reliability as the path-loss only channel case, either the destination has to be closer or we need to use some fading mitigation scheme to increase the reliability of the link.

For example, consider a broadcast packet transmission over a Rayleigh fading channel from a source node, S, to neighboring nodes A, B, and C as shown in Figure 6.1(a). Since the transmitted signal's power decreases as the distance between the source and destination increases, the relation between the average received power at the three nodes can be expressed as

$$\bar{\gamma_A} > \bar{\gamma_B} > \bar{\gamma_C} \tag{6.1}$$

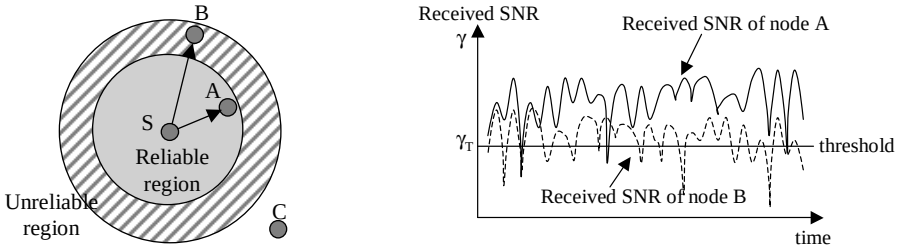

(a) A network configuration (b) Received SNR

Figure 6.1: An illustration of a packet transmission from the source node, S, to node A, B, and C.

where, $\bar{\gamma_A}$, $\bar{\gamma_B}$, and $\bar{\gamma_C}$ are the average received power of nodes A, B, and C, respectively. The reliability of a link gets weaker as the distance between the transmitter and receiver increases. Figure 6.1(b) illustrates the received SNR with fading at node A and B. Assuming all the nodes have the same packet reception threshold γ_T, which guarantees a certain level of packet error probability (PEP), the figure clearly shows that while node B suffers from packet drops due to fading, node A, which is closer to the transmitter than node B, receives most of the packets transmitted from node S successfully. Therefore, for a broadcast packet to reach its neighboring nodes reliably, the distance between the source and the neighboring nodes has to be sufficiently close (closer than the path-loss only channel case) or the nodes have to use a physical layer scheme that can mitigate fading.

In contrast to the broadcast packet transmission, a unicast packet transmission can take advantage of a retransmission mechanism. When a unicast packet is dropped due to fading, the transmitter can detect the packet drop and can retransmit the packet. As shown in Figure 6.1(b), since the received signal's SNR fluctuates over time, at the time of retransmission, the channel condition might be good enough and thus the receiver might receive the retransmitted packet successfully. Therefore, a unicast packet transmission can use the retransmission mechanism as a form of temporal diversity [10] and mitigate fading, which increases the reliability of a link.

6.2.2 Impact of a route discovery failure on system performance

Consider a network employing a reactive ad hoc routing protocol. When a source has data to send to its destination, which is, for example, n hops away from the source, it first initiates a route discovery by flooding a query packet, RREQ, to its neighboring nodes. If we assume a Rayleigh fading channel and assume that the distance between adjacent nodes are not sufficiently close enough for a successful packet transmission over a Rayleigh fading channel (i.e. a network with a low node density), the connectivity of the network is too weak for a broadcast packet transmission and thus the RREQ packet has a low probability of reaching its destination, which might lead to a route discovery failure. The source repeats broadcasting a RREQ packet until it finds the route or it fails. Obviously, as the number of route discovery attempts increases, the routing overhead increases and thus the throughput of the network is degraded by the increased routing overhead.

For example, AODV and DSR employ a flooding mechanism called "expanding ring search" to search for a destination [23, 27, 28]. The expanding ring search mechanism does not flood the entire network but tries a number of times expanding the searching area progressively for every attempt to reduce the flooding overhead at the cost of increased latency. Each RREQ packet has a limited number of hops that it can be re-broadcasted. Every time it is re-broadcasted by other nodes, the hop count value is decreased by one. When the count reaches zero, the RREQ is no longer re-broadcasted and thus we can control the size of the flooding area. If the RREQ fails to reach its destination, the source expands the size of the ring (increases the number of hops) and tries again. For example, in the case of the ns-2 implementation of AODV [23], the route-discovery-timeout value, TO_{RREQ}, is calculated as follows

$$TO_{RREQ} = 2 \times N_r \times N_{TTL} \times T_{RTT} \tag{6.2}$$

where, N_r is the number of retries for route discovery, N_{TTL} is the size of the ring for the expanding ring search in number of hops, and T_{RTT} is the estimated round trip time for a one-hop distance. For every retry, N_r and N_{TTL} is incremented by one and two, respectively, and thus from (6.2) TO_{RREQ} increases as the number of retrials increases until it reaches the maximum timeout value (10sec for the ns-2 implementation). Moreover, when the number of retransmissions reaches three, the source uses the maximum timeout value as the route-discovery-timeout. The increased route-discovery-timeout value increases the routing overhead even more and thus degrades the performance of the network.

6.3 Route Discovery: Conservative and Aggressive Approaches

We have shown how broadcast packet transmission over a wireless channel suffers from fading and its impact on the route discovery process of a routing protocol, which increases a route discovery overhead and thus degrades the system performance. Fortunately, when nodes are equipped with multiple antennas, we can mitigate fading and significantly reduce packet drops by simply utilizing multiple antennas in spatial diversity mode. We consider two approaches in using spatial diversity:

- **Conservative approach**: Increase the reliability of a link for both broadcast and unicast packet transmissions by employing spatial diversity for both types of packets.
- **Aggressive approach**: Use spatial diversity only for broadcast packet transmissions and use other transmission modes that can increase the capacity of the link such as spatial multiplexing for unicast packet transmissions.

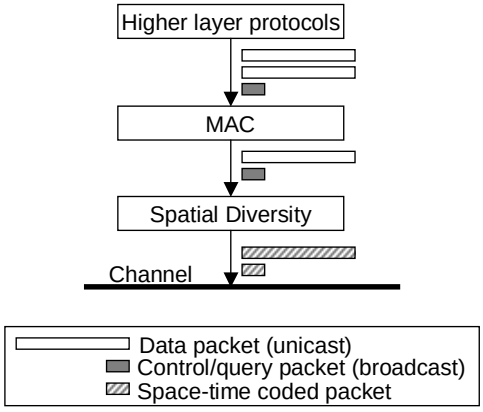

Figure 6.2: Illustration of a conservative MAC design utilizing multiple antennas in the physical layer for spatial multiplexing.

6.3.1 Conservative approach

In the conservative approach, we use spatial diversity for both broadcast and unicast packets. Spatial diversity, however, only provides a logarithmic increase of the channel capacity whereas spatial multiplexing provides a linear increase. As we have discussed in the previous section, since the route discovery packets (broadcast packets) are generally small in size and they are injected into the network only when the source needs to search for the route to the destination, which is not frequent, using spatial diversity for broadcast packet transmissions is a reasonable choice. After the source acquires the routing information, however, large data packets (unicast packets) are transmitted, which might also require increased link capacity. Since a unicast packet transmission can employ a retransmission scheme, this will work as temporal diversity [10] in a fading channel and will help compensate possible packet drops due to fading. Therefore, as shown in Figure 6.2, using spatial diversity for both broadcast and unicast packet transmissions might be too *conservative* and might limit the throughput of the network.

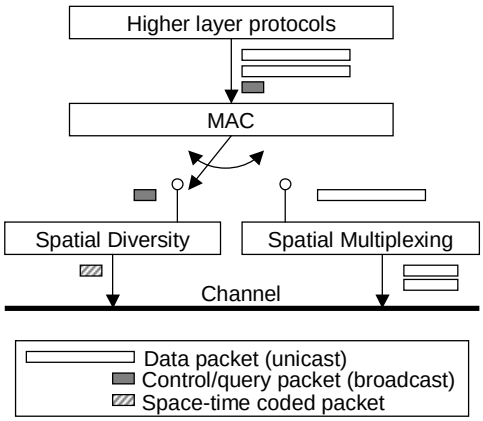

Figure 6.3: Illustration of the basic idea of an aggressive cross-layer MAC design using spatial diversity for broadcast packets and spatial multiplexing for unicast packets.

6.3.2 Aggressive approach

To improve the throughput of a multi-hop wireless network, we investigate transmission modes that can increase the data rate for the unicast packet transmissions. For example, as shown in 6.3, we may use spatial multiplexing for unicast packet transmissions and thus increase the link capacity, while using spatial diversity for broadcast packet transmissions and thus improve the link reliability. Using a different transmission mode for unicast packet transmission other than the one that the nodes used for the route discovery, however, might create another problem due to the discrepancy between the reliabilities provided by the different transmission modes, especially when the reliability of the broadcast packet transmission is higher than that of the unicast packet transmission. We present this problem and a possible solution in detail in the next section.

6.4 Aggressive MAC Design

In this section, we first present the basic idea of our aggressive MAC design approach, then present the a new problem arising from the use of different transmission modes for different types of packets, and finally present the details of the proposed aggressive MAC design.

6.4.1 Basic idea

Our basic idea is to control the transmission modes, which provide a variety of reliabilities and data rates, based on the "type" of a packet by utilizing a flexible MIMO physical layer. We can consider the flexible physical layer as a "knob" that provides a number of transmission modes that have different levels of reliability and rates, and the MAC protocol as a controller that controls the knob appropriately. Figure 6.3 shows this concept. In particular, for broadcast packet transmission, we increase the reliability of a link by using spatial diversity to improve the route discovery process, and for unicast packet transmission we increase the data rate (capacity) of the link by using spatial multiplexing or some other transmission scheme that can provide higher data rate than spatial diversity to improve the throughput of the network. This approach could be considered *aggressive* in the sense that we are using less reliable transmission scheme than that we used for the route discovery to increase the data rate. In the next subsection, we present the *unequal reliability problem*.

6.4.2 Unequal reliability problem

The unequal reliability problem arises when the reliability of the transmission mode used for actual data delivery process (unicast packet transmission) is lower than that of the transmission mode used for the route discovery process (broadcast packet transmission). For example, suppose we use spatial diversity for the broadcast

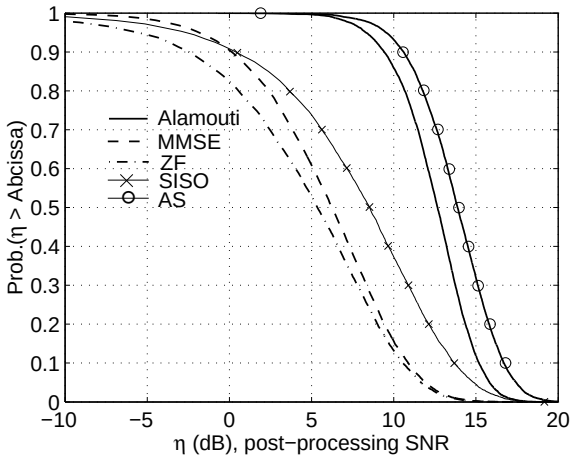

Figure 6.4: Comparison of the post-processing SNRs of the systems using the uncoded ZF, MMSE, Alamouti, antenna selection diversity (AS) receivers for the 2×2 MIMO configuration and a SISO system ($\rho = 10dB$).

packet transmission and use spatial multiplexing for the unicast packet transmission over a Rayleigh fading channel. Since the order of diversity provided by spatial diversity is higher than that provided by spatial multiplexing, the reliability of the link seen by the broadcast packet is higher than that seen by the unicast packet. In other words, although the link is not reliable enough to transmit a unicast packet using spatial multiplexing, it might successfully deliver a broadcast packet by using spatial diversity. Therefore, when a route request packet is broadcast over such a link by using spatial diversity, the link will successfully deliver the route request packet to the next hop and a routing protocol might consider this link as a part of a route to the destination. If, however, this link becomes a part of the route, a unicast packet transmission over the link using spatial multiplexing might fail because the link is not sufficiently reliable for a unicast packet transmission using spatial multiplexing. Since the purpose of a route discovery process is to find a route that can deliver unicast packets reliably to the destination, finding a route with unreliable links for a unicast packet transmission is a serious problem. Moreover,

when the routing protocol uses the hop count metric as the route selection criterion, which selects the shortest route to the destination, it will select a route with the longest possible hops [61], which means that it will select the weakest possible links seen by a route request packet using spatial diversity, and thus when a unicast packet is transmitted over the selected route using spatial multiplexing, the transmission will be more likely to fail.

We can measure the reliability of the transmission modes and receivers by measuring the post-processing SNR. Figure 6.4 shows a comparison of the distribution of the post-processing SNRs of the two spatial multiplexing systems using a zero-forcing (ZF) and a minimum mean-square error (MMSE) receiver, two spatial diversity systems using Alamouti encoding and antenna selection diversity (AS), and a conventional single-input-single-output (SISO) system. For multiple antenna systems, the simulations are performed for a MIMO configuration with two-transmit ($M_t = 2$) and two-receive ($M_r = 2$) antennas. The received SNR is set to $\rho = 10dB$. The post-processing SNRs are measured by Monte Carlo simulations. For the simulations, we generate 10,000 uncorrelated Rayleigh fading channel realizations. The simulation results show that the post-processing SNRs of the spatial diversity systems are much higher than those of the spatial multiplexing systems. The SNR loss of the spatial multiplexing systems using a linear receiver comes from the fact that only $\frac{1}{M_t}$ of the total transmit power is allocated to each transmit antenna and the receiver does not coherently combine the received signals across the receive antennas [5]. Moreover, of the spatial diversity systems, the system using antenna selection diversity is superior to the system using Alamouti encoding. This is because the transmitter of the antenna selection diversity system is utilizing feedback information from the receiver whereas the Alamouti system does not [5].

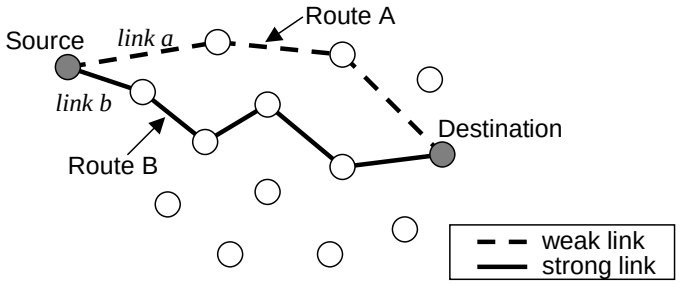

Figure 6.5: Illustration of two types of routes. *Route A*: a route discovered using the minimum number of hops as the route selection metric. *Route B*: a route discovered with the increased reception threshold.

6.4.3 The proposed aggressive MAC

We propose an aggressive MAC design that addresses the unequal reliability problem by increasing the reception threshold of the broadcast packet and by further improving the quality of a link with feedback information from the receiver.

Increased reception threshold

To address the unequal reliability problem, we increase the reception threshold, Th_r, by β (> 1) for the broadcast packets so that the route discovery packet does not find the route with the weakest possible links. In other words, we are shrinking the transmission range for the broadcast packets. This will increase the number of hops to the destination but makes the reliability of each link not too low for the unicast packet transmission to succeed. For example, in Figure 6.5, instead of selecting the shortest route with the weak links (Route A) to the destination, by increasing the reception threshold to $\beta \cdot \mathrm{Th}_r$, we select Route B, which consists of more hops but stronger links than those of Route A. In our experiment, we choose the value of β by simulations so that the throughput is maximized. If β is too small (≈ 1), the unicast packet transmission will suffer from low channel reliability. On the other hand, if β is too large, the number of hops to the destination will increase too much

and eventually degrade the system performance. One drawback of increasing the reception threshold is that it might reduce the network connectivity.

Unicast packet transmission with feedback information

To improve the reliability of the unicast packet transmission, besides spatial multiplexing, we employ antenna selection diversity and an adaptive modulation scheme with feedback information from the receiver. The feedback information can be obtained by employing the basic request-to-send (RTS)/clear-to-send (CTS) exchange protocol before the actual data packet transmission. The receiver first estimates the channel during the period of the RTS packet reception and sees if the channel is appropriate for spatial multiplexing. That is, the receiver calculates the post-processing SNRs of the data streams and sees if they are all above the reception threshold. If all the estimated post-processing SNRs are above the reception threshold, this information is fedback to the transmitter using the CTS packet and then the transmitter uses spatial multiplexing for the data packet transmission. Otherwise, the receiver feedbacks the indexes of the transmit antennas that satisfy the reception threshold of the lowest data rate to the transmitter and the information of the modulation schemes each transmit antenna can use in the CTS packet. Since, we will not use some of the transmit antennas, whose data streams' post-processing SNRs are lower than the lowest reception threshold, we can increase the selected antennas' transmit power. The receiver takes this into account in determining the modulation scheme for the selected transmit antennas. The transmitter then uses the information extracted from the CTS packet to select the transmit antennas and the modulation schemes for the unicast packet transmission.

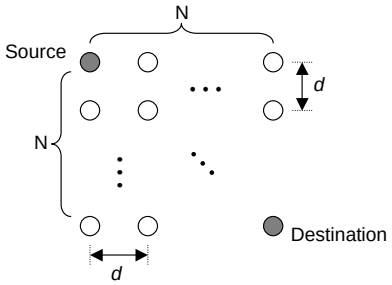

Figure 6.6: Illustration of the $N \times N$ lattice topology network.

6.5 Simulation Results

To validate our approach, we compare the aggressive MAC system and the conservative MAC system. Both approaches are implemented in ns-2. We use AODV for an ad hoc routing protocol. We measure the performance of the systems by measuring the constant-bit-rate (CBR) throughput of the network by varying the size and density of the network. The throughput is measured after the source finds the route to the destination and we turn off the link failure reporting function at the MAC layer to exclude the effect of the link failure due to interference from neighboring nodes.

6.5.1 Simulation setup

The simulation setup is as follows:

Network topology

As shown in Figure 6.6, we use a lattice topology network for the simulations to provide a number of routes from the source to destination. The source and destination (colored in gray) are located at the upper left corner and the lower right corner of the network, respectively. We vary the size of the network from 3×3 (9 nodes) to 7×7 (49 nodes) and vary the density of the network by changing the distance

between the adjacent nodes d=50m, 75m, and 100m.

Traffic model

We use a CBR traffic model to measure the throughput of the network. The CBR packet size is set to 2048 bytes and the interval between the packets is set so that it will fully consume the channel. The CBR packets are transmitted from the source to destination.

Physical layer parameters

Each node is equipped with two antennas. For spatial diversity mode, we use Alamouti encoding with the data rate of 1Mbps assuming BPSK modulation. For spatial multiplexing mode, the data rate of each transmit antenna is set to 1Mbps with BPSK modulation and thus the total data rate of the link is 2Mbps. For spatial multiplexing, we use a ZF receiver to differentiate two independent data streams. The transmit power is set to 24.5dBm and the reception threshold, $Th_{r,\mathrm{BPSK}}$, is set to -63.5dBm for BPSK modulation. The carrier sensing threshold is set to -70.4dBm. When we are using antenna selection diversity, since the reception threshold of QPSK, $Th_{r,\mathrm{QPSK}}$ is double the reception threshold of BPSK [62], if the post-processing SNR is greater than or equal to double the reception threshold of BPSK, we use QPSK modulation, which increases the data rate of the link to 2Mbps.

6.5.2 Evaluation

We first search for the appropriate value of β for our aggressive MAC approach to increase the reception threshold for the broadcast packets. We use the 5×5 lattice topology network and measure the throughput of CBR traffic from the source to destination by varying β from 1 to 4 in 0.5 step increments. Figure 6.7(a) shows the

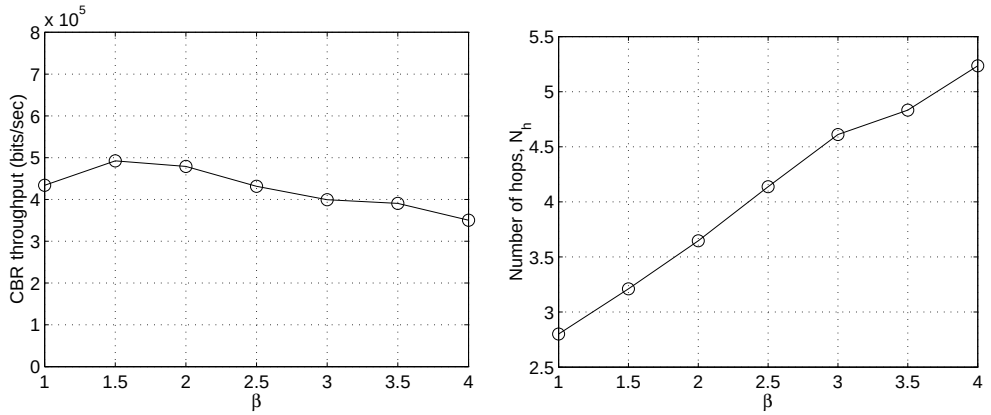

(a) Throughput (b) Number of hops

Figure 6.7: (a) CBR throughput and (b) the number of hops from the source to destination for a variety of β for the system using aggressive MAC with feedback in 5×5 lattice topology network with d=75m.

throughput of the CBR traffic and the number of hops from the source to destination as a function of β. The simulation results show that for $1 \leq \beta \leq 1.5$, the throughput increases as β increases. This is because the increased reception threshold for the broadcast packet shrinks the transmission range of the route discovery packet and thus the routing protocol finds the route with the shorter (stronger) links than for the case of $\beta = 1$. As shown in Figure 6.7(b), although the average number of hops to the destination is increased, the gain obtained from the increased reliability of the links of the route for the unicast packet transmission is larger than the loss from the increased number of hops to the destination and thus the overall throughput of the network improves. If however we increase the reception threshold for the broadcast packet too much (e.g. $\beta \geq 2$), the throughput degradation due to the increased number of hops to the destination dominates the overall network performance and thus the network throughput starts to degrade. Therefore, for our experiment, we select β=1.75, which is a value between 1.5 and 2.

Figure 6.8 shows the comparison of the systems using the aggressive MAC

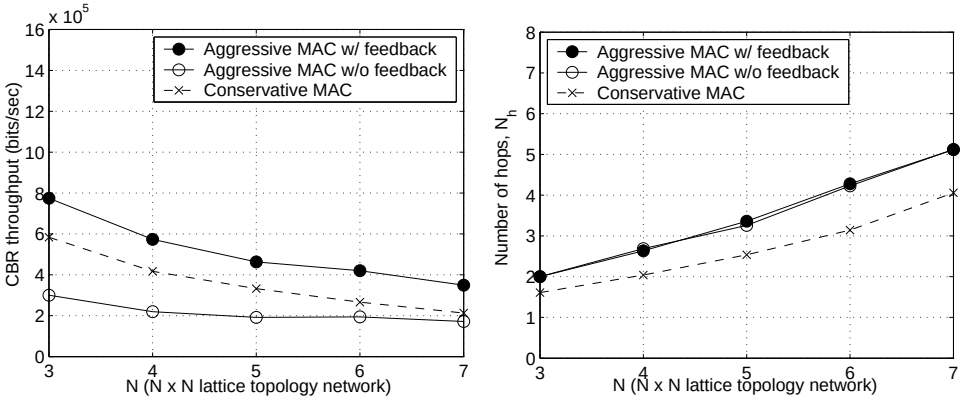

(a) Throughput (b) Number of hops

Figure 6.8: Comparison of the systems using the aggressive MAC with feedback information, the aggressive MAC without feedback information, and the conservative MAC for d=75m.

with feedback, the aggressive MAC without feedback, and the conservative MAC for d=75m. Figure 6.8(a) compares the CBR throughput by varying the size of the lattice topology network from 3×3 to 7×7. Figure 6.8(b) compares the three systems in terms of the number of hops of the discovered route. The simulation results show that when the transmitter does not utilize feedback information from the receiver, the conservative MAC system performs better than the aggressive MAC system due to the low reliability of the link for the unicast packet transmission. By improving the reliability of the link for the unicast packet transmission using the feedback information from the receiver and employing antenna selection diversity, the aggressive MAC system with feedback information outperforms the conservative MAC system. Since the aggressive MAC system increases the reception threshold for the broadcast packet, the number of hops of the discovered route is larger than that of the discovered route of the conservative MAC system. The system using the aggressive MAC with feedback information outperforms that using the conservative MAC by 33% to 64% in terms of throughput.

Now we decrease the distance between the neighboring nodes d from 75m to

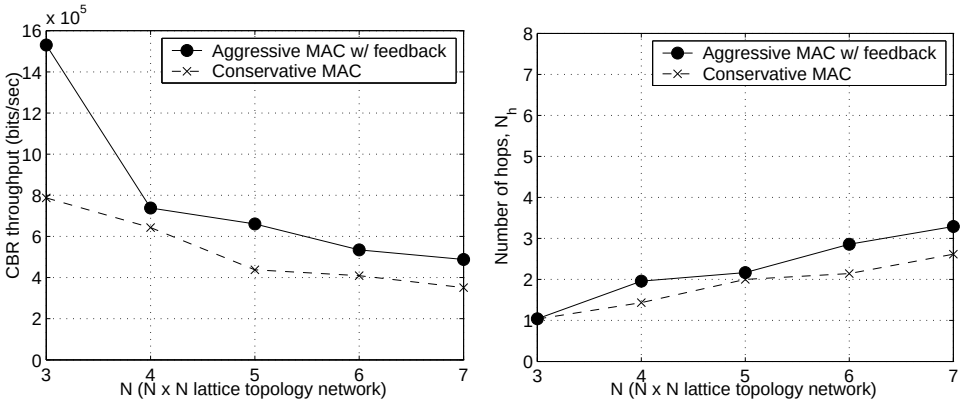

(a) Throughput (b) Number of hops

Figure 6.9: Comparison of the systems using the aggressive MAC with feedback information and the conservative MAC for d=50m.

50m to increase the density of the network. Figure 6.9 shows the simulation results for d=50m. We compare the aggressive MAC system with feedback and the conservative MAC system. Since the destination gets closer to the source, the number of hops to the destination becomes smaller and thus both systems' throughput is higher than the case of d=75m. Again, the system using spatial multiplexing and antenna selection diversity for the unicast packet transmission outperforms the one using spatial diversity. The throughput gain obtained from the use of the aggressive MAC with feedback information is approximately 14% to 94%. For the 3×3 lattice topology network, the distance between the source and destination is so close that the hop count for both of the systems equals approximately 1 and thus the throughput of the aggressive MAC system with feedback information is almost twice that of the conservative MAC system.

Figure 6.10 shows the simulation results for d=100m. When we increase the distance between the adjacent nodes, the hop count between the source and destination increases and thus the throughput of both systems gets lower than the cases of d=50m and 75m. The simulation results show that the aggressive MAC

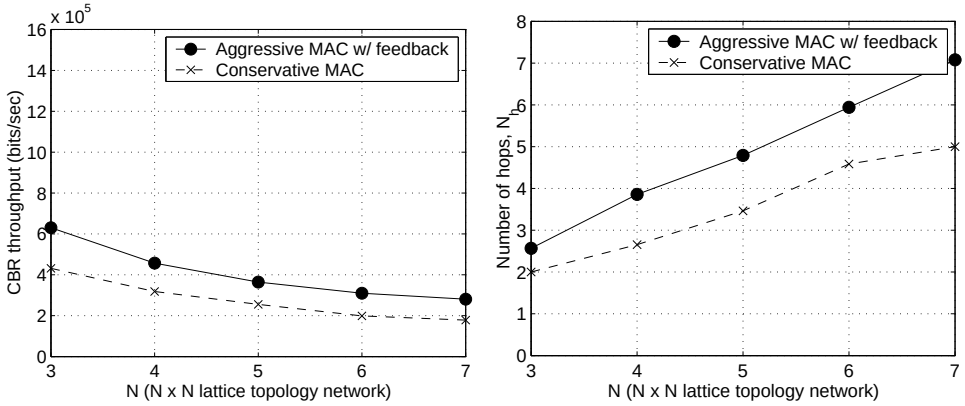

(a) Throughput (b) Number of hops

Figure 6.10: Comparison of the systems using the aggressive MAC with feedback information and the conservative MAC for d=100m.

system with feedback outperforms the conservative MAC system by approximately 43% to 57% in terms of throughput.

Discussion

The simulation results show that we can improve overall network performance by controlling the transmission mode of the physical layer based not only on the channel condition or the type of MAC packets but also on the type of higher layer packets, which need to utilize different capabilities of physical layer technologies. As an example, in our experiments, we investigated a system that uses a reactive ad hoc routing protocol that has two types of networking layer packets to transmit: broadcast packets for a route discovery and unicast packets for actual data transmission. As we described earlier, to improve overall network performance, we need to increase the reliability of a broadcast packet transmission rather than to increase its data rate whereas we need to increase the data rate of a unicast packet by sacrificing its reliability to a certain degree. To satisfy these requirements, we used MIMO in spatial diversity mode for broadcast packet transmission to increase the reliability

of a link and used MIMO in spatial multiplexing together with antenna selection diversity and the adaptive modulation scheme to increase the capacity of the link. The underlying intuition here is that we can address the problems of a certain layer by appropriately controlling the transmission mode of a physical layer and this can be accomplished by designing a MAC protocol with these problems in mind.

Chapter 7

Contributions and Conclusion

Our main contribution is to show that we are able to solve a number of problems across the protocol stack in multi-hop wireless networks by jointly designing MAC protocols with flexible MIMO physical layer techniques.

We first designed the Mitigating Interference using Multiple Antennas MAC (MIMA-MAC), which exploits the ability to mitigate interference from neighboring nodes by using MIMO in spatial multiplexing mode and thereby addresses the unfairness and throughput degradation problems of the conventional CSMA/CA based MAC protocols for multi-hop wireless networks.

Second, we further enhanced MIMA-MAC to mitigate fading as well as interference by fully utilizing multiple antennas in the physical layer. We proposed Mitigating Interference using the Multiple Antennas with Antenna Selection diversity MAC (MIMA/AS-MAC), which employs antenna selection diversity together with spatial multiplexing to achieve this goal.

Third, we showed preliminary simulation results of the MIMA-MAC system for TCP traffic in a multi-hop network and observed its benefit for TCP traffic, which suffers from self generated interference, as well as its limitation for small-sized packet transmissions. We proposed the TCP enhanced MIMA/AS-MAC, which addresses

the inefficiency problem for small-sized packet transmissions by concatenating a small packet with a large packet and transmitting it in the same data slot. By extensive simulations, we showed that designing the MAC jointly with the MIMO physical layer improves TCP performance.

Finally, we extended our study to a network using a flooding based target discovery protocol over a fading channel. Instead of using a conservative approach, which employs spatial diversity for both broadcast and unicast packet transmissions to mitigate fading, we proposed an aggressive approach, which controls a flexible MIMO physical layer to increase the capacity of a link for unicast packet transmission by using either spatial multiplexing or antenna selection diversity with an adaptive modulation scheme based on the channel condition and to increase the reliability of a link for broadcast packet transmission by using spatial diversity. By simulations, we showed that by controlling physical layer's transmission mode based on the type of a packet and channel condition, we can improve overall network performance.

Our study clearly showed that designing a cross-layer MAC protocol jointly with a flexible MIMO physical layer addresses a number of problems spanning the protocol stack: from a MIMO physical layer to TCP.

In fairness, our MIMA-MAC approach has drawbacks. First of all, the MIMA-MAC assumes that all the nodes are synchronized, which is a significant assumption that makes this protocol hard to deploy in a real world. Second, since the MIMA-MAC frame is fixed and large in size, it is inefficient for applications that transmit small packets most of the time.

As future work, we will extend our synchronous MIMA-MAC design with a fixed length MAC frame to an asynchronous design with a variable length MAC frame and will address some of the practical issues in deploying the MIMA-MAC. Moreover, we will apply our MAC design approach to other higher layer protocols

that might suffer from dynamically varying wireless channel conditions by first identifying communication patterns of the protocols and then designing a MAC protocol that controls the transmission mode of flexible physical layer technologies to address the problems of the protocol. It would also be of interest to design a MAC protocol for a network consisting of nodes with different number of antennas, which will generally be the case in a real world. In such a heterogeneous environment, the nodes will need to negotiate with each other about the number of antennas they should use so that they do not interfere each other's transmission and also improve overall network performance.

Appendix A

Abbreviations and Symbols

A.1 Abbreviations

ACK	acknowledgement
AIMD	additive-increase multiplicative-decrease
AODV	ad-hoc on-demand distance vector
ARP	address resolution protocol
AS	antenna selection
BER	bit-error-rate
CBR	constant-bit-rate
CSI	channel state information
CSMA/CA	carrier sense multiple access with collision avoidance
CTS	clear-to-send
CW	contention window
D-MAC	directional MAC
DCF	distributed coordination function
DIFS	DCF inter frame space
DSR	dynamic source routing

ECN	explicit congestion notification
EIFS	extended inter frame space
ETD	extreme throughput degradation
FCS	frame check sequence
FR	fairness ratio
FTP	file transport protocol
GPS	global positioning system
HTTP	hyper text transfer protocol
IP	Internet protocol
LAN	local area network
LFR	link failure report
LOS	line-of-sight
MAC	medium access control
MIMA-MAC	mitigating interference using multiple antennas MAC
MIMA/AS-MAC	MIMA-MAC with antenna selection diversity
MIMO-OFDM	MIMO orthogonal frequency division multiplexing
MIMO	multiple-input multiple-output
ML	maximum-likelihood
MMSE	minimum mean-square error
MTU	maximum transmission unit
NAV	network allocation vector
ODT	opposite direction traffic
OSI	open system interconnection
PEP	packet error probability
PLCP	physical layer convergence procedure
RERR	route error

RREQ	route request
RTS	request-to-send
SCMA	stream control medium access
SD	spatial diversity
SD-MAC	spatial diversity MAC
SDT	same direction traffic
SIFS	short inter frame space
SIMO	single-input multiple-output
SINR	signal-to-interference and noise ratio
SIR	signal-to-interference ratio
SISO	single-input single-output
SM	spatial multiplexing
SMTP	simple mail transfer protocol
SNR	signal-to-noise ratio
SSH	secure shell
STBC	space-time block coding
STTC	space-time trellis coding
TCP	transport control protocol
UDP	user datagram protocol
ZF	zero-forcing
ZMCSCG	zero mean circularly symmetric complex Gaussian

A.2 Symbols

$\approx$	approximately equal to
$\mathbf{0}_{m,n}$	$m \times n$ all zeros matrix
$\|a\|$	magnitude of a
$\mathbf{A}^{\dagger}$	pseudo inverse of $\mathbf{A}$
$[\mathbf{A}]_{i,j}$	i th row and j th column element of $\mathbf{A}$
$\|\mathbf{A}\|_F^2$	squared Frobenius norm of $\mathbf{A}$
$\mathbf{A}^H$	Hermitian of $\mathbf{A}$
$\mathbf{A}^T$	transpose of $\mathbf{A}$
$\mathcal{E}$	expectation operator
$\mathbf{I}_m$	$m \times m$ identity matrix
$\max(a_1, a_2, ..., a_n)$	maximum of $a_1, a_2, ..., a_n$
$\min(a_1, a_2, ..., a_n)$	minimum of $a_1, a_2, ..., a_n$
x^*	conjugate of x

Bibliography

[1] H. Zimmerman, "The OSI Model of Architecture for Open Systems Interconnection," *IEEE Trans. Commun.*, vol. 28, no. 4, pp. 425–432, Apr. 1980.

[2] *Wireless LAN Medium Access Control (MAC) and Physical Layer (PHY) Specification*, IEEE Std. 802.11, 1997.

[3] S. Xu and T. Saadawi, "Does the IEEE 802.11 MAC Protocol Work Well in Multihop Wireless Ad Hoc Networks?" *IEEE Commun. Mag.*, vol. 39, no. 6, pp. 130–137, June 2001.

[4] K. Xu, M. Gerla, and S. Bae, "How Effective is the IEEE 802.11 RTS/CTS Handshake in Ad Hoc Networks?" in *Proc. of IEEE Global Telecommunications Conf.*, Taipei, Taiwan, R.O.C., Nov. 2002, pp. 17–21.

[5] A. J. Paulraj, R. Nabar, and D. A. Gore, *Introduction to Space-Time Wireless Communications*. Cambridge University Press, 2003.

[6] I. E. Telatar, *Capacity of Mulit-antenna Gaussian Channels*, 3rd ed. Harlow, England: Addison-Wesley, 1999.

[7] P. W. Wolniansky, G. J. Foschini, G. D. Golden, and R. A. Valenzuela, "V-BLAST: An Architecture for Realizing Very High Data Rates Over the Rich-Scattering Wireless Channel," in *Proc. of ISSSE'98*, Pisa, Italy, Sept. 1998, pp. 295–300.

[8] D.-S. Shiu, G. J. Foschini, M. J. Gans, and J. M. Kahn, "Fading Correlation and Its Effect on the Capacity of Multielement Antenna Systems," *IEEE Trans. Commun.*, vol. 3, no. 48, pp. 502–513, 2000.

[9] S. M. Alamouti, "A Simple Transmitter Diversity Scheme for Wireless Communications," *IEEE J. Select. Areas Commun.*, vol. 16, no. 8, pp. 1451–1458, Oct. 1998.

[10] V. Tarokh, N. Seshadri, and A. R. Calderbank, "Space-Time Codes for High Data Rate Wireless Communication: Performance Criterion and Code Construction," *IEEE Trans. Inform. Theory*, vol. 44, no. 2, pp. 744–765, Mar. 1998.

[11] G. Holland, N. H. Vaidya, and P. Bahl, "A Rate-adaptive MAC Protocol for Multi-Hop Wireless Networks," in *Proc. of ACM Int. Conf. on Mobile Computing and Networking (MobiCom)*, Rome, Italy, July 2001, pp. 236–251.

[12] J. P. Monks, V. Bharghavan, and W. W. Hwu, "A Power Controlled Multiple Access Protocol for Wireless Packet Networks," in *Proc. of IEEE INFOCOM*, Anchorage, AL, Apr. 2001, pp. 219–228.

[13] E.-S. Jung and N. Vaidya, "A Power Control MAC Protocol for Ad Hoc Networks," in *Proc. of ACM Int. Conf. on Mobile Computing and Networking (MobiCom)*, Atlanta, Georgia, Sept. 2002, pp. 36–47.

[14] Y.-B. Ko, V. Shankarkumar, and N. H. Vaidya, "Medium Access Control Protocols Using Directional Antennas in Ad Hoc Networks," in *Proc. of IEEE INFOCOM*, Tel-Aviv, Israel, Mar. 2000, pp. 13–21.

[15] S. Bandyopadhyay, K. Hasuike, S. Horisawa, and S. Tawara, "An Adaptive MAC and Directional Routing Protocol for Ad Hoc Wireless Network Using

ESPAR Antenna," in *Proc. of ACM Int. Symposium on Mobile Ad Hoc Networking and Computing (MobiHoc)*, Long Beach, CA, Oct. 2001, pp. 243–246.

[16] A. Nasipuri, S. Ye, J. You, and R. E. Hiromoto, "A MAC Protocol for Mobile Ad Hoc Networks Using Directional Antennas," in *Proc. of IEEE Wireless Communications and Networking Conf. (WCNC)*, vol. 3, Chicago, IL, Sept. 2000, pp. 1214–1219.

[17] R. R. Choudhury, X. Yang, R. Ramanathan, and N. H. Vaidya, "Using Directional Antennas for Medium Access Control in Ad Hoc Networks," in *Proc. of ACM Int. Conf. on Mobile Computing and Networking (MobiCom)*, Atlanta, GA, Sept. 2002, pp. 59–70.

[18] S. Bellofiore, J. Foutz, R. Govindarajula, I. Bahceci, C. A. Balanis, A. S. Spanias, J. M. Capone, and T. M. Duman, "Smart Antenna System Analysis, Integration and Performance for Mobile Ad-Hoc Networks (MANETs)," *IEEE Trans. Antennas Propagat.*, vol. 50, no. 5, pp. 571–581, May 2002.

[19] M. F. Demirkol and M. A. Ingram, "Stream Control in Networks with Interfering MIMO Links," in *Proc. of IEEE Wireless Communications and Networking Conf. (WCNC)*, vol. 1, New Orleans, LA, Mar. 2003, pp. 16–20.

[20] K. Sundaresan, R. Sivakumar, M. A. Ingram, and T.-Y. Chang, "A Fair Medium Access Control Protocol for Ad-hoc Networks with MIMO Links," in *Proc. of IEEE INFOCOM*, Hong Kong, China, Mar. 2004, pp. 2559–2570.

[21] M. Hu and J. Zhang, "MIMO Ad Hoc Networks: Medium Access Control, Satuation Throughput, and Optimal Hop Distance," *Journal of Communications and Networks, Special Issue on Mobile Ad Hoc Networks*, vol. 6, no. 4, pp. 317–330, Dec. 2004.

[22] J.-S. Park, A. Nandan, M. Gerla, and H. Lee, "SPACE-MAC: Enabling Spatial Reuse in Using MIMO-Channel Aware MAC," in *Proc. of Int. Conf. on Comm.*, Seoul, Korea, May 2005.

[23] "The Network Simulator - ns-2," http://www.isi.edu/nsnam/ns/.

[24] C.-K. Toh, *Ad Hoc Mobile Wireless Networks: Protocols and Systems.* Prentice Hall, 2002.

[25] A. Kamerman and L. Monteban, "WaveLAN-II: A High-Performance Wireless LAN for the Unilicensed Band," *Bell Labs Technical Journal*, vol. 2, no. 3, pp. 118–133, Summer 1997.

[26] T. S. Rappaport, *Wireless Communications: Principles and Practice*, 2nd ed. Prentice Hall, 1996.

[27] C. E. Perkins and E. M. Royer, "Ad Hoc On-demand Distance Vector Routing," in *Proc. of IEEE Workshop on Mobile Computing Systems and Applications (WMCSA)*, New Orleans, LA, Feb. 1999, pp. 90–100.

[28] D. B. Johnson and D. A. Maltz, "Dynamic Source Routing in Ad Hoc Wireless Networks," in *Mobile Computing.* Kluwer Academic Publishers, 1996, ch. 5, pp. 153–181.

[29] V. Bharghavan, A. Demers, S. Shenker, and L. Zhang, "MACAW: A Media Access Protocol for Wireless LAN's," in *Proc. of ACM SIGCOMM'94*, New Orleans, LA, Aug. 1994, pp. 212–225.

[30] E. G. Larsson and P. Stoica, *Space-Time Block Coding for Wireless Communications.* Cambridge University Press, 2003.

[31] R. W. Heath Jr., *Space-Time Signaling in Multi-Antenna Systems.* Ph.D. Thesis, Stanford University, 2001.

[32] B. Holter, "On the Capacity of the MIMO Channel : A Tutorial Introduction," in *Proc. of IEEE Norwegian Symposium on Signal Processing*, Trondheim, Norway, Oct. 2001, pp. 167–172.

[33] D. Gesbert, H. Bölcskei, D. A. Gore, and A. J. Paulraj, "MIMO Wireless Channels: Capacity and Performance Prediction," in *Proc. of IEEE Global Telecommunications Conf.*, San Francisco, CA, Nov. 2000, pp. 1083–1088.

[34] R. W. Heath Jr., S. Sandhu, and A. J. Paulraj, "Antenna Selection for Spatial Multiplexing Systems with Linear Receivers," *IEEE Commun. Lett.*, vol. 5, no. 4, pp. 142–144, Apr. 2001.

[35] A. Ebner, H. Rohling, R. Halfmann, and M. Lott, "Synchronization in Ad Hoc Networks Based on UTRA TDD," in *Proc. of IEEE Int. Symposium on Personal, Indoor and Mobile Radio Communications (PIMRC)*, Lisbon, Portugal, Sept. 2002, pp. 15–18.

[36] M. A. Lombardi, L. M. Nelson, A. N. Novick, and V. S. Zhang, "Time and Frequency Measurements Using the Global Positioning System," *Cal Lab Int. J. Metrology*, vol. 8, pp. 26–33, July 2001.

[37] T. Tang and R. W. Heath Jr., "Joint Frequency Offset Estimation and Interference Cancellation for MIMO-OFDM Systems," in *Proc. of IEEE Vehicular Tech. Conf.*, Los Angeles, CA, Sept. 2004, pp. 1553–1557.

[38] T. Nandagopal, T.-E. Kim, X. Gao, and V. Bharghavan, "Achieving MAC Layer Fairness in Wireless Packet Networks," in *Proc. of ACM Int. Conf. on Mobile Computing and Networking (MobiCom)*, Boston, MA, Aug. 2000, pp. 87–98.

[39] *Wireless LAN Medium Access Control (MAC) and Physical Layer (PHY) Spec-*

ification: Higher-Speed Physical Layer Extension in the 2.4 GHz Band, IEEE Std. 802.11b, 1999.

[40] L. Peterson and B. S. Davie, *Computer Networks: A Systems Approach*, 2nd ed. Morgan Kaufmann, 2000.

[41] G. D. Golden, C. J. Foschini, R. A. Valenzuela, and P. W. Wolniansky, "Detection Algorithm and Initial Laboratory Results Using V-BLAST Space-Time Communication Architecture," *Electron. Lett.*, vol. 35, no. 1, pp. 14–15, Jan. 1999.

[42] C. B. Papadias and G. J. Foschini, "On the Capacity of Certain Space-Time Coding Schemes," *EURASIP Journal on Applied Signal Processing*, vol. 2002, no. 5, pp. 447–458, May 2002.

[43] A. Kochut, A. Vasan, A. U. Shankar, and A. Agrawala, "Sniffing Out the Correct Physical Layer Capture Model in 802.11b ," in *Proc. of ICNP'04*, Berlin, Germany, Oct. 2004, pp. 252–261.

[44] G. L. Stüber, *Principals of Mobile Communication*, 2nd ed. Kluwer Academic Publishers, 2000.

[45] G. Holland, *Adaptive Protocols for Mobile Ad Hoc Networks*. Ph.D. Thesis, Texas A&M University, 2004.

[46] C.-N. Chuah, J. M. Kahn, and D. Tse, "Capacity of multi-antenna array systems in indoor wireless environment," in *Proc. of IEEE Global Telecommunications Conf.*, Sydney, Australia, Nov. 1998, pp. 1894–1899.

[47] D. A. Gore, R. W. Heath Jr., and A. J. Paulraj, "Transmit Selection in Spatial Multiplexing Systems," *IEEE Commun. Lett.*, vol. 6, no. 11, pp. 491–493, Nov. 2002.

[48] A. F. Naguib, N. Seshadri, and A. R. Calderbank., "Increasing Data Rate over Wireless Channels: Space-Time Coding and Signal Processing for High Data Rate Wireless Communications." *IEEE Signal Processing Mag.*, vol. 17, no. 3, pp. 76–92, May 2002.

[49] H. Balakrishnan, S. Seshan, E. Amir, and R. H. Katz, "Improving TCP/IP Performance over Wireless Networks," in *Proc. of ACM Int. Conf. on Mobile Computing and Networking (MobiCom)*, Berkeley, CA, Nov. 1995, pp. 2–11.

[50] M. Mathis, J. Mahdavi, S. Floyd, and A. Romanow, "TCP Selective Acknowledgment Options," IETF, RFC 2018, October 1996, http://www.ietf.org/rfc/rfc2018.txt.

[51] H. Balakrishnan, V. Padmanabhan, S. Seshan, and R. H. Katz, "A Comparison of Mechanisms for Improving TCP Performance over Wireless Links," *IEEE/ACM Trans. Networking*, vol. 5, no. 6, pp. 756–769, Dec. 1997.

[52] K. Ramakrishnan, S. Floyd, and D. Black, "The Addition of Explicit Congestion Notification (ECN) to IP," IETF, RFC 3168, September 2001, http://www.ietf.org/rfc/rfc3168.txt.

[53] A. Stamoulis and N. Al-Dhahir, "Impact of Space-Time Block Codes on 802.11 Network Throughput," *IEEE Trans. Wireless Commun.*, vol. 2, no. 5, pp. 1029–1039, Sept. 2003.

[54] D. Plummer, "An Ethernet Address Resolution Protocol," IETF, RFC 826, November 1982, http://www.ietf.org/rfc/rfc826.txt.

[55] R. K. Jain, D.-M. W. Chiu, and W. R. Hawe, "A Quantitative Measure of Fairness and Discrimination for Resource Allocation in Shared Computer Systems," DEC Research Report, TR 301, September 1984.

[56] Z. Cheng and W. B. Heinzelman, "Flooding Strategy for Target Discovery in Wireless Networks," in *Proc. of MSWiM'03*, San Diego, CA, Sept. 2003, pp. 33–41.

[57] C. Intanagonwiwat, R. Govindan, and D. Estrin, "Directed Diffusion: A Scalable and Robust Communication Paradigm for Sensor Networks," in *Proc. of ACM Int. Conf. on Mobile Computing and Networking (MobiCom)*, Boston, MA, Aug. 2000, pp. 56 – 67.

[58] E. Woodrow and W. Heinzelman, "SPIN-IT: A Data Centric Routing Protocol for Image Retrieval in Wireless Networks," in *Proc. International Conference on Image Processing (ICIP)*, Rochester, NY, Sept. 2002, pp. 913–916.

[59] J. Broch, D. A. Maltz, D. B. Johnson, Y.-C. Hu, and J. Jetcheva, "A Performance Comparsion of Multi-Hop Wireless Ad Hoc Network Routing Protocols," in *Proc. of ACM Int. Conf. on Mobile Computing and Networking (MobiCom)*, Dallas, TX, Oct. 1998, pp. 85–97.

[60] S. R. Das, C. E. Perkins, E. M. Royer, and M. K. Marina, "Performance Comparison of Two On-demand Routing Protocols for Ad Hoc Networks," *IEEE Personal Commun. Mag.*, vol. 8, no. 1, pp. 16–29, Feb. 2001.

[61] V. Kawadia and P. R. Kumar, "A Cautionary Perspective on Cross Layer Design," *IEEE Wireless Commun. Mag.*, vol. 12, no. 1, pp. 3–11, Feb. 2005.

[62] B. Sklar, *Digital Communications: Fundamentals and Applications*. Prentice-Hall, 1988.

Vita

Minyoung Park was born in Seoul, Korea on October 15, 1970. He received his Bachelor of Science and Master of Science degrees in Electrical Engineering from Yonsei University in February 1993 and February 1995, respectively. From 1995 to 2001, he was a senior research engineer at LG Electronics Inc. in Korea. In August 2001, he joined the Electrical and Computer Engineering at the University of Texas at Austin to pursue his doctoral degree. During his study, he was a member of the Wireless Networking and Communications Group.

Permanent Address: 244-65 Shinlim9-Dong Kwanak-Gu
Seoul, 151-019, Korea

This dissertation was typeset with LaTeX 2_ε[1] by the author.

[1] LaTeX 2_ε is an extension of LaTeX. LaTeX is a collection of macros for TeX. TeX is a trademark of the American Mathematical Society. The macros used in formatting this dissertation were written by Dinesh Das, Department of Computer Sciences, The University of Texas at Austin, and extended by Bert Kay, James A. Bednar, and Ayman El-Khashab.